AN ABSTRACT OF DISSERTATION OF

Olga Golonzhka for the degree of Doctor of Philosophy in Biochemistry and Biophysics presented on June 9, 2008

Title: Characterization of the Mechanism and Function of C_2H_2 Zinc Finger Protein CTIP2 in the Developmental Processes

Abstract approved:

_____

Mark Leid

CTIP2 is a C_2H_2 zinc finger transcription factor that plays important yet poorly understood roles in mouse development. CTIP2 is known to be highly expressed in the central nervous system, skin and T lymphocytes during embryogenesis. CTIP2-null mice die perinatally of unknown causes and exhibit defects in multiple organ systems including nervous and immune systems. The goals of our studies described herein were to characterize the mechanism of CTIP2-mediated transcriptional regulation and determine the role of CTIP2 during mouse development, focusing primarily on that of skin and the craniofacial complex.

We analyzed the mechanisms of CTIP2-mediated repression in the neuronal context and uncovered that CTIP2 regulates transcription through recruitment of the

nucleosome remodeling and deacetylation (NuRD) repressor complex to the target promoters. We also identified p57Kip2 as novel target gene of CTIP2 in neuroblastoma cells and showed that CTIP2 directly or indirectly binds to the promoter of p57Kip2 gene.

We demonstrated for the first time that CTIP2 is highly expressed in the developing epidermis and in the underlying dermis. Analyses of the CTIP2-null mice revealed that CTIP2 controls both the terminal differentiation of keratinocytes and the establishment of the epidermal permeability barrier in a cell-autonomous manner. Our results also indicate that CTIP2 controls proliferation and early differentiation events of keratinocyte in a non-cell-autonomous manner by regulating the expression of growth factors, such as keratinocyte growth factor (KGF), that are expressed by the dermal fibroblast, and exert regulatory control over epidermal keratinocytes.

CTIP2 is also highly expressed in the oral epithelium and the developing tooth. CTIP2 controls the terminal differentiation of ameloblasts, which are the enamel-producing cells of teeth, and in the absence of CTIP2 these cells do not differentiate, fail to polarize and do not express ameloblast-specific genes. Additionally, CTIP2 appears to be involved in the establishment of the asymmetry of the mouse incisors by inhibiting formation of the ameloblasts on the lingual aspect of the developing tooth.

Together, our results provide new evidence that CTIP2 is involved in controlling development of the several ectoderm-derived tissues and regulates the differentiation of specific cell lineages.

Characterization of the Mechanism and Function of C_2H_2 Zinc Finger Protein CTIP2 in the Developmental Processes

by

Olga Golonzhka

A DISSERTATION

submitted to

Oregon State University

In partial fulfillment of

the requirements for the

degree of

Doctor of Philosophy

Presented June 9, 2008

Commencement June 2009

Doctor of Philosophy dissertation of Olga Golonzhka presented on June 9, 2008.

APPROVED:

_____

Major Professor, representing Biochemistry and Biophysics

_____

Chair of the Department of Biochemistry and Biophysics

_____

Dean of the Graduate School

I understand that my dissertation will become part of the permanent collection of the Oregon State University libraries. My signature below authorizes release of my dissertation to any reader upon request.

_____

Olga Golonzhka, Author

CONTRIBUTION OF AUTHORS

Dr. Mark Leid designed research. Olga Golonzhka performed research. Dr. Khamsiritrakul Topark-Ngarm assisted with the data collection and Chapter 2 preparation. Olga Golonzhka and Dr. Mark Leid analyzed and wrote the manuscripts.

TABLE OF CONTENTS

Page

CHAPTER 1 INTODUCTION.....1
Transcriptional regulation and in vivo function of CTIP2,
a C2H2 zinc finger protein

Introduction.....2
C_2H_2 zinc finger proteins.....3
History of the CTIP proteins.....4
CTIP2 as a transcriptional regulator.....6
In vivo function of CTIP2.....9
CTIP2 in T lymphocyte development.....9
CTIP2 in the developing nervous system.....11

CHAPTER 2 16
CTIP2 associates with the NuRD complex on the promoter of p57KIP2,
a newly identified CTIP2 target gene

ABSTRACT.....17
INTRODUCTION.....18
MATERIALS AND METHODS.....21
RESULTS.....29
The Class I and Class II histone deacetylase inhibitor TSA partially reverses transcriptional repression mediated by Gal4-CTIP2 on a minimal promoter 29
Deacetylation of histone H3/H4 associated with the reporter template in cells expressing GAL4-CTIP2.....30
CTIP2 complexes harbor TSA-sensitive HDAC activity.....30
CTIP2 associates with the NuRD complex in HEK293T cells.....32
CTIP2 associates with the NuRD complex in SK-N-MC cells.....33
CTIP2 interacts directly with RbAp46 and RbAp48 in vitro.....35
GAL4-CTIP2 recruits the NuRD complex to the promoter template.....36
Identification of CTIP2 target genes in SK-N-MC cells.....38
p57KIP2 is a direct Target of CTIP2 in SK-N-MC cells.....39
DISCUSSION.....41

CHAPTER 3.....63
Expression of COUP-TF-interacting protein 2 (CTIP2) in mouse skin
during development and in adulthood

ABTRACT.....64
INTRODUCTION.....65

TABLE OF CONTENTS (CONTINUED)

Page

MATERIAL AND METHODS.....66
RESULTS AND DISCUSSION.....68
Expression of CTIP2 during epidermal morphogenesis.....68
CTIP2 expression in proliferating cells.....70
Expression of CTIP2 in adult skin.....72
CTIP2 expression in stem cells present in the bulge of the adult.....73

CHAPTER 4 82
Dual role of COUP-TF-interacting protein 2 (CTIP2) in regulating epidermal homeostasis and skin barrier formation during mouse fetal development

ABTRACT.....83
INTRODUCTION.....83
MATERIAL AND METHODS.....86
RESULTS.....91
Generation of CTIP2$^{-/-}$ mice.....91
Loss of CTIP2 results in compromised barrier function, epidermal hypoplasia and increased transepidermal water loss.....92
CTIP2$^{-/-}$ mice exhibit altered expression of markers of epidermal proliferation and early differentiation.....93
CTIP2$^{-/-}$ mice exhibit alterations in expression of terminal epidermal differentiation markers and genes implicated in epidermal homeostasis and permeability barrier formation.....94
CTIP2$^{-/-}$ mice exhibit defects in surface lipid distribution and decreased expression of lipid-metabolizing enzymes.....95
Generation of epidermis-specific CTIP2 knockout mice.....97
CTIP2$^{ep-/-}$ mice exhibit compromised barrier function and increased transepidermal water loss during development.....98
CTIP2$^{ep-/-}$ mice develop histologically normal epidermis.....99
Microarray analysis of CTIP2$^{ep-/-}$ skin revealed downregulation of enzymes involved in lipid metabolism and alterations in the epidermal differentiation complex (EDC).....99
CTIP2 is involved in controlling the mesenchymal-epithelial crosstalk through regulation of KGF expression in the dermis. 101
DISCUSSION.....102

CHAPTER 5.....122
CTIP2 controls the terminal differentiation of ameloblasts

ABSTRACT.....123

TABLE OF CONTENTS (CONTINUED)

Page

INTRODUCTION.....124
MATERIALS AND METHODS.....129
RESULTS.....135
CTIP2 is expressed in developing mandible and tooth.....135
CTIP2 is expressed in ameloblasts.....136
CTIP2-null mice exhibit defects in tooth development.....136
CTIP2 controls terminal cytodifferentiation and polarization of ameloblasts.....139
CTIP2 controls the expression of a network of genes implicated in ameloblastogenesis.....141
DISCUSSION.....143

CHAPTER 6 CONCLUSION.....162

BIBLIOGRAPHY.....166

LIST OF FIGURES

Figure Page

1.1 Mouse CTIP2/Bcl11 locus……15

2.1 CTIP2-mediated transcriptional repression of a minimal promoter is partially reversed by TSA……47

2.2 CTIP2 complexes harbor TSA-sensitive HDAC activity *in vitro*……49

2.3 Coimmunoprecipitation of CTIP2 with components of the NuRD complex……51

2.4 Co-fractionation of CTIP2 and components of NuRD complex on a Superose 6 size-exclusion column……53

2.5 CTIP2 interacts directly with RbAp46 and RbAp48 *in vitro*……54

2.6 CTIP2-dependent recruitment of endogenous NuRD complex proteins to the promoter template……56

2.7 CTIP2 knockdown in SK-N-MC cells results in increased expression of p57KIP2……58

2.8 CTIP2 and components of NuRD complex co-associate with *p57KIP2* promoter in SK-N-MC cells……60

3.1 Expression of CTIP2 in the mouse fetal skin……75

3.2 CTIP2 expression in proliferating cells……77

3.3 Expression of CTIP2 in the adult mouse skin……79

3.4 Immunoblot analysis of CTIP2 expression in fetal and adult skin……80

3.5 Expression of CTIP2 in stem cells of the bulge region of the mouse hair follicle……81

4.1 Floxing the CTIP2 locus……109

4.2 $CTIP2^{-/-}$ mice exhibit permeability barrier defects and epidermal hypoplasia……111

LIST OF FIGURES (CONTINUED)

Figure Page

4.3 Decreased expression of epidermal markers and genes involved in epidermal barrier establishment in CTIP2$^{-/-}$ mice……113

4.4 Defects in lipid distribution and expression of lipid-processing enzymes in CTIP2$^{-/-}$ mice……115

4.5 CTIP2$^{ep-/-}$ mice exhibit barrier defects, increased water loss and normal epidermis……117

4.6 Microarray analyses of CTIP2$^{ep-/-}$ mice indicate that CTIP2 is a top-level transcription factor in skin development……119

4.7 CTIP2 regulates expression of growth factors involved in mesenchymal-epithelial crosstalk for maintaining epidermal homeostasis……121

5.1 CTIP2 is expressed in the developing tooth……149

5.2 CTIP2$^{-/+}$ mice experience malocclusion……151

5.3 CTIP2 mice exhibit defects in tooth development……152

5.4 CTIP2-null mice exhibit defects in the terminal differentiation of the ameloblast cell lineage……154

5.5 CTIP2-null odontoblast display minor defects……156

5.6 CTIP2 regulates expression of other transcription factor involved in the ameloblast differentiation……157

5.7 CTIP2 interacts with promoter regions of several ameloblast-related genes……159

5.8 The model for the action of CTIP2 during tooth morphogenesis……161

.

CHAPTER 1

Transcriptional regulation and in vivo function of CTIP2, a C_2H_2 zinc finger protein

INTRODUCTION

Introduction

The fascinating subject of developmental biology occupies a central position in a modern biology. It is a captivating discipline that unites genetics, morphogenesis, molecular and cell biology.

Recent years can be characterized by enormous technological advances. Novel genetic and biochemical approaches offer colossal opportunities for advancing our understating of embryogenesis. The importance of such advances is well-recognized as it has become clear that the molecular components of many developmental processes are present and active in the adult organisms and developmental pathways are important not only for generating but also for maintaining an adult form.

Transcriptional regulators play a central role in controlling the developmental processes. The genetic programs governed by the specific transcription factors leading to the generation of all the different cell types of an embryo and ultimately the adult, begin immediately after fertilization. The complex regulation of gene expression results in changes in a number of embryonic cells and their interactions, specification of the different cell types and establishment of the organ systems. However, our knowledge of genetic programs and the cell-cell interactions that influence these programs is by no means complete.

Understanding the genetic programs and signaling pathways of normal development will provide us with an invaluable tool for understanding the pathways and mechanisms of the adult tissue maintenance, repair and regeneration. It will enable us to manipulate genetic and environmental factors that lead to the development of the complex organ system and ultimately aid in the development of disease therapies.

C_2H_2 zinc finger proteins

There are a number of families of zinc finger proteins that contain multiple cysteine and histidine residues and use zinc coordination to stabilize their structure (Coleman, 1992; Berg and Shi, 1996; Berg and Godwin, 1997). C_2H_2 zinc finger proteins were the founding members of zinc finger family and this group is one of the most common DNA-biding motifs found in eukaryotic transcription factors (Wolfe et al., 2000; Tupler et al., 2001). However, the C_2H_2 domain is used not only for DNA interactions but also for RNA and protein interactions (Shastry, 1996; Mackay and Crossley, 1998).

C_2H_2 zinc finger was originally discovered as a repetitive motif in the transcription factor TFIIIA of Xenopus laevis (Miller et al., 1985). Each zinc finger is characterized by the conserved structure. A typical zinc binding domain includes about 30 amino acids with the following consensus sequence: (Tyr,Phe)-X-Cys-X2,4-

Cys-X3-Phe-X5-Leu-X2-His-X3-5-His-X2-6, where as X is a variable amino acid (Lee et al., 1989). These sequences fold in the presence of zinc and form a compact domain (Parraga et al., 1988; Lee et al., 1989). Each finger binds a single zinc ion that is positioned in between the two-stranded antiparallel β-sheet and the α-helix. The zinc ion is tetrahedrally coordinated between two cysteines at one end of the β-sheet and two histidines in the C-terminal portion of the α-helix. Zinc finger proteins usually contain several fingers that make tandem contacts with the major groove of the DNA. C_2H_2 zinc fingers usually bind to DNA target sites with high affinity and specificity.

A colossal amount of evidence exists supporting the crucial role of C_2H_2 zinc finger proteins in regulating normal mammalian physiology as well as their role in instructing developmental processes of multiple organ systems (Polimeni et al., 1996; Relaix et al., 1996; Tsai and Reed, 1997; Ganss and Kobayashi, 2002; Ganss et al., 2002; Herman and El-Hodiri, 2002; Trappe et al., 2002; Ganss and Jheon, 2004; Parrish et al., 2004; De et al., 2005; Zhang et al., 2006).

History of the CTIP proteins

COUP-TF-interacting proteins 1 (CTIP1) and 2 (CTIP2), also known as Bcl11a and Bcl11b, respectively, are highly related C_2H_2 zinc finger proteins that were originally cloned in Dr. Leid's lab (Avram et al., 2000). CTIP1 and CTIP2 were isolated

through yeast two-hybrid screening and had been shown to interact directly with all members of the COUP-TF family of orphan nuclear receptors in yeast and *in vitro*. These two proteins also mediate transcriptional repression of COUP-TF proteins (Avram et al., 2000). The analysis of the amino acid sequence revealed highly conserved and repeated C_2H_2 zinc finger motifs (Avram et al., 2000).

Shortly after the Leid group's characterization of CTIP proteins, Neal Copeland's group reported the identification of Bcl11a (which they named ectopic viral integration site 9, *Evi9*) as a site of retroviral integration that was associated with murine myeloid leukemia, perhaps by virtue of interacting with Bcl6 (Nakamura et al., 2000) It was proposed that Evi9 could potentially represent a new leukemia gene. Copeland's lab was the first to show that Bcl11a may regulate the proliferative state of specific cell types within the hematopoietic system, and several reports were subsequently published that implicated Bcl11a in human B cell leukemias (Satterwhite et al., 2001; Kuppers et al., 2002; Martin-Subero et al., 2002; Martinez-Climent et al., 2003).

Bcl11b, so re-named by NCBI because of its close sequence identity to Bcl11a (Avram et al., 2002), has never been implicated in B cell leukemia. CTIP2/Bcl11b was recloned by Kominami's group in 2003, and this group referred to CTIP2 as radiation-induced transcript-1b (Rit-1b) because it was found that Bcl11b was mutated in mouse thymocytes in the process of gamma radiation-induced tumorigenesis (Wakabayashi et al., 2003b). This finding led Kominami's group to hypothesize that

CTIP2 may function as a tumor suppressor gene in T cells (Wakabayashi et al., 2003b), and this has been supported by reports of LOH at the human CTIP2 locus (MacLeod et al., 2003; Nagel et al., 2003; MacLeod et al., 2004; Su et al., 2004; Okazuka et al., 2005; Przybylski et al., 2005). Kominami's group also cloned two other splice variants of CTIP2/ Bcl11b, defined herein as Bcl11b-long (containing exon 3) and Bcl11b-short (lacking exons 2 and 3; see Fig. 1.1).

The organization of the mouse CTIP2 genomic locus is shown in Fig. 1.1. The CTIP2 gene (both mouse and human) contains 4 exons (Fig. 1.1 A) and the majority of the CTIP2 open reading frame is encoded by exon 4 (Fig. 1.1 B). CTIP2 harbors 7 zinc fingers, 6 of which are encoded in the exon 4. CTIP2 protein is characterized by the basic region at the N-terminus of the proteins, several proline and serine-rich regions, as well as acidic domain located within the fourth exon (Fig. 1.1 B)

Both CTIP2 (Fig. 1.1) and CTIP1 (not shown) are highly conserved at the amino acid level across species (Fig. 1.1 C), suggesting that each likely serves a crucial function(s) in vertebrate organisms.

CTIP2 as a transcriptional regulator

COUP-TF proteins are generally considered as repressors of transcription (Tsai and Tsai, 1997). CTIP2 was found to be tethered to promoters through COUP-TF

proteins and potentiate transcriptional repression of COUP-TF-mediated repression of reporter constructs in transiently transfected cells. Such repression was found to be Trichostatin A (TSA)-insensitive, suggesting that the mechanism of repression is independent of class I and II of histone deacetylases (HDAC) (Avram et al., 2002).

It was also shown that CTIP2 can act through direct, sequence-specific DNA binding activity *in vitro* and act independently of COUP-TF family members (Avram et al., 2002). The regulatory element to which CTIP2 binds contains a core motif, 5'-GGCCGG-3', which is reminiscent of a canonical GC-box (5-'GGGCGG-3'), as was revealed by a binding-site selection technique (Avram et al., 2002). In a context of the thymidine kinase promoter which carried CTIP2 biding sites, CTIP2 repressed transcription of the reporter construct and such repression was not enhanced by the co-transfection of the COUP-TF proteins. Repression by CTIP2 in this context did not involve recruitment of HDACs of class I or II (Avram et al., 2002).

Further experiments provided evidence that CTIP2-mediated transcriptional repression can result from the recruitment of the class III histone deacetylase SIRT1 *in vitro* (Senawong et al., 2003; Senawong et al., 2005). SIRT1 interacted with CTIP2 directly and was recruited to the promoter template in a CTIP2-dependent manner in transiently transfected HEK293 cells. The recruitment of SIRT1 enhanced CTIP2-meidated repression and was accompanied by the deacetylation of histones H3 and H4 present at the promoter. SIRT1 and CTIP2 also co-purified as a part of a bigger protein complex from the nuclear extracts in Jurkat cells.

Further studies reported that CTIP2 can recruit HDACs, HDAC1 and HDAC2 (Cismasiu et al., 2005) to the promoter template in T lymphocytes, within the context of the Nucleosome Remodeling and Deacetylation (NuRD) complex (Cismasiu et al., 2005). Yet another study indicated that CTIP2 can represses HIV-1 transcription through recruitment of deacetylaseas HDAC1 and HDAC2 as well as methyltransferase SUV39H1 with subsequent heterochromatin formation (Marban et al., 2007).

Multiple lines of evidence supported the hypothesis that CTIP2 functions primarily as a transcriptional repressor in neuroblasoma cells (Topark-Ngarm et al., 2006), T cells (Leid, et al., in preparation), and skin (Golonzhka et al., submitted), in which the majority of CTIP2 target genes that were identified were derepressed in the absence of CTIP2. However, approximately one third of the genes that are dysregulated in the T cells of CTIP2-null mice are down-regulated relative to the control, suggesting that CTIP2 may act as a transcriptional activator in some promoter and/or cell contexts (Leid et al., in preparation). To date, only one study has addressed the activator function of CTIP2. It was demonstrated that CTIP2 activates expression of *IL2* gene upon T cell activation. CTIP2 also interacted with the p300 coactivator protein in the extracts of activated lymphocytes. Therefore it was proposed that CTIP2 may activate transcription of its target genes through recruitment of p300. Nevertheless, the mechanisms of CTIP2-mediated transcription

activation remain to be examined in detail and are likely to be cell type and promoter context dependent.

In vivo function of CTIP2

CTIP2 is expressed early during mouse development as well as in the adult animal, and in both cases, expression is most predominant in the CNS, thymus, and epithelial tissues (Leid et al., 2004; Golonzhka et al., 2007). Mice null for expression of CTIP2 (CTIP2$^{-/-}$)exhibit perinatal lethality (Wakabayashi et al., 2003b), which is reminiscent of the COUP-TFI$^{-/-}$ phenotype (Qiu et al., 1997; Yamaguchi et al., 2004), and severe phenotypes in all tissues that express the gene.

CTIP2 in the T lymphocyte development

CTIP2 is highly expressed in T cells and is crucial for their normal development , differentiation and function (Wakabayashi et al., 2003b; Leid et al., 2004; Cismasiu et al., 2006; Albu et al., 2007; Grabarczyk et al., 2007; Tydell et al., 2007).

CTIP2 is expressed in the developing thymus as early as E14.5. At this stage most of the thymic cells are double negative T cell precursors (CD4^{-}CD8^{-}) (Leid et al., 2004). CTIP2 expression persists in the thymus throughout all the stages of mouse development and is present in more mature neonatal T lymphocytes (Wakabayashi

et al., 2003b; Leid et al., 2004). The function of CTIP2 in T cells was addressed by the analysis of T cell phenotype in CTIP2-null mice. CTIP2-null mice die perinatally of unknown causes (Wakabayashi et al., 2003b) and therefore all the further studies were limited to the neonatal or earlier developmental stages. CTIP2–null mice show a block at the double-negative stage of thymocyte development and lack of pre-T cell receptor (TCR) complex on the cell surface. These cell exhibit a profound apoptosis as a result of the lack of the pre-TCR signaling (Wakabayashi et al., 2003b), and it was concluded that CTIP2 serves as a T cell survivor signal.

Further dissection of the signaling pathways that control T cell lineage development of the role of CTIP2 in these processes established that expression of CTIP2 in T cell progenitors is downstream of Notch/Delta signaling in the very early stages of T cell development (Tydell et al., 2007), and later is tightly coupled with the maintenance of T cell lineage identity (Franco et al., 2006).

The role of CTIP2 in later stages of T cell development was examined by conditionally deleting CTIP2 in double positive thymocytes using CD4-cre transgenic animals. It was shown that CTIP2 controls the positive selection of both CD4 and CD8 lineages. CTIP2-null thymocytes rearranged T cell receptor $(TCR)_{\alpha}$ normally, however, the TCR signaling in these cell was impaired and they displayed an increased susceptibility to spontaneous apoptosis.

CTIP2 has been implicated in lymphoproliferative disorders (MacLeod et al., 2003; Nagel et al., 2003; Wakabayashi et al., 2003a; Przybylski et al., 2005). Loss of heterozygocity at the mouse CTIP2 locus resulted in the development of thymic lymphomas and it was suggested that CTIP2 can act as a tumor suppressor. Interestingly, introduction of CTIP2 into HeLa cells, which normally lack CTIP2 expression, suppressed cell growth. These results indicated that loss-of-function mutations of CTIP2 can contribute to mouse lymphomagenesis and possibly to human neoplastic transformations (Wakabayashi et al., 2003a).

The inversion involving the CTIP2 locus resulted in its disruption, lack of the wt CTIP2 transcripts and T cell lymphoblastic leukemia development (Przybylski et al., 2005). It was later shown that CTIP2 is necessary for survival of human T-cell leukemia and lymphoma cell lines and knock-down of CTIP2 resulted in apoptosis in transformed but not normal T cells (Grabarczyk et al., 2007).

CTIP2 in the developing nervous system

CTIP2 is expressed at high levels in the developing central nervous system and in the adult brain (Leid et al., 2004). The expression domains include numerous subdivisions of the brain. CTIP2 was prominent in the cerebral cortex. Later it was shown that CTIP2 expression is specific to layer V of the cortex and it was proposed that CTIP2 can be used as a marker for layer V cortical neurons.

High expression of CTIP2 is detected in the developing olfactory bulb as well as the olfactory epithelium. Basal ganglia, hippocampus, thalamus, hypothalamus and cerebellum, all express high levels of CTIP2. In the spinal cord CTIP2 is expressed predominantly in the dorsal side. This expression pattern of CTIP2 persisted in the adult brain in all the structures mentioned above (Leid et al., 2004).

As was mentioned above CTIP2 is present at very high levels in layer V of the cerebral cortex. Jeff Macklis's lab undertook a detailed investigation to identify the cell types that are positive for CTIP2 expression and examined the function of CTIP2 in these cells. It was shown that CTIP2 is present in the corticospinal motor neurons and corticotectal neurons specifically (Arlotta et al., 2005).

At E12 CTIP2 was expressed in a cluster of cells in the ventrolateral cortex but not in either the ventricular or subventricular zones. At E14.5 and at E16.5 CTIP2 expression was observed in the corticospinal motor neurons of the cortical plate. These data suggested that CTIP2 is not expressed in the neural precursors and is not involved in the early specification of the cortical neurons, but is present in the postmitotic neurons and perhaps is involved in their differentiation. Corticospinal motor neurons of the CTIP2-null mice exhibited defects in fasciculation, outgrowth and pathfinding, accompanied by the abnormal pruning of the axons of these cells. This resulted in the failure of these neurons to connect to their targets in the spinal cord. No changes in the apoptosis of these cells were detected. Further examination

revealed abnormalities of axonal fiber tracts of the cortex and disorganization of the internal capsule.

Recent findings postulated a novel role of CTIP2 in medium spiny neurons (MSN) differentiation and striatal development and architecture (Arlotta et al., 2008).

CTIP2 is highly expressed in the striatum. The striatum is involved in the coordination of movements, emotions and cognition (Graybiel, 2005). A more detailed examination and the co-staining with specific markers revealed that CTIP2 is expressed by all medium spiny neurons (which account for 90-95 % of all the striatal neurons (Gerfen, 1992)), but is excluded from the striatal interneurons (Arlotta et al., 2008). Medium spiny neurons are involved in controlling the body's motor function and are implicated in the Huntington's disease (Albin et al., 1989; Stenman et al., 2003). In the absence of CTIP2, medium spiny neurons fail to differentiate and are characterized by the dramatically reduced expression of a large number of MSN markers. These neurons fail to aggregate into characteristic patches and this ultimately leads to the disruption of the structure of the striatum. The disorganization of the patches also results in the abnormal dopaminergic innervations of the striatum. This was linked to the defects in the repulsion of neurons during development and it was suggested that CTIP2 controls expression of molecules involved in neuron repulsion during development of the nervous system (Arlotta et al., 2008).

In the studies described below, we addressed the mechanisms of the CTIP2-meidated transctipional regulation in the neuronal context and identified several target genes of CTIP2 in the neuroblastoma cells. We then further examined the expression pattern of CTIP2 in a mouse embryo and analyzed the function of CTIP2 in the developing skin and dentition.

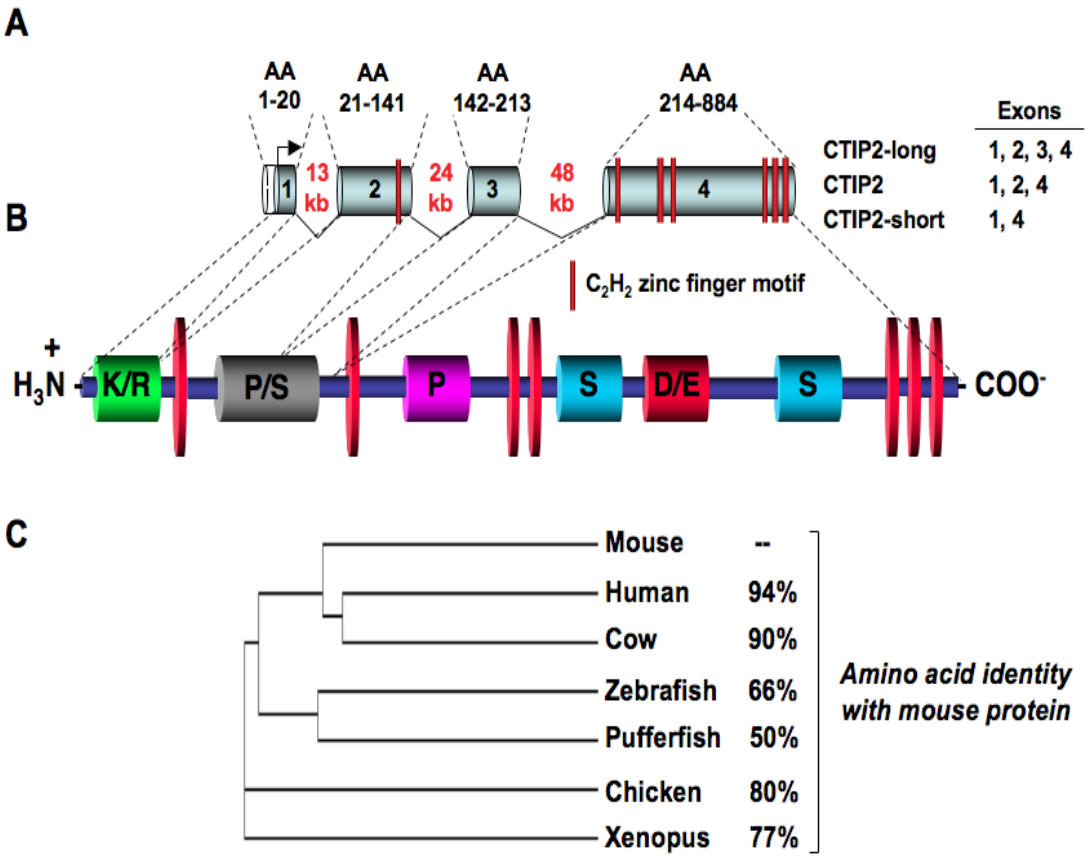

Figure. 1.1. Mouse CTIP2/Bcl11b locus.

A, organization of mouse CTIP2/Bcl11b genomic locus with the corresponding amino acid numbers (AA) and known splice variants. Exons are represented by grey bars.
B, relationship of exonic structure to the full-length protein. Red discs represent zinc fingers; K/R-basic region; P-proline-rich region, S-serine rich region; P/S – proline and serine-rich region, D/E – acidic region.
C, phylogram depicting sequence identity of the Bcl11b protein across vertebrate species indicated. Phylogeny analyses were performed using ClustalW.

CHAPTER 2

CTIP2 Associates with the NuRD Complex on the Promoter of p57KIP2, a Newly Identified CTIP2 Target Gene

Olga Golonzhka*, Acharawan Topark-Ngarm*, Valerie J. Peterson, Brian Barrett Jr,

Brigetta Martinez, Kristi Crofoot, Theresa M. Filtz and Mark Leid

*contributed equally to this work

The journal of Biological Chemistry **281**: 32272-32283

2006

Abstract

Chicken ovalbumin upstream promoter-transcription factor (COUP-TF)-interacting protein 2 (CTIP2), also known as Bcl11b, is a transcriptional repressor that functions by direct, sequence-specific DNA binding activity or by recruitment to the promoter template by interaction with COUP-TF family members. CTIP2 is essential for both T cell development and axonal projections of corticospinal motor neurons in the central nervous system. However, little is known regarding the molecular mechanism(s) by which CTIP2 contributes to either process. CTIP2 complexes that were isolated from SK-N-MC neuroblastoma cells were found to harbor substantial histone deacetylase activity, which was likely conferred by the Nucleosome Remodeling and Deacetylation (NuRD) complex. CTIP2 was found to associate with the NuRD complex through direct interaction with both RbAp46 and RbAp48, and components of the NuRD complex were found to be recruited to an artificial promoter template in a CTIP2-dependent manner in transfected cells. Finally, the NuRD complex and CTIP2 were found to co-occupy the promoter template of p57KIP2, a gene encoding a cyclin-dependent kinase inhibitor, and identified herein as a novel transcriptional target of CTIP2 in SK-N-MC cells. Therefore, it seems likely that the NuRD complex may be involved in transcriptional repression of CTIP2 target genes and contribute to the function(s) of CTIP2 within a neuronal context.

Introduction

CTIP2 (Bcl11b, Rit-1β) is a novel C_2H_2 zinc finger protein that was first isolated and identified as a COUP-TF-interacting protein (Avram et al., 2000). Within the immune system, CTIP2/Bcl11b is predominantly expressed in mouse thymocytes, and is required for development and survival of αβ T lymphocytes (Wakabayashi et al., 2003b). Inactivation of CTIP2/Bcl11b by homozygous deletions and point mutations of CTIP2 gene are associated with γ-ray induced thymic lymphomas in mouse (Wakabayashi et al., 2003a; Sakata et al., 2004), and ectopic expression of CTIP2/Bcl11b in HeLa cells results in suppression of cell growth (Wakabayashi et al., 2003a). Although these findings suggest that CTIP2 may function as a tumor suppressor, its involvement in human carcinogenesis remains unclear. However, several reports have described a link between chromosomal rearrangements of CTIP2 and human T-cell acute lymphoblastic leukemia (T-ALL) (MacLeod et al., 2003; Nagel et al., 2003; Bezrookove et al., 2004; Su et al., 2004; Przybylski et al., 2005).

In addition to substantial expression in thymocytes, CTIP2/Bcl11b (CTIP2 hereafter) is also expressed at a high level in the central nervous system (CNS) of pre- and post-natal mouse brain, more specifically in developing cerebral cortex primarily in layer V, the striatum, olfactory bulb, hippocampus, limbic system, basal ganglia, and also in the intermediate region of the spinal cord (Leid et al., 2004; Arlotta et al., 2005; Chen et al., 2005; Molyneaux et al., 2005). *Ctip2*-null mice exhibit defective axonal projections of corticospinal motor neurons (CSMNs), indicating that CTIP2 plays a critical role in development of the CNS (Arlotta et al., 2005). Although several

lines of evidence have shown that CTIP2 is required for T cell and CNS development, little is known concerning the mechanism(s) by which CTIP2 may function in these processes, or transcriptional targets of CTIP2 in any cell or tissue.

CTIP2, and the highly related protein CTIP1, are transcriptional repressors that are recruited to the template either by interaction with COUP-TFs (Ref (Avram et al., 2000), and unpublished data) or by direct, sequence-specific DNA binding activity (Avram et al., 2002). In both cases, CTIPs mediate transcriptional repression that has been found to be largely insensitive to reversal by trichostatin A (TSA), an inhibitor of class I and class II histone deacetylases (HDACs). SIRT1 (sirtuin 1), a class III HDAC, may underlie TSA-insensitive transcriptional repression mediated by CTIPs (Senawong et al., 2003; Senawong et al., 2005), but it is not known if TSA- insensitive histone deacetylation entirely underlies CTIP2-mediated transcriptional repression in all cell types and/or promoter contexts.

The NuRD complex harbors ATP-dependent, nucleosome remodeling and histone deacetylase activities, and consists of several subunits, minimally including RbAp46, RbAp48, HDAC1, HDAC2, MTA1, MTA2, MTA3, MBD3, and Mi-2α and β (Xue et al., 1998; Zhang et al., 1999; Yao and Yang, 2003; Fujita et al., 2004). The NuRD complex is considered to play a key role in transcriptional repression mediated by sequence specific transcription factors including p53 (Luo et al., 2000), Ikaros (Kim et

al., 1999), Hunchback (Kehle et al., 1998), Tramtrack69 (Murawsky et al., 2001), KAP-1 (Schultz et al., 2001), BCL-6 (Fujita et al., 2004), and FOG-1 (Hong et al., 2005).

In the present report, we found that transcriptional repression mediated by CTIP2 was partially sensitive to inhibition by TSA in the context of a minimal promoter. Consistently, both ectopically expressed and endogenous CTIP2 complexes were found to harbor TSA-sensitive HDAC activity *in vitro*. We found that CTIP2 associated with the NuRD complex in both transfected HEK293T and in untransfected SK-N-MC neuroblastoma cells, and this appeared to be via direct interaction with RbAp46 and/or RbAp48. We also found that the NuRD complex was recruited to a CTIP2-responsive promoter template in a CTIP2-dependent manner in transfected HEK293T cells. Here we report a newly identified CTIP2 target gene, *p57KIP2*, which encodes a cyclin-dependent kinase (cdk) inhibitor. p57KIP2 plays important roles in control of cell cycle and neuronal differentiation, and was found herein to be repressed by CTIP2 in SK-N-MC cells. Subsequent ChIP and re-ChIP analyses of the *p57KIP2* promoter demonstrated co-occupancy by CTIP2, MTA2, HDAC2, and RbAp46/48, suggesting that CTIP2-mediated repression of this target gene is likely to involve recruitment of the NuRD complex to the template. Together, these findings suggest that the NuRD complex may play a role in CTIP2-mediated transcriptional repression, at least on a subset of genes, and in a neuron-like context.

Material and methods

Constructs

The Lex-Gal-Luc reporter and LexA-VP16 constructs were kind gifts from Dr. Malcolm G. Parker (Imperial College, London; Ref (Christian et al., 2004). The Gal4-CTIP2, FLAG-CTIP2, and deletion mutants of the latter were previously described (Senawong et al., 2003). FLAG-CTIP2-(129-350) was prepared by PCR amplification with primers containing appropriate restriction sites for insertion into pcDNA3.1/HisC (Invitrogen), and verified by complete DNA sequencing. Recombinant baculoviruses expressing Mi-2β, MTA2, HDAC1, HDAC2, RbAp46 and RbAp48 were kind gifts from Dr. Danny Reinberg (University of Medical and Dentistry of New Jersey; Ref (Zhang et al., 1999).

Cell Culture

HEK293T cells were cultured on 10 cm plates in high glucose Dulbecco's modified Eagle's medium (Gibco) with 10% (v/v) fetal bovine serum (Atlas Biologicals) and 1% (v/v) penicillin/streptomycin (Invitrogen). SK-N-MC neuroblastoma cells were grown under identical conditions except that 1% sodium pyruvate (Invitrogen) was added to the media.

Transfection and reporter assays

At approximately 60% confluence, HEK293T cells were transiently transfected with 3 μg of the Lex-Gal-Luc reporter gene, 0.1 μg of an expression vector encoding the LexA-VP16 fusion protein, and 1 or 5 μg of either Gal4-DBD or Gal4-DBD-CTIP2 (Gal4-CTIP2), using the calcium phosphate method. Twenty-four h after transfection, cells were treated with TSA (100 ng/mL) or vehicle, and harvested 24 h later. Whole cell lysates were subjected to a luciferase assay (Promega). Luciferase levels were measured using a LUMAT LB 9507 (EG&G Berthold) luminometer. Luciferase activities were normalized across all samples by protein concentration as determined using the Bradford assay.

Antibodies

Anti-acetylated-histone H3 and -H4 antibodies were purchased from Upstate. Anti-CTIP2 antisera was raised against CTIP2 peptide corresponding to amino acids 25-44 and purified on a peptide affinity column. Anti-Mi-2α/β and -FLAG M5 monoclonal antibodies were obtained from BD Biosciences and Sigma, respectively. Anti-RbAp46/RbAp48, -CTIP2 (25B6), and -β-actin monoclonal antibodies were obtained from Abcam. Anti-MTA2, -HDAC1, -HDAC2, and -HA polyclonal antibodies were purchased from Santa Cruz Biotechnology and Abcam, and anti-p57KIP2 was obtained from BD Pharmingen.

Immunoprecipitation (IP) analyses

HEK293T cells were transiently transfected as described above with 10 μg of an expression vector encoding FLAG-CTIP2 or the corresponding empty vector (pcDNA3.1). Forty-eight h after transfection, cells were lysed with NET-N buffer (150 mM NaCl, 0.5% Nonidet P-40 (NP 40), 10% glycerol, 1 mM EDTA, 20 mM Tris-HCl, pH 8 and a protease inhibitor mixture), and incubated on ice for 30 min with occasional vortexing prior to centrifugation (16,000 x *g* for 15 min). Cell lysates (800 μg protein per IP reaction) were precleared with protein G-Sepharose (Amersham Biosciences) in Buffer IP (10 mM HEPES, pH 7.5, 10% glycerol, 1 mM EDTA, 150 mM NaCl, 0.05% NP 40) at 4^{o}C for 60 min to reduce nonspecific protein binding. After centrifugation, the precleared samples were incubated with 2 μg of an anti-MTA2 or irrelevant (anti-HA) antibody on ice for 60 min, followed by addition of protein G-Sepharose. Samples were then incubated at 4^{o}C overnight with rocking. The Sepharose beads were collected by centrifugation, washed three times with buffer IP, and resuspended in denaturing sample buffer. Immune complexes were separated by SDS-PAGE and analyzed by western blotting with appropriate antibodies. For SK-N-MC cells, the nuclear extract was made as described previously (Dignam et al., 1983), except buffer C was modified to contain 0.72 M NaCl and the pellet remaining after nuclear lysis was re-extracted with an equal volume of this buffer followed by brief sonication and centrifugation. Final nuclear extracts were dialyzed against buffer D (20 mM HEPES, pH 8.0, 10% glycerol, 0.1 mM EDTA, 300 mM NaCl), aliquoted, and quickly frozen or used directly in IP assays, which were performed as described above using 300 μg

nuclear protein, and in buffer D containing 0.05% NP40. SF9 cells were infected with baculovirus individually directing expression of Mi-2β, MTA2, HDAC1, HDAC2, RbAp46, and RbAp48. Cell pellets were resuspended in hypotonic buffer (10 mM HEPES, pH 7.9, 10% glycerol, 0.5 M NaCl, 0.2 mM EDTA, 0.5 mM DTT), and sonicated 3 times for 20 s to lyse cells, followed by centrifugation. Approximately 120-160 μg of total protein from cell lysates was used per IP reaction**,** which was performed in buffer IP using 1 μg of specific antibodies against individual NuRD complex proteins.

GST Pull-down Experiments

GST pull-down experiments were conducted as described previously (Dowell et al., 1997).

HDAC activity assays

Immunoprecipitation assays were performed essentially as described above except that more protein was used (HEK293T, 2 mg/IP; SK-N-MC, 500 μg/IP). Immunoprecipitates obtained from SK-N-MC cells or transiently transfected HEK293T cells were analyzed for HDAC activity using an HDAC Fluorescent Activity Assay kit (Biomol Research Laboratories, Inc.), in the absence or presence of TSA (0.25 μM). The fluorophore produced from the reactions was excited at 360 nm light and emission was followed at 460 nm on a Gemini XPS microplate spectrofluorometer (Molecular Devices).

Superose 6 size-exclusion column chromatography

SK-N-MC nuclear extract was dialyzed against buffer D. Approximately 6 mg of nuclear protein was concentrated to 1 ml using a Millipore Ultrafree centrifugal filter apparatus (10 kDa nominal molecular mass limit), and then applied to an 850 mm x 20 mm Superose 6 size exclusion column (Amersham Biosciences) that had been equilibrated with buffer D containing 1 mM DTT, and calibrated with protein standards (blue dextran, 2000 kDa; thyroglobulin, 669 kDa; ferritin, 440 kDa; catalase, 232 kDa; bovine serum albumin, 67 kDa; RNAse A, 13.7 kDa, all from Amersham Biosciences). The column was eluted at a flow rate of 0.4 ml/min and fractions were collected for 5 min (2 mL). The chromatographic elution profiles of CTIP2 and the NuRD complex proteins were determined by immunoblotting with appropriate antibodies and chemiluminescence detection.

Chromatin Immunoprecipitation (ChIP) assays

ChIP assays were conducted as previously described (Senawong et al., 2003; Senawong et al., 2005) with some modifications. Briefly, HEK293T cells were washed sequentially after cross-linking with PBS, buffer I (0.25% TritonX-100, 10 mM EDTA, 0.5 mM EGTA, 10 mM HEPES, pH 6.5), and buffer II (200 mM NaCl, 1 mM EDTA, 0.5 mM EGTA, 10 mM HEPES, pH 6.5), and then lysed followed by brief sonication. The sonicated lysates were diluted 3.5-fold with ChIP dilution buffer, and 10% of the diluted lysates was reserved as an input sample to determine the total amount of

reporter plasmid in transfected cells for subsequent normalization procedures. The remaining lysates were aliquoted equally and used for IP with and without the addition of 5 μg of anti-MTA2 (Santa Cruz Biotechnology), -RbAp46/48 (Abcam), or -HDAC2 (Santa Cruz Biotechnology) antibody. Chromatin complexes were subjected to reversal of protein-DNA cross-links at 65 ^{o}C overnight and proteinase K treatment at 45 ^{o}C for 2 h. DNA was recovered by using a Qiaquick Spin kit (Qiagen) and amplified using a forward primer (5'-GTCGAGGGGATGATAATGC-3') upstream of the multimerized 17-mer, and a reverse primer (5'-ACAGTACCGGAATGCCAAG-3') downstream of the promoter but upstream of a transcriptional start site of the luciferase gene. Amplification of *GAPDH* promoter region (negative control) was performed with a forward primer (5'-TCCTCCTGTTTCATCCAAGC-3'), and a reverse primer (5'-TAGTAGCCGGGCCCTACTTT-3'). Conditions of the amplification reactions were as follows; a predenaturation step of 2 min at 94 ^{o}C was followed by 23 (for the reporter) and 31 (for GAPDH) cycles of 94 ^{o}C (denaturation) for 40 s, 56 ^{o}C (annealing) for 45 s, 70 ^{o}C (elongation) for 1 min, and a final elongation step of 5 min at 72 ^{o}C. The resulting 210 bp PCR product of the reporter gene promoter region and 218 bp PCR product of the *GAPDH* promoter region were analyzed by agarose gel electrophoresis and ethidium bromide staining. Experiments were performed at least three times. ChIP assays in SK-N-MC cells were performed as described above except that the antibodies (anti-CTIP2 and RbAp46/48, respectively) were coupled to magnetic Dynabeads (Dynal/Invitrogen).

Re-ChIP assays

The 1st ChIP was performed as described above using anti-CTIP2 antibody. Immune complexes were eluted from the beads with 20 mM DTT. Eluates were then diluted 30-fold with ChIP dilution buffer, and subjected to the 2nd immunoprecipiation reaction using either anti-MTA2, -HDAC2 or -RbAp46/48 antibody. The final elution step was performed using 1% SDS solution in Tris-EDTA buffer, pH 8.0. The enrichment of DNA template was analyzed by conventional PCR using primers specific for *p57KIP2* proximal promoter (forward: 5'-GCCAATCGCCGTGGTTGTTGT-3'; reverse: 5'-GTGGTGGACTCTTCTGCGTC- 3'). Amplification of *HMOX-1* proximal promoter was performed using a forward primer 5'-GCCAGACTTTGTTTCCCAAGG-3', and a reverse primer 5'-GAGGAGGCAGGCGTTGACTG –3'.

Quantitative Real-Time PCR (qPCR)

Purified immunoprecipitated promoter fragments were analyzed by quantitative real time-PCR (DNA Engine Opticon® 2 Thermal Cycler, MJ Research, Inc.) using SYBR Green I methodology. Amplification reactions were performed as follows; a predenaturation step of 10 min at 95 ^{o}C was followed by 35 cycles of 94 ^{o}C (denaturation) for 10 s, 56 ^{o}C (annealing) for 20 s, 70 ^{o}C (elongation) for 20 s, and a final elongation step of 5 min at 72 ^{o}C.

siRNA transfection

Transfections of SK-N-MC cells were performed using Lipofectamine 2000 (Invitrogen) and a siRNA pool targeting CTIP2 (custom synthesized by Dharmacon). Lipofectamine (60μl) as well as siRNA (60 μl of 15 μM SMARTPOOL or nonspecific siRNA) were pre-incubated in Opti-MEM media for 5 min. After pre-incubation, the two reagents were mixed together and allowed to incubate for additional 20 min. Immediately before transfection, SK-N-MC cells were transferred from DMEM media to Opti-MEM (without serum), and the transfection mix was added dropwise to the plates (siRNA final concentration 100 nM). Four independent plates were used for each condition (CTIP2 siRNA and nonspecific siRNA). After 24 h, the cells were transferred back to DMEM and allowed to incubate for another 24 h prior to harvesting for either RNA preparation or protein isolation (see below).

RNA preparation and microarray analysis

Total RNA was prepared using QIAGEN RNeasy Mini Kit, labeled using the ENZO RNA Transcript Labeling Kit, and used to probe the Affymetrix human microarray chip HG-U133. Results were analyzed using GeneSpring 7.2 (Silicon Genetics) software, and genes that differed from the control by at least two-fold ($p < 0.05$ as determined by 1-way ANOVA), such as *p57KIP2*, were identified, and confirmed to be regulated by CTIP2 by immunoblotting and/or RT-PCR.

Whole cell extract preparation

SK-N-MC cells (from a 100 mm plate at approximately 80% confluence) were lysed with 100 μl of lysis buffer (0.5 M NaCl, 1% Triton X-100, 5 mM EDTA, 5 mM Tris-HCl, pH 7.8) containing a protease inhibitor cocktail. The supernatant was clarified by centrifugation at 16,000 x *g* for 20 min, aliquoted, and stored at –80°C. Extracts were analyzed by western blot.

Results

The Class I and Class II histone Deacetylase inhibitor TSA partially reverses transcriptional repression mediated by Gal4-CTIP2 on a minimal promoter

Gal4-CTIP2 has been previously shown to possess strong, and predominantly TSA-insensitive transcriptional repression activity in the context of the *herpes simplex* thymidine kinase (tk) promoter, which may be due to CTIP2-mediated recruitment of the histone deacetylase SIRT1 to the template (Senawong et al., 2003). In order to determine if the TSA insensitivity of CTIP2-mediated transcriptional repression generalizes to other promoter contexts, we assessed the ability of CTIP2 to mediate repression of a luciferase reporter gene driven by a minimal promoter (Lex-Gal-Luc; Ref.(Christian et al., 2004) in transiently transfected HEK293T cells. Expression of the reporter gene was stimulated by co-expression with LexA-VP16 in order to facilitate evaluation of GAL4-CTIP2-mediated repression. TSA stimulated expression of the reporter gene over seven-fold in the presence of GAL4-DBD (Fig. 2.1*A, lane 2*). Gal4-

CTIP2 strongly repressed expression of the reporter gene (Fig. 2.1*A, lane 3*), as previously described within the tk promoter (Senawong et al., 2003). However, in the context of this minimal promoter, Gal4-CTIP2-mediated repression was found to be partially reversed by TSA (Fig. 2.1*A*, compare *lanes 3* and *4*), indicating the possible involvement of class I and class II histone deacetylases (HDACs).

Deacetylation of Histone H3/H4 Associated with the Reporter Template in Cells Expressing GAL4-CTIP2

Chromatin immunoprecipitation (ChIP) experiments were conducted to determine if transfection of Gal4-CTIP2 resulted in deacetylation of template-associated histones H3 and/or H4. Transfection of Gal4-DBD minimally reduced the level of acetylated H3/H4 associated with the template as determined by both conventional and quantitative PCR (qPCR; Fig. 2.1*B, compare lanes 6* and *8*). This effect was consistent with the lack of transcriptional repression activity of Gal4-DBD observed in reporter assays (data not shown). However, the level of acetylated H3/H4 associated with the template decreased by over four-fold upon transfection with Gal4-CTIP2 as determined by both conventional and qPCR (Fig. 2.1*B*, compare *lanes 6, 8,* and *10*). Together, these findings indicate that transfection of Gal4-CTIP2 resulted in deacetylation of H3/H4 on the template of the minimal promoter.

CTIP2 complexes harbor TSA-sensitive HDAC activity

To determine if TSA-sensitive histone deacetylase activity is associated with CTIP2 complexes in mammalian cells, histone deacetylase activity assays were performed *in vitro* using whole cell lysates from HEK293T cells, which had been transiently transfected with an expression vector encoding FLAG-CTIP2 or the corresponding empty vector. Immunoprecipitates of FLAG-CTIP2 complexes indeed harbored HDAC activity that was nearly ten-fold greater than that observed with control immunoprecipitates (Fig. 2.2*A*, *lanes 1* and *3*). Inclusion of TSA in the *in vitro* assay completely abolished the *in vitro* HDAC activity of FLAG-CTIP2 immunoprecipitates (Fig. 2.2*A*, compare *lanes 1, 2* and *3*). To investigate if complexes containing CTIP2 harbor TSA-sensitive histone deacetylase activity in a more natural cellular context, the HDAC activity assays were performed similarly as above on nuclear extracts derived from SK-N-MC human neuroblastoma cells, which like Jurkat cells (Senawong et al., 2003), endogenously express two splice variants of CTIP2 (see Fig. 2.3*B* below). CTIP2 complexes from SK-N-MC cells possessed robust HDAC activity (Fig. 2.2*B*, *lane 1*). In contrast, the immunoprecipitation performed with an irrelevant antibody (anti-HA) exhibited only negligible amounts of HDAC activity (Fig. 2.2*B*, *lane 3*). As observed in transfected HEK293T cells, TSA completely inhibited HDAC activity in CTIP2 immunoprecipitates from SK-N-MC cells (Fig. 2.2*B*, compare *lanes 1* and *2*). These data suggest that class I and/or class II HDACs mediate the TSA-sensitive HDAC activity that is associated with CTIP2 complexes *in vitro*. It is important to note that the HDAC activity assays reported herein were performed

without addition of NAD^+, a cofactor that is required for deacetylation mediated by SIRT1 (Smith et al., 2000; Bitterman et al., 2002), a class III HDAC that interacts with CTIP2 in HEK293 and Jurkat cells (Senawong et al., 2003). Thus, the HDAC activity of CTIP2 immunoprecipitates that we observed in the present studies was most likely due to the catalytic activity of class I and/or class II HDACs. We have not observed either NAD^+-stimulated or nicotinamide-inhibited HDAC activity in CTIP2 immunoprecipitates from SK-N-MC cells under the conditions used herein (data not shown). However, we cannot exclude the possibility that SIRT1 may also contribute to HDAC activity of CTIP2 complexes in cells. Indeed, we note that TSA only reversed a fraction of transcriptional repression mediated by GAL4-CTIP2 in transiently transfected HEK293T cells (Fig. 2.1*A*, *lanes 3* and *4*).

CTIP2 associates with the NuRD complex in HEK293T cells

CTIP2 has been recently demonstrated to interact with the NuRD complex in Jurkat cells (Cismasiu et al., 2005). To investigate the physical association between CTIP2 and components of the NuRD complex in HEK293T cells, immunoprecipitation (IP) experiments were performed on whole cell extracts from cells overexpressing FLAG-CTIP2. As expected, Mi-2α/β and HDAC2 were co-immunoprecipitated with MTA2 by an anti-MTA2 antibody in the absence of FLAG-CTIP2 expression (Fig. 2.3*A*, *lane 4*). MTA1 was also detected in MTA2 immunoprecipitates (Fig. 2.3*A*, *lanes 4* and *6*) and this was due to the cross-reactivity of the anti-MTA2 antibody used in

immunoprecipitation and/or immunoblotting procedures. However, none of these proteins was co-immunoprecipitated by an irrelevant antibody (anti-HA, Fig. 2.3*A*, *lane 3*). Overexpressed FLAG-CTIP2 was co-immunoprecipitated with MTA2 and the other NuRD components by the anti-MTA2 antibody (Fig. 2.3*A*, *lane 6*), but not by anti-HA antibody (*lane 5*), suggesting that FLAG-CTIP2 associates with the NuRD complex in transiently transfected HEK293T cells. It is interesting to note that upon overexpression of FLAG-CTIP2 in HEK293T cells, we observed substantially decreased expression of MTA1, MTA2 and Mi-2α/β, but not of HDAC2 (Fig. 2.3*A*, compare *lanes 1* and *2*). In addition, we observed significantly less Mi-2α/β in the NuRD complexes when CTIP2 was overexpressed (Fig. 2.3*A*, compare *lanes 4* and *6* of *first panel*). Although we do not know yet the mechanism for this effect, we speculate that Mi-2α/β, MTA1, and MTA2, but not HDAC2, may be direct or indirect targets of CTIP2-mediated transcriptional repression in HEK293T cells. It is also possible that CTIP2 may be a general repressor of transcription in HEK293T cells, although this is not consistent with the lack of effect of CTIP2 on expression of HDAC2. (Fig. 2.3*A*, compare *lanes 1* and *2* of *last panel*). These data clearly demonstrate that NuRD complex proteins interact with CTIP2 either directly or indirectly in transfected HEK293T cells.

CTIP2 associates with the NuRD complex in SK-N-MC Cells

The co-IP results shown above were performed using transiently transfected cells overexpressing CTIP2. However, it is important to verify association of CTIP2 with the NuRD complex when expressed at physiological levels, and in untransfected cells. To assess these possibilities, IP experiments were performed using nuclear extracts derived from SK-N-MC cells. Endogenous MTA2, HDAC2, RbAp46/48, and to some extent Mi-2α/β, were co-immunoprecipitated with CTIP2 by an anti-CTIP2 antisera (Fig. 2.3*B*, *lane 3*), but not by an irrelevant antibody (anti-HA, *lane 7*). The results from reciprocal experiments revealed that endogenous CTIP2 was efficiently co-immunoprecipitated by anti-MTA2, -Mi-2α/β, -HDAC2, and -RbAp46/48 antibodies (second panel of Fig. 2.3*B*, *lanes 2, 4, 5,* and *6*, respectively), but not by an anti-HA antibody (*lane 7*). These findings indicate that endogenous CTIP2 stably associates with the NuRD complex when expressed at physiological levels in SK-N-MC neuroblastoma cells.

To determine the mass of native CTIP2 complexes in SK-N-MC cells, nuclear extracts were fractionated on a Superose 6 size-exclusion column. CTIP2 immunoreactivity eluted from the Superose 6 column as a relatively symmetrical peak centered between 669 and ~ 1000 kDa. (Fig. 2.4*A*, and *first panel* of Fig. 2.4*B*, *fractions 13-33*). The elution pattern of CTIP2 appeared to overlap that of some NuRD complex proteins including MTA2, HDAC1, and HDAC2. (*third, fourth, and fifth panels* of Fig. 2.4*B*), but only partially overlapped that of Mi-2α/β (*second panel*). The partial co-elution of Mi-2α/β with CTIP2 and other NuRD proteins may explain, at least in

part, why Mi-2α/β was weakly detected in anti-MTA2, -CTIP2 and -HDAC2 immunoprecipitates from SK-N-MC nuclear extracts (Fig. 2.3*B*, *lanes 2, 3,* and *5*). These size-exclusion chromatography results demonstrated that native CTIP2 in SK-N-MC cells eluted with an apparent mass greater than that of the monomeric protein for the two relevant CTIP2 splice variants (95.5 and 88.5 kDa, respectively), consistent with the possibility that CTIP2 exists within a large complex in SK-N-MC cells. Moreover, the partial co-elution of CTIP2 with most NuRD complex proteins further confirms the interaction of CTIP2 with this complex, which was maintained through a high salt extraction and size-exclusion chromatography.

CTIP2 interacts directly with RbAp46 and RbAp48 in vitro

The co-IP results demonstrated that CTIP2 associated with the NuRD complex both in transfected and untransfected cells. To determine the component(s) of the NuRD complex with which CTIP2 may interact directly, IP assays were conducted using lysates of SF9 cells infected with recombinant baculoviruses directing the expression of individual components of the NuRD complex and [^{35}S]-labeled FLAG-CTIP2. FLAG-CTIP2 was found to interact strongly with RbAp46 and RbAp48 (Fig. 2.5*A*, *lanes 7* and *8*), but not with other components of the NuRD complex tested (Fig. 2.5*A*, *lanes 3-6*). This interaction is most likely specific as FLAG-CTIP2 was not immunoprecipitated by non-specific IgG (a negative control; Fig. 2.5*A*, *lane 2*). The efficiency of the IP reactions was confirmed by immunoblotting with cognate

antibodies (Fig. 2.5*B*). These results indicate that CTIP2 interacts directly with RbAp46 and RbAp48 *in vitro*.

Next, GST pull-down assays were performed to map RbAp46- and RbAp48-interaction interfaces of CTIP2. CTIP2 deletion mutants containing amino acids 129-350 strongly interacted with both GST-RbAp46 (Fig. 2.5*C*, *lanes 8, 9,* and *11*) and GST-RbAp48 (*lane 15, 16,* and *18*), but not with GST alone (data not shown for simplicity). Deletion mutants of CTIP2 lacking this region weakly interacted (Fig. 2.5*C*, *lanes 12-14*, and *19-21*, respectively), or did not interact at all (*lanes 10* and *17*, respectively) with GST-RbAp46 and GST-RbAp48. As CTIP2-(129-350) interacted strongly (Fig. 2.5*C*, *lanes 11* and *18*, respectively), whereas CTIP2-(171-350) interacted more weakly (Fig. 2.5*C*, *lanes 12* and *19*, respectively) with GST-RbAp46 and -RbAp48, amino acids 129-171 of CTIP2 are likely to be important for mediating interaction with GST-RbAp46 and -RbAp48. Accordingly, we tested the interaction between CTIP2-(129-171) and GST-RbAp46 and -RbAp48. To our surprise, we did not observe appreciable interaction of this CTIP2 fragment and RbAp proteins (data not shown). However, these results indicate that CTIP2-(129-350), a region including a C_2H_2 zinc finger motif and also a proline-rich domain (Avram et al., 2000), appears to be primarily responsible for interaction of CTIP2 with RbAp46 and RbAp48 *in vitro*.

GAL4-CTIP2 recruits the NuRD complex to the promoter template

CTIP2 represses transcription and is associated with TSA-sensitive histone deacetylase activity *in vitro* and in cells, which may be conferred by components of the NuRD complex, such as HDAC1 and/or HDAC2 (Xue et al., 1998; Zhang et al., 1999). However, the NuRD complex must be recruited to a CTIP2-responsive promoter in a CTIP2-dependent manner in order to play a role in transcriptional repression mediated by this repressor. To investigate this directly, ChIP experiments were performed in HEK293T cells that had been co-transfected with the Lex-Gal-Luc reporter (the same reporter construct used in Fig. 2.1), and either Gal4-DBD or Gal4-CTIP2. The presence of Gal4-CTIP2 on this template was confirmed by ChIP (data not shown). We found that Lex-Gal-Luc reporter template was immunoprecipitated by anti-MTA2, -RbAp46/48, and -HDAC2 antibodies in the manner that was stimulated by co-expression of Gal4-CTIP2 (Fig. 2.6*A*, compare *lane 7* to *lane 5* of *all panels*). In contrast, very little template was mock-immunoprecipitated (Fig. 2.6*A*, *lanes 4* and *6* of *all panels*). These results suggest that MTA2, RbAp46/48, and HDAC2 are recruited to the promoter template of this transfected reporter in a CTIP2-dependent manner. This effect was specific to the promoter template, as expression of Gal4-CTIP2 did not affect the enrichment of MTA2, RbAp46/48, and HDAC2 on the *GAPDH* promoter (Fig. 2.6*B*). The results of these experiments demonstrate that CTIP2 recruits endogenous NuRD complex proteins to the promoter template of a transfected reporter gene in HEK293T cells, suggesting that the NuRD complex may potentially play a role in CTIP2-mediated transcriptional repression.

Identification of CTIP2 target genes in SK-N-MC cells

SK-N-MC human neuroblastoma cells express high levels of two splice variants of CTIP2 (Fig. 2.3*B*), but undetectable levels of CTIP1 (data not shown). Therefore, these cells were chosen as a model system for the identification of CTIP2 target genes in a neuron-like context, without the potentially confounding effects of complementation by CTIP1. Transcriptome analyses were performed on SK-N-MC cells that had been transfected with CTIP2-specific ($CTIP2^{KD}$) or mock ($CTIP2^{Mock}$) siRNAs. The microarray analyses confirmed that CTIP2 knockdown was achieved in $CTIP2^{KD}$ cells (~60% knockdown at the mRNA level; compare *lanes 1* and *2* of Fig. 2.7*A*; see also immunoblot in *top panel* of Fig. 2.7*B*). The expression of a number of genes was increased in the $CTIP2^{KD}$ relative to $CTIP2^{Mock}$ cells, consistent with the previously described role of CTIP2 as a repressor of transcription (Avram et al., 2000; Avram et al., 2002; Senawong et al., 2003). Four of these genes, which have been confirmed as CTIP2 target genes at the mRNA and/or protein levels (data not shown), are listed in Table 1.1. These genes are *heme oxygenase-1* (HMOX-1), fibronectin-1 (FN-1), cadherin-10, and p57KIP2. In light of the neuronal phenotype of $CTIP2^{-/-}$ mice, i.e., defective axonal projections of CSMN (Arlotta et al., 2005), it is of interest that two of these genes encode proteins involved in the function of the extracellular matrix. For the purposes of this manuscript, we chose to focus on *p57KIP2*, which encodes a cyclin-dependent kinase inhibitor belonging to the CIP/KIP family (Cunningham and Roussel, 2001). Affymetrix microarray analyses revealed that the

expression of *p57KIP2* was increased 4-fold in CTIP2^{KD} cells (compare *lanes 3* and *4* of Fig. 2.7*A*), and this, as well as knockdown of CTIP2 protein, was confirmed at the protein level (Fig. 2.7*B*, compare *lanes 1* and *2* of *middle panel*).

Induction of *p57KIP2* expression was also observed at the protein level in cells treated with the HDAC inhibitor, TSA (Fig. 2.7C, compare *lanes* 1 and 2), consistent with the hypothesis that TSA-sensitive HDACs, such as those present within the NuRD complex, may be involved in dictating the basal expression of *p57KIP2* in SK-N-MC cells.

p57KIP2 is a direct target of CTIP2 in SK-N-MC cells

As the *p57KIP2* proximal promoter region contains several putative CTIP2 binding sites (Fig. 2.8*A*), ChIP experiments were carried out to determine if CTIP2 is bound to this promoter in SK-N-MC cells. CTIP2 was found to associate strongly with *p57KIP2* promoter, but not with that of *heme oxygenase-1* (*HMOX-1;* Fig. 2.8*B*), even though the latter contains multiple consensus CTIP2 binding sites, and was similarly identified as an induced gene in our transcriptome analyses of CTIP2^{KD} cells (Table 1.1 and data not shown). Although we found that CTIP2 did not associate with the promoter region of HMOX-1 we tested (see materials and methods), we cannot exclude the possibility that CTIP2 may associate with other upstream or downstream regulatory regions of *HMOX-1,* and/or CTIP2 may regulate *HMOX-1* expression indirectly via a mechanism(s) that remains to be investigated. These findings

demonstrate that endogenously expressed CTIP2 in SK-N-MC cells is associated with the *p57KIP2* promoter either directly or indirectly. In light of the transcriptome analyses of CTIP2^{KD} cells, we hypothesize that transcriptional repression is the functional outcome of the interaction of CTIP2 with this promoter template.

In transient transfection experiments with the Lex-Gal-Luc reporter gene, we showed that components of the NuRD complex were recruited to the promoter template upon co-expression with Gal4-CTIP2 (Fig. 2.6). Therefore, we looked for the presence of the NuRD complex on the promoter of *p57KIP2* gene in untransfected SK-N-MC cells by ChIP/re-ChIP analyses. Soluble chromatin was immunoprecipitated with the anti-CTIP2 antibody; immune complexes were released and then subjected to a second immunoprecipitation with the antibodies against different components of the NuRD complex, namely MTA2, HDAC2 and RbAp46/48. Of these proteins, MTA2 appears to be specific for and define the presence of the NuRD complex (Avram et al., 2000; Avram et al., 2002; Senawong et al., 2003), and our re-ChIP analyses demonstrated the association of MTA2 and CTIP2 with the same fragment of *p57KIP2* promoter (*upper panel of* Fig. 2.8C), but not with the *HMOX-1* promoter (*lower panel* of Fig. 2.8C). These findings demonstrate that CTIP2 and the NuRD complex co-occupy the *p57KIP2* promoter. To establish this further, we performed re-chip analyses with CTIP2 and two additional NuRD complex proteins, HDAC2 and RbAp46/48. HDAC2 and RbAp46/48 were both found to co-occupy the promoter of *p57KIP2* (*upper panels* of Fig. 2.8 D and E) but not that of *HMOX-1* (*lower panels* of

Fig. 2.8D and E) with CTIP2. Given our findings that CTIP2 and several components of the NuRD complex (MTA2, HDAC2, RbAp46/48) co-occupy the proximal promoter region of *p57KIP2*, and that CTIP2 and RbAp46/48 interact directly (Fig. 2.5), we conclude that CTIP2 recruits the NuRD complex to the *p57KIP2* template resulting in transcriptional repression of this gene under basal conditions.

Discussion

Previously, CTIP1 and CTIP2 were demonstrated to repress transcription in a predominantly TSA-insensitive manner, possibly due to recruitment of SIRT1 to CTIP1/2-responsive promoters, at least in transiently transfected cells, and in the context of the *tk* promoter (Avram et al., 2000; Avram et al., 2002; Senawong et al., 2003; Senawong et al., 2005). However, in the context of the minimal promoter, we found herein that transcriptional repression mediated by CTIP2 was partially sensitive to inhibition by TSA (see Fig. 2.1), suggesting that TSA-insensitive, SIRT1-mediated histone deacetylation may not necessarily generalize to all CTIP2-responsive promoters and/or cell types. Other transcriptional repressors have been similarly found to function in TSA-sensitive and –insensitive manners, as well as in a cell- and promoter-dependent contexts. For example, the retinoblastoma tumor suppressor protein (Rb) represses expression of *Cdc2, topoisomerase IIα, and thymidylate synthase* in a TSA-sensitive manner, but Rb-mediated repression of *cyclin A* is not

reversed by TSA, demonstrating that the mechanism of Rb-mediated transcriptional repression is promoter-specific (Siddiqui et al., 2003). Similarly, RE-1 silencing transcription factor (REST)-mediated repression of *connexin36* was found to be reversible by TSA, whereas that of the two other REST target genes, *BDNF* and *GluR2*, was not (Hohl and Thiel, 2005). Moreover, REST-mediated repression of *connexin36* was TSA-sensitive only in pancreatic α and β cells, but not in neuronal cells, indicating that REST represses transcription in both promoter- and cell type-specific manners (Hohl and Thiel, 2005). The differential responses of promoters and cell types to TSA may be an important scheme for transcriptional repressors, perhaps including CTIP2, to function in transcriptional regulation. In addition to TSA-sensitive and NAD^+-dependent HDACs, histone and DNA methylation may also be involved in transcriptional repression (Blander and Guarente, 2004; Wang et al., 2004). As we did not observe complete inhibition of CTIP2-mediated repression by TSA in our present studies, we cannot exclude the possibility that CTIP2 may use other mechanism(s), in addition to TSA-sensitive histone deacetylation, to repress transcription in the context of the minimal promoter.

The CTIP2 complex in from SK-N-MC cells appeared to migrate with a peak centered between 669 to 1000 kDa (see Fig. 2.4). In contrast, the size of CTIP2 complex in Jurkat cells was found be up to 2000 kDa (Senawong et al., 2003). Although we found that the NuRD complex proteins co-fractionated with CTIP2 in Jurkat cells (data not shown), the difference in apparent masses of the CTIP2

complexes in these two cell types possibly suggests differing compositions of CTIP2 complexes, which may be of functional significance.

The components of the NuRD complex were recruited to a CTIP2-targeted promoter in a CTIP2-dependent manner (see Fig. 2.6), and were found to co-occupy the promoter of an endogenous CTIP2-target gene in SK-N-MC neuroblastoma cells (see Fig. 2.8). This recruitment is likely mediated by the direct interaction of CTIP2 with the histone binding proteins, RbAp46 and/or RbAp48 (see Fig. 2.5). Additionally, many other transcription factors involved in transcriptional repression have been reported to interact with different subunits of the NuRD complex (Kehle et al., 1998; Kim et al., 1999; Luo et al., 2000; Murawsky et al., 2001; Schultz et al., 2001; Fujita et al., 2004; Hong et al., 2005), suggesting the possibility that the NuRD complex is involved in many pathways leading to transcriptional repression. However, it is presently unknown if the potentially differential recruitment of the NuRD complex to a particular, nucleating transcription factor may result in the formation of a gene-specific repressor complex(es).

Extensive studies of the biological function of the NuRD complex have shown that the components of this complex are required for morphogenesis of *Drosophila* (Kehle et al., 1998), embryonic patterning, vulva development and signaling in *Caenorrhabditis elegans* (Solari et al., 1999; von Zelewsky et al., 2000), and mouse embryogenesis (Hendrich et al., 2001). In combination with the data from RT-PCR analysis illustrating the expression of MBD3, Mi2, HDAC1, and HDAC2 from a very

early stage of embryonic development (Kantor et al., 2003), transcriptional silencing by the NuRD complex may play a significant role in embryonic development in many species ranging from nematodes to mammals. In addition, recent reports revealed an important role of the NuRD complex in control cell fate determination during B and T cell development (Fujita et al., 2004; Williams et al., 2004).

The crucial function of CTIP2 in the context T cell development, as well as in the development of corticospinal motor neurons (CSMN), suggests that this protein may play a global role during mammalian development. As both CTIP2 and the NuRD complex appear to play significant, and possibly convergent, roles in cell fate determination and differentiation, association of CTIP2 with this complex raises the possibility that the histone deacetylase and chromosome remodeling activities of the NuRD complex may be implicated in regulation of both T cell and CSMN specification and development by CTIP2. This hypothesis may be tested in vivo by analysis of compound mutant mice.

The cyclin-dependent kinase (cdk) inhibitor *p57KIP2* was newly identified in this report as one of the putative CTIP2 target genes in SK-N-MC neuroblastoma cells. The cdk inhibitor p57KIP2 is a putative tumor suppressor, and has the ability to associate with and inhibit the catalytic activity of a number of cyclin-cdk complexes (Cunningham and Roussel, 2001). The human *p57KIP2* gene is paternally imprinted in both humans and mice, and the human *p57KIP2* locus is on chromosome 11p15, a

region that has been implicated in various sporadic human malignancies, and also in Beckwith-Wiedemann syndrome (Matsuoka et al., 1995).

Several studies suggest that p57KIP2 plays a distinct role in neuronal differentiation, which may or may not be related to the function of this protein as a cdk inhibitor. During embryogenesis, *p57KIP2* is expressed in mitotic progenitor cells that migrate away from retinal ventricular zone, and in this context p57KIP2 appears to be required for proper exit from cell cycle (Dyer and Cepko, 2000). Postnatally, however, *p57KIP2* is expressed in a restricted population of amacrine neurons, and it has been proposed that p57KIP2 can influence cell fate specification and differentiation long after terminal mitosis (Dyer and Cepko, 2000). In addition, p57KIP2 is expressed in postmitotic differentiating midbrain dopaminergic neurons and is required for the maturation of these cells (Joseph et al., 2003). Interestingly, the mechanism by which p57KIP2 promotes maturation of dopaminergic neuronal cells does not require cdk inhibitor activity but rather is achieved through the direct protein-protein interaction of p57KIP2 with orphan nuclear receptor Nurr1 (Joseph et al., 2003).

The likely recruitment of the NuRD complex to the promoter of *p57KIP2* via direct interaction with CTIP2 suggests that the NuRD complex plays a role in transcriptional repression mediated by CTIP2 in a neuron-like context. At present, we do not know if CTIP2 directly regulates expression of *p57KIP2* within neuronal subpopulations in vivo, or the possible contribution of the NuRD complex to this and

other CTIP2-mediated transcriptional repressive events. Further studies employing the power of *Ctip2*$^{-/-}$ mice are necessary to clarify role(s) of this protein and the corresponding transcriptional repression pathway(s) *in vivo*.

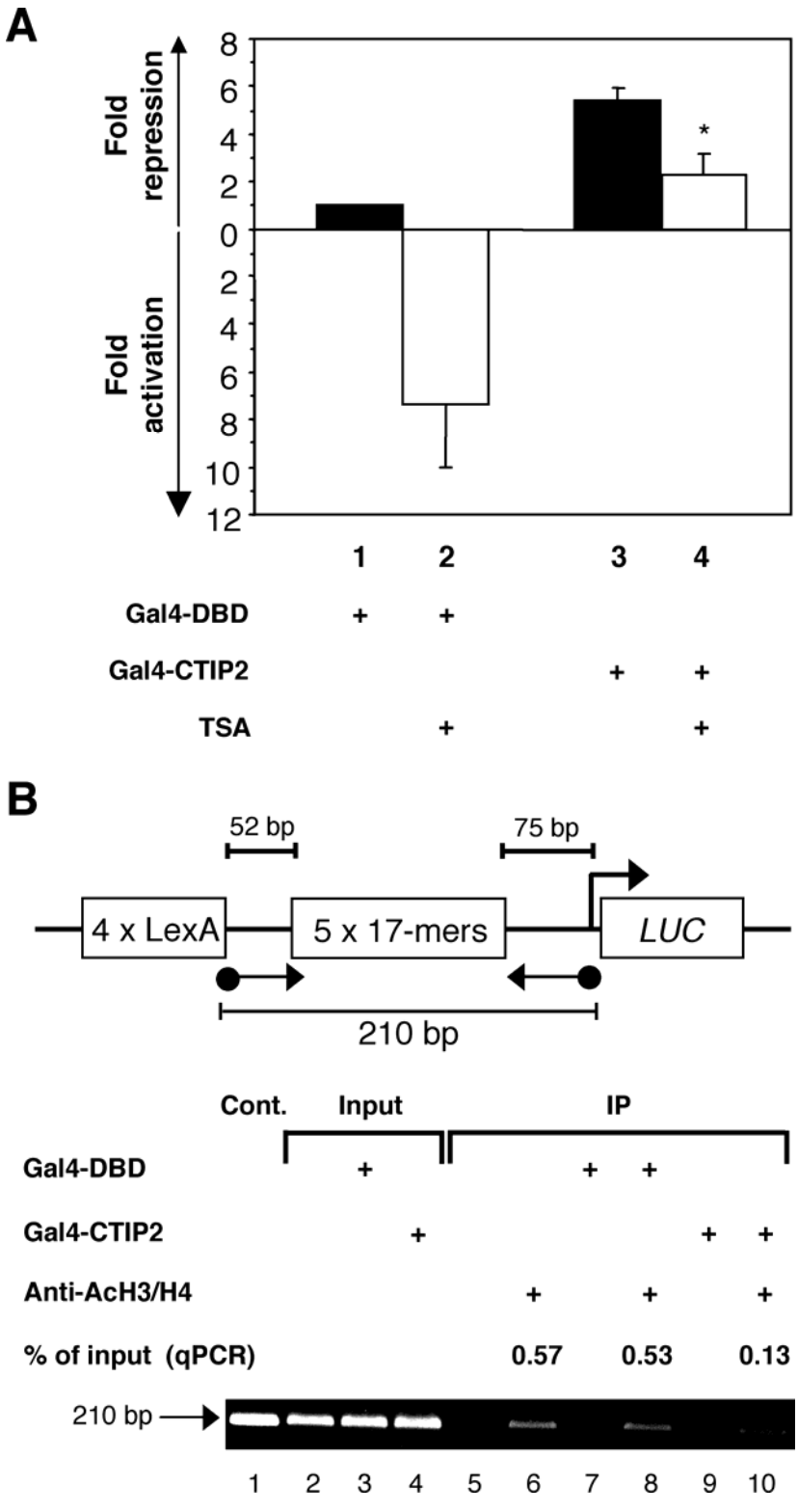
A
Fold repression
Fold activation
8
6
4
2
0
2
4
6
8
10
12
*
1
2
3
4
Gal4-DBD + +
Gal4-CTIP2 + +
TSA + +
B
52 bp
75 bp
4 x LexA
5 x 17-mers
LUC
210 bp
Cont.
Input
IP
Gal4-DBD + + +
Gal4-CTIP2 + + +
Anti-AcH3/H4 + + +
% of input (qPCR) 0.57 0.53 0.13
210 bp
1 2 3 4 5 6 7 8 9 10

Figure 2.1. CTIP2-mediated transcriptional repression of a minimal promoter is partially reversed by TSA.

A, HEK293T cells were co-transfected with 3 μg of Lex-Gal-Luc reporter, 0.1 μg of LexA-VP16 and either 1 μg of Gal4-DBD or Gal4-CTIP2 using the calcium phosphate method. Twenty-four h after transfection, cells were treated with TSA (100 ng/ml; *open bars*) or vehicle (*solid bars*) as indicated for 24 h prior to harvesting for luciferase reporter assays. Light units were normalized across all samples by protein concentration and expressed as fold-repression or fold-activation relative to lane 1 (Gal4-DBD). The data shown here represent the mean fold-repression or -activation ± S.E.M. derived from three independent experiments. Statistical significance is indicated by asterisk ($p < 0.05$, Student's *t* test) when comparing lane 4 to lane 3.

B, *(Upper)* Schematic diagram of a Lex-Gal-Luc reporter illustrating LexA and Gal4 (17-mer) binding sites, which are upstream of *LUC.* Arrows represent positions of forward and reverse primers for PCR amplification shown in the lower panel. The size of PCR product (210 bp) present in the lower panel is indicated. (*Lower*) ChIP assays were performed on HEK293T cells following transient transfection as described above. *Lane 1* corresponds to a template control in which a reporter plasmid was used directly in the amplification reaction. Inputs in *lanes 2-4* were 5% of total amount of template used in the reactions. *Lanes 5-10* represent template amplification reactions from samples immunoprecipitated (IP) with or without antibodies specific for acetylated histone H3 and H4 as indicated. The numbers above *lanes 6, 8, and 10* represent quantification of the template present, expressed as percent of input, as determined by qPCR. Results are representative of three independent experiments.

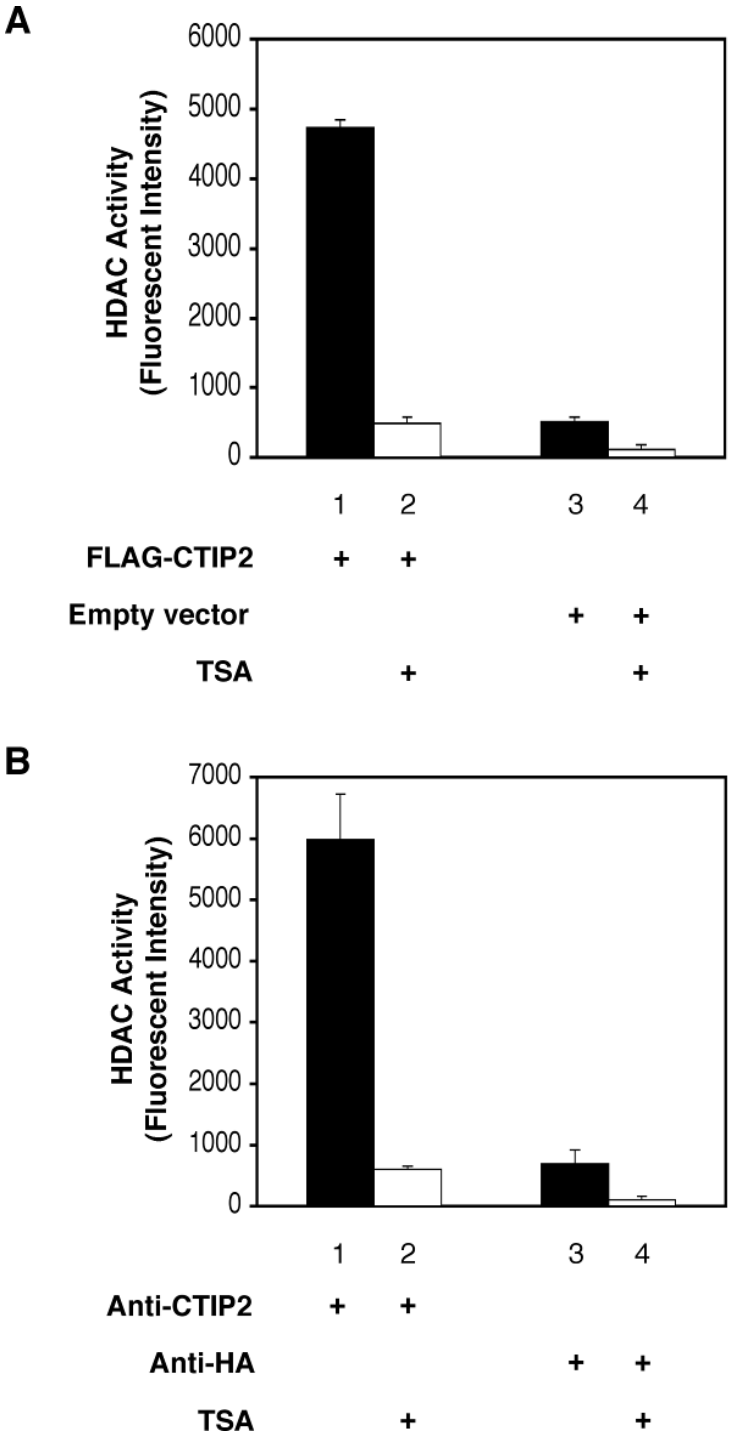
A
HDAC Activity
(Fluorescent Intensity)
6000
5000
4000
3000
2000
1000
0
1 2 3 4
FLAG-CTIP2 + +
Empty vector + +
TSA + +
B
HDAC Activity
(Fluorescent Intensity)
7000
6000
5000
4000
3000
2000
1000
0
1 2 3 4
Anti-CTIP2 + +
Anti-HA + +
TSA + +

Figure 2.2. CTIP2 complexes harbor TSA-sensitive HDAC activity *in vitro*.

A, HEK293T cells were transiently transfected with a eukaryotic expression vector encoding FLAG-CTIP2 or the corresponding empty vector as indicated. Immunoprecipitations (IPs) were performed on whole cell extracts using an anti-FLAG antibody and the immunoprecipitates were assayed for histone deacetylase activity in the presence (*lane 2*) or absence (*lane 1*) of TSA (0.25 μM). An irrelevant antibody (anti-HA) was used as a control (*lanes 3* and *4*).
B, HDAC activity assays performed on CTIP2 immunoprecipitates from SK-N-MC nuclear extracts in the presence (*lane 2*) or absence (*lane 1*) of TSA (0.25 μM). An anti-HA was again used as a control in these experiments (*lanes 3* and *4*). Relative HDAC activities present in *A and B* represent the mean (± S.E.M.) fluorescent intensity values derived from three independent experiments.

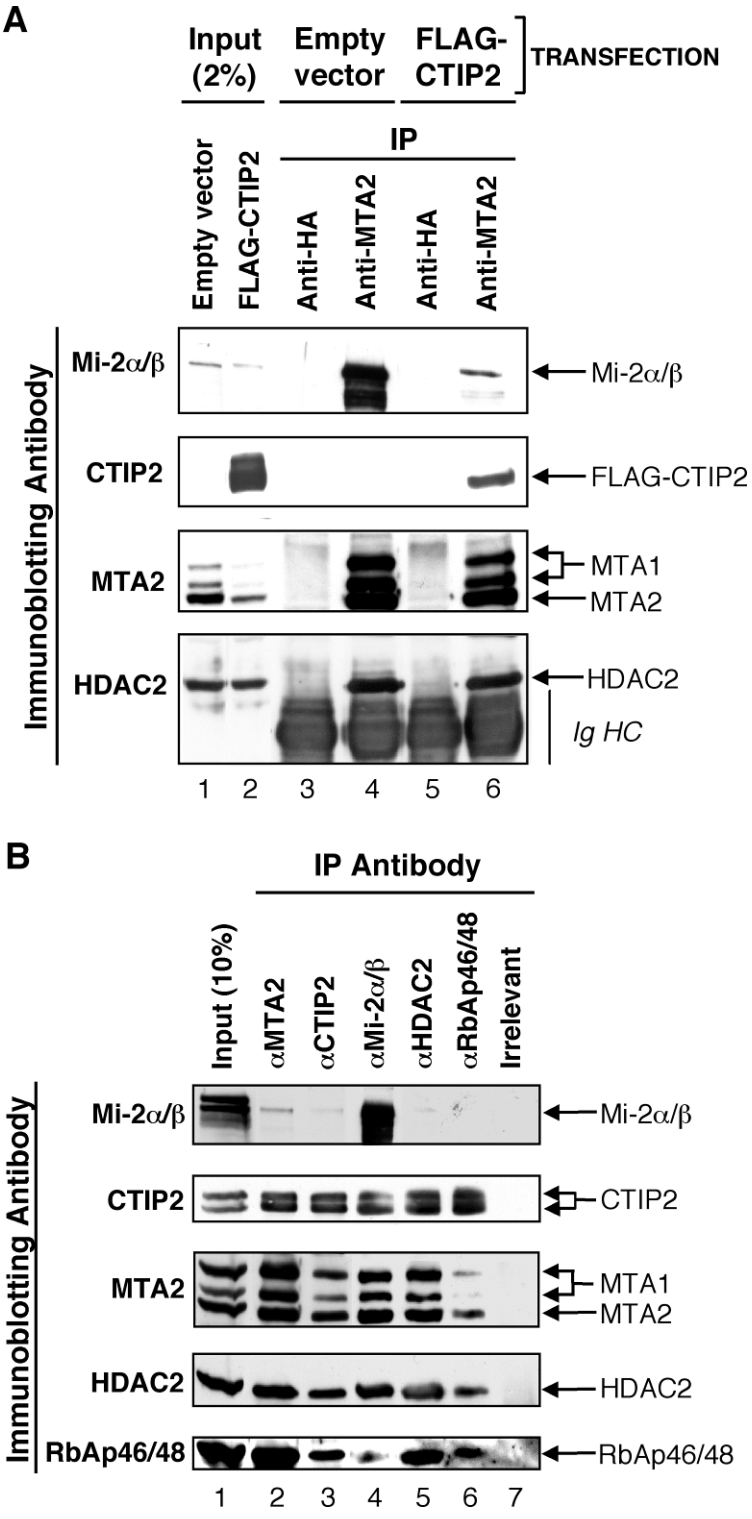
A
Input (2%)
Empty vector
FLAG-CTIP2
TRANSFECTION
IP
Empty vector
FLAG-CTIP2
Anti-HA
Anti-MTA2
Anti-HA
Anti-MTA2
Immunoblotting Antibody
Mi-2α/β
CTIP2
MTA2
HDAC2
Mi-2α/β
FLAG-CTIP2
MTA1
MTA2
HDAC2
Ig HC
1 2 3 4 5 6
B
IP Antibody
Input (10%)
αMTA2
αCTIP2
αMi-2α/β
αHDAC2
αRbAp46/48
Irrelevant
Immunoblotting Antibody
Mi-2α/β
CTIP2
MTA2
HDAC2
RbAp46/48
Mi-2α/β
CTIP2
MTA1
MTA2
HDAC2
RbAp46/48
1 2 3 4 5 6 7

Figure 2.3. Coimmunoprecipitation of CTIP2 with components of the NuRD complex.

A, FLAG-CTIP2 associates with endogenous NuRD complex in transfected HEK293T cells. Whole cell extracts from HEK293T cells transiently transfected with 10 μg of an expression vector encoding FLAG-CTIP2 or the corresponding empty vector were immunoprecipitated with an irrelevant (anti-HA) or anti-MTA2 antibody as indicated. Immunoprecipitates were subjected to SDS-PAGE and immunoblotting using the indicated antibodies. FLAG-CTIP2 was immunoprecipitated by anti-MTA2 antibody and detected by an anti-CTIP2 monoclonal antibody (25B6). Both MTA1 and MTA2 were detected by the anti-MTA2 antibody as indicated. The positions of Mi-2-α/β, FLAG-CTIP2, MTA1, MTA2 and HDAC2 are indicated. Ig HC = Immunoglobulin heavy chain.
B, Association of endogenous CTIP2 with the NuRD complex in SK-N-MC cells. Nuclear extracts from SK-N-MC cells were immunoprecipitated with the indicated antibodies. Immunocomplexes were resolved by SDS-PAGE and analyzed by western blotting using the indicated antibodies. The antibody used for IP and immunoblotting of CTIP2 was anti-CTIP2 antisera. The positions of Mi-2α/β, two splice variants of CTIP2, MTA1, MTA2, HDAC2 and RbAp46/48 are indicated.

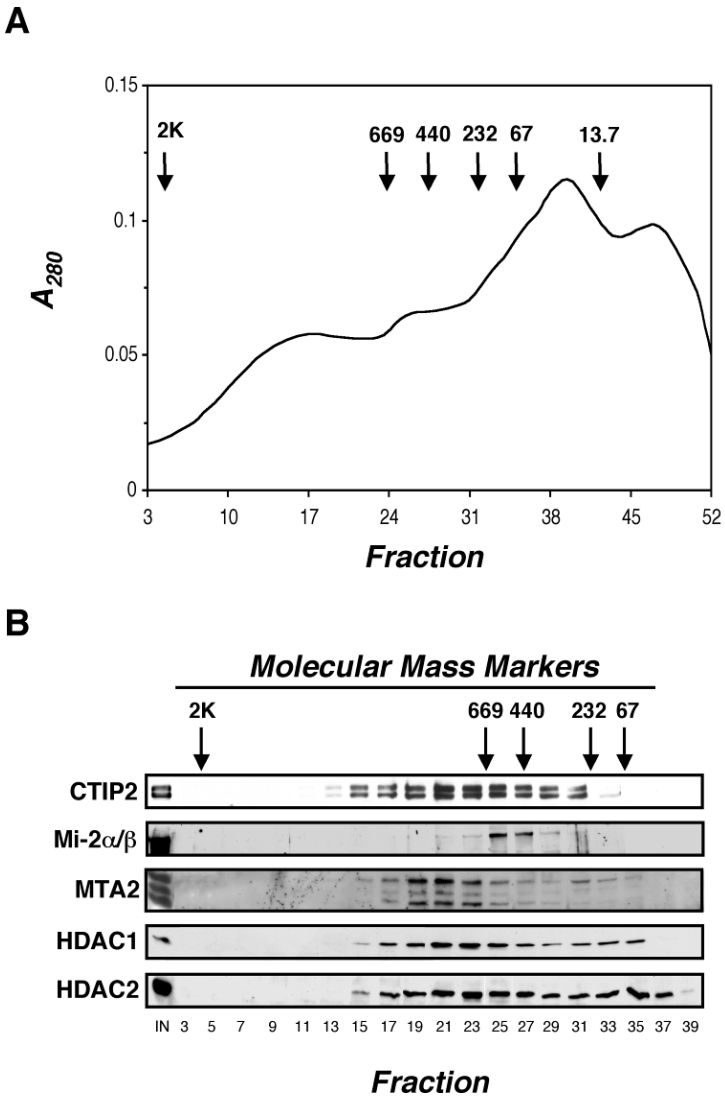

Figure 2.4. Co-fractionation of CTIP2 and components of NuRD complex on a Superose 6 size-exclusion column.

A-B, Fractionation of nuclear extracts from SK-N-MC cells on a Supersoe 6 size-exclusion column.

A, The chromatographic elution profile.

B, Analysis of chromatographic fractions by immunoblotting (equal volumes from each fractions were analyzed; IN = 30 μg of nuclear extract protein as input, and fraction numbers are also indicated). The elution positions of calibrating proteins of known molecular weights (kDa) are indicated by downward arrows in both *A and B*.

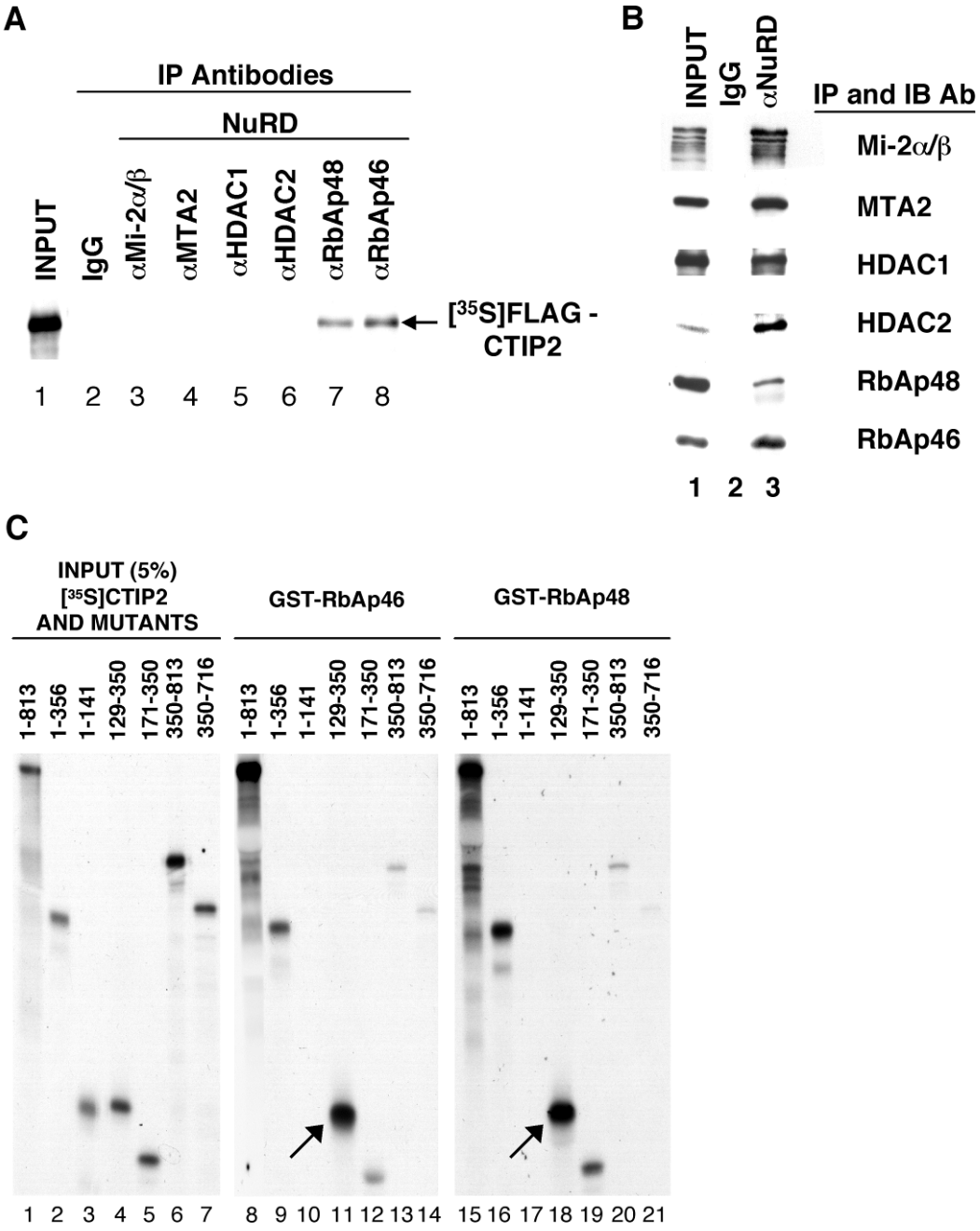
A
IP Antibodies
NuRD
INPUT
IgG
αMi-2α/β
αMTA2
αHDAC1
αHDAC2
αRbAp48
αRbAp46
[35S]FLAG - CTIP2
1 2 3 4 5 6 7 8
B
INPUT
IgG
αNuRD
IP and IB Ab
Mi-2α/β
MTA2
HDAC1
HDAC2
RbAp48
RbAp46
1 2 3
C
INPUT (5%) [35S]CTIP2 AND MUTANTS
GST-RbAp46
GST-RbAp48
1-813
1-356
1-141
129-350
171-350
350-813
350-716
1 2 3 4 5 6 7 8 9 10 11 12 13 14 15 16 17 18 19 20 21

Figure 2.5. CTIP2 interacts directly with RbAp46 and RbAp48 *in vitro*.

A-B, *In vitro* translated and [^{35}S]Met-labeled, full-length FLAG-CTIP2 was mixed with SF9 cell extracts containing individual recombinant NuRD complex proteins and these mixtures were immunoprecipitated with antibodies against the NuRD complex proteins, or non-specific antibody (IgG), as indicated.
A, Immunoprecipitates were resolved by SDS-PAGE and the presence of [^{35}S]Met-labeled FLAG-CTIP2 was determined by autoradiography (*lanes 2-8*). Input [^{35}S]Met-labeled FLAG-CTIP2 is shown in *lane 1.*
B, Controls demonstrating efficiency of immunoprecipitation reactions. All NuRD complex proteins were efficiently immunoprecipitated by cognate antibodies. ***C**, In vitro* translated and [^{35}S]Met-labeled, full-length CTIP2 and truncation mutants were incubated with equivalent amounts of bacterially expressed GST-RbAp46 (*lanes 8-14*) and GST-RbAp48 (*lanes 15-21*) fusion proteins or GST (*data not shown for simplicity*). After extensive washing, [^{35}S]Met-labeled CTIP2 associated with the affinity resin was resolved by SDS-PAGE and visualized by autoradiography. *Arrows* indicate strong interaction between [^{35}S]Met-labeled CTIP2-(129-350) and GST-RbAp46, -RbAp48 fusion proteins.

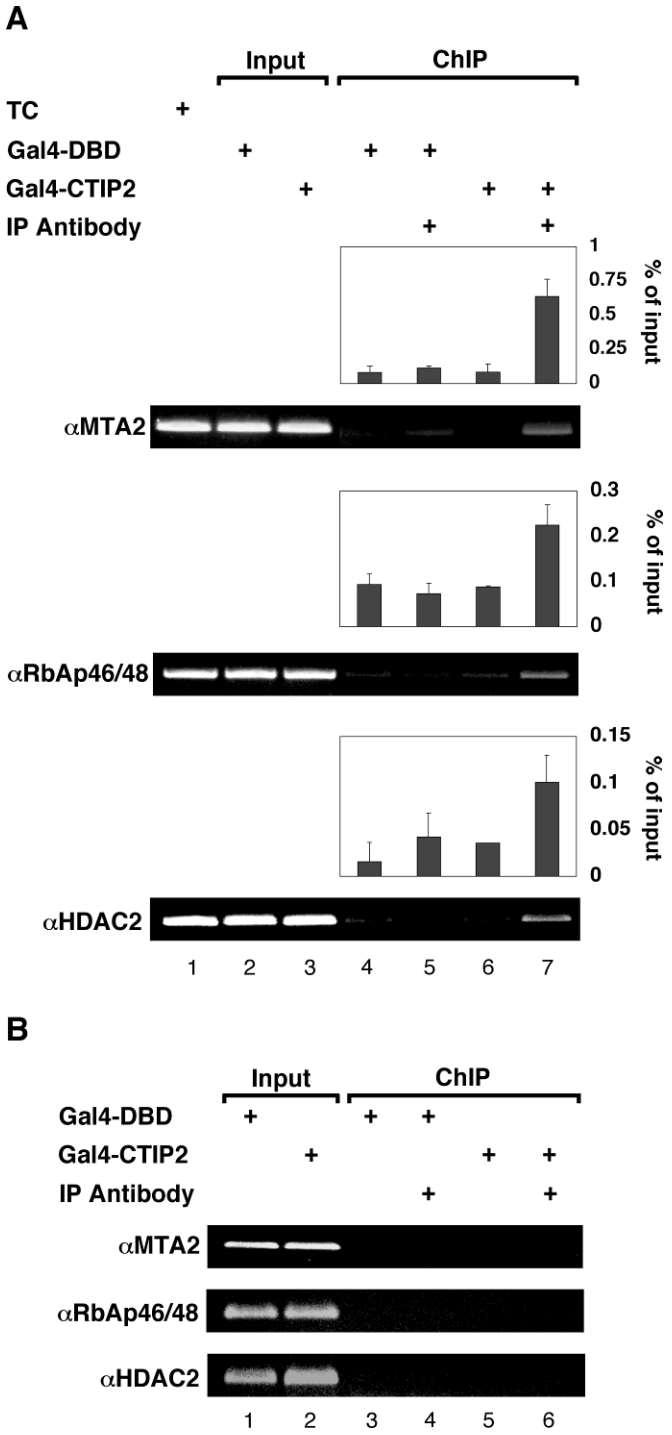
A
Input
ChIP
TC
Gal4-DBD
Gal4-CTIP2
IP Antibody
1
0.75
0.5
0.25
0
% of input
αMTA2
0.3
0.2
0.1
0
% of input
αRbAp46/48
0.15
0.1
0.05
0
% of input
αHDAC2
1 2 3 4 5 6 7
B
Input
ChIP
Gal4-DBD
Gal4-CTIP2
IP Antibody
αMTA2
αRbAp46/48
αHDAC2
1 2 3 4 5 6

Figure 2.6. CTIP2-dependent recruitment of endogenous NuRD complex proteins to the promoter template.

A, ChIP assays were performed on HEK293T cells following transient transfection of 3 μg of Lex-Gal-Luc reporter and 5 μg of an expression vector encoding either Gal4-DBD or Gal4-CTIP2. Conventional PCR amplification of a promoter template from samples immunoprecipitated with or without specified antibodies (*lanes 4-7*) is shown *(lower)* together with quantification by qPCR amplification *(upper)* in each panel. *Lane 1* corresponds to a template control (*TC*) in which a reporter plasmid was used directly in the amplification reaction. *Lanes 2* and *3* represent amplification reactions conducted utilizing 5% of the input lysate that was used for IP reactions. The result of conventional PCR (ethidium bromide-stained gels) is a representative of three independent experiments. CTIP2-dependent enrichment of MTA2, RbAp46/48, and HDAC2 on the promoter template was quantified by qPCR and presented as the mean percentage of input ± S.E.M. derived from three independent experiments
B, PCR amplification of a genomic *GAPDH* promoter region from samples immunoprecipitated with or without specified antibodies (*lanes 3-6*). Inputs (*lanes 1-2*) were as described in *A*.

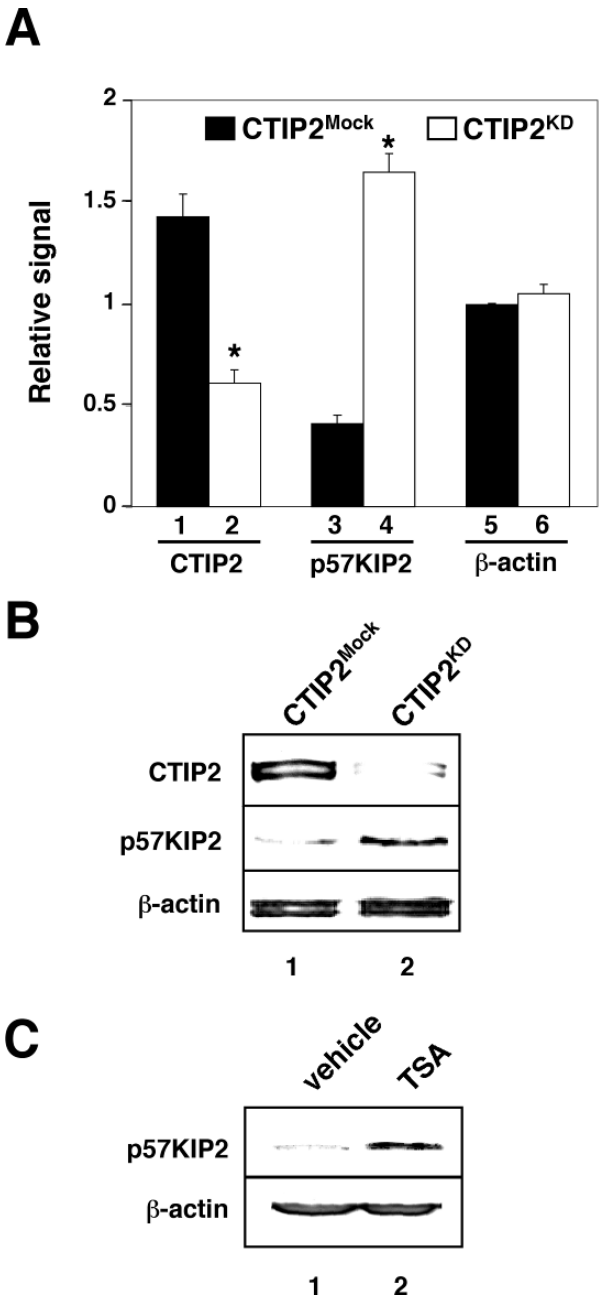
A
CTIP2Mock
CTIP2KD
Relative signal
2
1.5
1
0.5
0
*
*
1 2
3 4
5 6
CTIP2
p57KIP2
β-actin
B
CTIP2Mock
CTIP2KD
CTIP2
p57KIP2
β-actin
1
2
C
vehicle
TSA
p57KIP2
β-actin
1
2

Figure 2.7. CTIP2 knockdown in SK-N-MC cells results in increased expression of p57KIP2.

SK-N-MC cells were transfected with 100 nM CTIP2 siRNA ($CTIP2^{KD}$) or nonspecific siRNA ($CTIP2^{Mock}$).

A, Microarray analyses of mRNA levels of CTIP2, p57KIP2, and β-actin in $CTIP2^{KD}$ and $CTIP2^{Mock}$ cells. The results represent mean mRNA levels (shown as *relative signal*) ± S.E.M. derived from three independent experiments. The difference of mRNA levels between $CTIP2^{KD}$ and $CTIP2^{Mock}$ cells is statistically significance for CTIP2 and p57KIP2 ($p < 0.05$; indicated by an asterisk).

B, Protein expression of CTIP2, p57KIP2, and β-actin as analyzed by immunoblotting in $CTIP2^{KD}$ and $CTIP2^{Mock}$ cells. β-actin was used as a negative and loading control (*bottom panel*). ***C***, Induction of *p57KIP2* expression at the protein level by TSA treatment as demonstrated by immunoblot analysis. SK-N-MC cells were treated with 100 ng/mL TSA or vehicle for seven hours, prior to harvesting, whole cell extract preparation and immunoblotting. Again, β-actin serves a loading control.

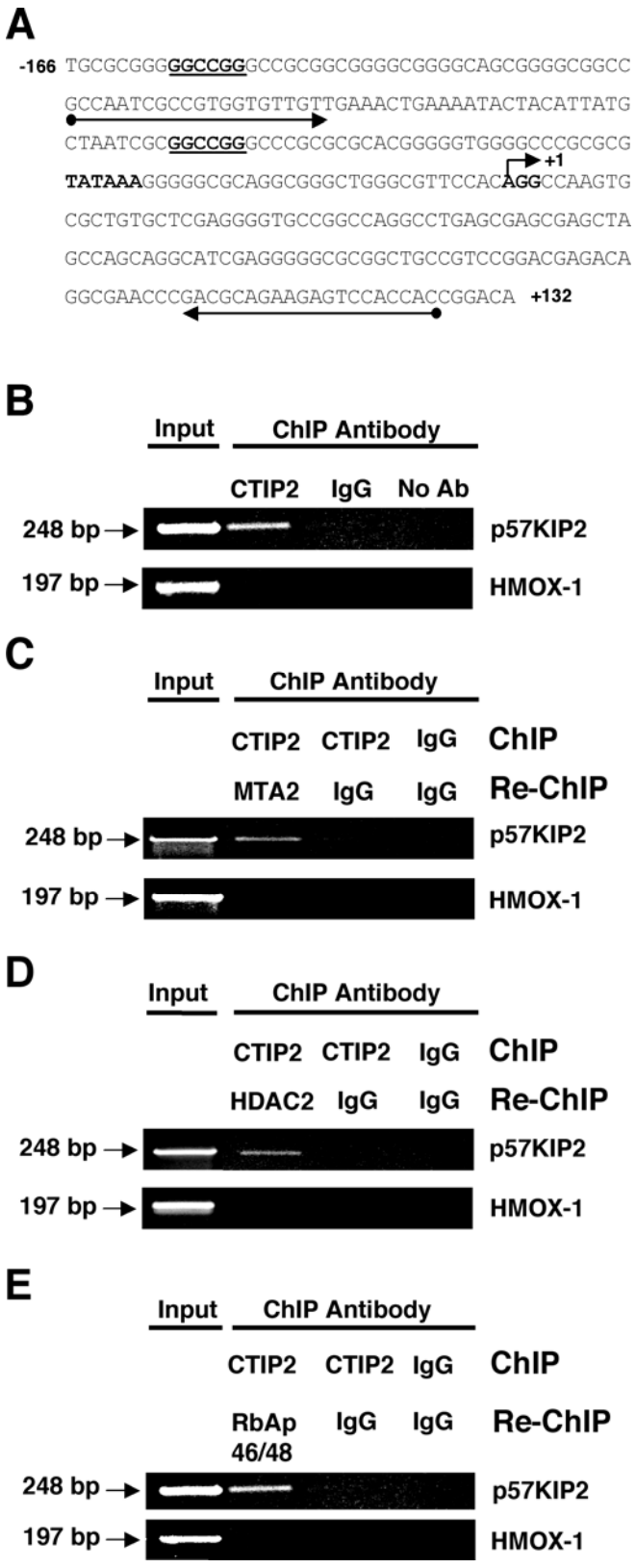
A
-166 TGCGCGGGGGCCGGGCCGCGGCGGGGCGGGGCAGCGGGGCGGCC
GCCAATCGCCGTGGTGTTGTTGAAACTGAAAATACTACATTATG
CTAATCGCGGCCGGGCCCGCGCGCACGGGGGTGGGGCCCGCGCG
+1
TATAAAGGGGGCGCAGGCGGGCTGGGCGTTCCACAGGCCAAGTG
CGCTGTGCTCGAGGGGTGCCGGCCAGGCCTGAGCGAGCGAGCTA
GCCAGCAGGCATCGAGGGGGCGCGGCTGCCGTCCGGACGAGACA
GGCGAACCCGACGCAGAAGAGTCCACCACCGGACA +132
B
Input
ChIP Antibody
CTIP2 IgG No Ab
248 bp
p57KIP2
197 bp
HMOX-1
C
Input
ChIP Antibody
CTIP2 CTIP2 IgG ChIP
MTA2 IgG IgG Re-ChIP
248 bp
p57KIP2
197 bp
HMOX-1
D
Input
ChIP Antibody
CTIP2 CTIP2 IgG ChIP
HDAC2 IgG IgG Re-ChIP
248 bp
p57KIP2
197 bp
HMOX-1
E
Input
ChIP Antibody
CTIP2 CTIP2 IgG ChIP
RbAp 46/48 IgG IgG Re-ChIP
248 bp
p57KIP2
197 bp
HMOX-1

Figure 2.8. CTIP2 and components of NuRD complex co-associate with *p57KIP2* promoter in SK-N-MC cells.

A*,* The *p57KIP2* proximal promoter region. Putative CTIP2 binding sites (Ref. 14) are underlined; arrows represent positions of forward and reverse primers for ChIP, and the transcriptional start site is denoted as +1.
B*,* Chromatin immunoprecipitation was performed in SK-N-MC cells using indicated antibodies, and results were analyzed by conventional PCR using primers described in ***A***. The *heme oxygenase-1* (*HMOX-1*) promoter was used as a negative control to demonstrate the specificity of CTIP2 binding to *p57KIP2* promoter. The input lane represents 10% of the total chromatin used for immunoprecipitation.
C, **D, and E**, CTIP2, MTA2, HDAC2 and RbAp46/48 co-occupy the promoter of *p57KIP2* gene. ChIP and re-ChIP studies were performed using the specified antibodies in the orders indicated. The proximal *HMOX-1* promoter was again used as a negative control. ChIP/re-ChIP studies shown are representative of three independent experiments. The sizes of PCR products (*p57KIP2*, 248 bp; *HMOX-1*, 197 bp) are indicated by arrows.

Table 1.1. Up-regualted genes in CTIP2 knockdown SK-N-MC cells

GenBank	Identity	Fold up-regulation
NM_006727	Cadherin 10, type 2	6.5
NM_002133	Heme Oxygenase 1 (HMOX-1)	5.1
N33167	CDK inhibitor 1C (p57KIP2)	4.3
X02761	Fibronectin-1 (FN-1)	3.8

CHAPTER 3

Expression of COUP-TF-interacting Protein 2 (CTIP2) in Mouse Skin During Development and in Adulthood

Olga Golonzhka, Mark Leid, Gitali Indra, Arup Indra

Gene Expression Patterns **7(7)**:754-760

2007

Abstract

COUP-TF-interacting protein 2 (CTIP2), also known as Bcl11b, is a transcriptional regulatory protein that is highly expressed in and plays a critical role(s) during development of T lymphocytes and the central nervous system. We demonstrate herein that CTIP2 is also highly expressed in mouse skin during embryogenesis and in adulthood as revealed by immunohistochemical analyses. CTIP2 expression in the ectoderm was first detected at embryonic day 10.5 (E10.5), and became increasingly restricted to proliferating cells of the basal cell layer of the developing epidermis in later stages of fetal development and in adult skin. In addition, CTIP2 expression was also detected in some cells of the suprabasal layer of the developing epidermis, as well as in developing and mature hair follicles. Relatively fewer cells of the developing dermal component of skin were found to express CTIP2, and the adult dermis was devoid of CTIP2 expression. Some, but not all, of the cells present within hair follicle bulge were found to co-express CTIP2, keratin K15, and CD34, indicating that a subset of $K15^{+}$ $CD34^{+}$ skin stem cells may express CTIP2. Considered together, these findings suggest that CTIP2 may play a role(s) in skin development and/or homeostasis.

Introduction

CTIP2 (Chicken ovalbumin upstream promoter transcription factor (COUP-TF)–interacting protein 2), also known as Bcl11b, is a C_2H_2 zinc finger protein (Avram et al., 2000) that has been shown to repress transcription though interaction with COUP-TF nuclear receptor proteins as well as through direct, sequence-specific DNA binding (Avram et al., 2002). CTIP2 is required for normal T cell development and CTIP2-null mice exhibit arrested thymocyte development (Wakabayashi et al., 2003b). Additionally, deregulation of CTIP2 may be implicated in immune system malignant transformation (Wakabayashi et al., 2003a; Bezrookove et al., 2004; Kamimura et al., 2007). It was shown that CTIP2 is also expressed in layer V of cerebral cortex and plays a critical role in the establishment of connections of corticospinal motor neurons to the spinal cord (Arlotta et al., 2005).

Mouse epidermis develops from a single-layered embryonic ectoderm (Mack et al., 2005). Subsequent stratification events lead to the formation of the periderm (around E9-E12), which overlies the ectoderm (Byrne et al., 2003; Mack et al., 2005). Cells of this two-layered epidermis then undergo a series of proliferation and terminal differentiation events which results in the formation of new cell layers of the future epidermis. Formation of the mature epidermis is completed by E18, at which the epidermis consists of four layers: the basal, spinous, granular and cornified layer (Mack et al., 2005).

Epidermis undergoes constant renewal, which is required to maintain normal tissue homeostasis. This is possible due to the presence of two populations of proliferating cells: transit amplifying cells with limited proliferative potential and keratinocyte stem cells, which are slow-cycling cells with high proliferative capacity (Lavker et al., 1993; Slack, 2000).

Previous RNA *in situ* hybridization using a CTIP2 RNA probe performed in our laboratory demonstrated that CTIP2 was highly expressed in developing and mature central nervous system and spinal cord as well as in the thymus (Leid et al., 2004). The epidermis was not specifically identified as a site of CTIP2 expression in the previous *in situ* hybridization studies, although CTIP2 mRNA is found in the skin (see Fig. 1G and I from Leid et al., 2004). Preliminary attempts to define CTIP2 expression pattern during mouse embryogenesis using a CTIP2-specific monoclonal antibody revealed high-level expression of CTIP2 in developing skin. To our knowledge this is the first evidence for expression of CTIP2 in skin, during development or in the adulthood, and it therefore provided a rationale to perform additional analyses.

Materials and methods

Sample preparation

Wild type fetuses from CD1 outbred mice strain (ICR or Swiss Mice from Charles River) were collected at stages E10.5, E12.5, E14.5, E16.5, E18.5, rinsed with

PBS and fixed with 4% paraformaldehyde at 4˚C. Fixed embryos were then washed with PBS overnight, cryopreserved in 30% sucrose, frozen in Optimum Cutting Temperature embedding compound (OCT) and stored at -80˚C until used. For the purpose of developmental timing, 12:00 pm on the day after the night of mating was considered as E0.5. For adult skin studies, dorsal skin biopsies were taken from 8-10 week-old shaved mice and processed as described for fetal skin biopsies.

Immunohistochemistry

OCT-embedded embryos and adult skin samples were cross-sectioned at 10 µm intervals. Sections were mounted on "superfrost" slides and allowed to air dry. Sections were rinsed with PBS three times (5 min each) and permeabilized with ice-cold methanol for 3 min. Sections were allowed to dry and nonspecific binding of antibody was blocked with blocking buffer (0.3% Boehringer Mannheim Blocking reagent, 5% horse serum, 5% fetal Calf serum, 0.1 % triton X-100 in PBS) for 1 h. Slides were then incubated with rat anti-CTIP2 primary monoclonal antibody (Abcam product number 18465; clone 25B6) overnight in a humidified chamber. Primary antibody incubation was followed by three washes with PBST and incubation with fluorescently-labeled [Cy2 (1:250) or Cy3(1:500); Jackson ImmunoResearch] secondary antibody for 2 hours. Nuclei were counterstained with DAPI. Finally, sections were rinsed with PBST, dehydrated through sequential washes in 50, 70, 95 and 100% ethanol and then cleared in xylene. Slides were mounted with DPX mounting media and allowed to dry overnight. Images were captured at 40X

magnification using Leica DMRA fluorescent microscope and Hamamatsu C4742-95 digital camera and processed using OpenLab software and Adobe Photoshop 7.0.

Whole skin protein extract preparation and Immunoblot analysis

Dorsal skin biopsies from E18.5 fetuses or adult mice were homogenized in RIPA buffer (50 mM Tris pH7.5, 1% NP-40, 0.5% Sodium Deoxycholate, 0.1 %SDS, 150 mM NaCl, 5mM EDTA, proteinase inhibitors) using tissue grinder and cleared by centrifugation. Supernatants were collected and equal amounts of protein (determined using the Bio-Rad Protein Assay Kit) were analyzed by immunoblotting using antibodies against CTIP2 and β-actin as a loading control.

Antibodies

The following antibodies and their dilutions were used for immunohistochemical studies: anti-CTIP2 (Abcam, 1:300), -K14 (Covance, 1:1000), -K10 (Covance, 1:1000), -Ki67 (Abcam, 1:500), -K15 (Covance, 1:500), -CD34 (Santa Cruz, 1:50). Antibodies used for Western blot analysis: anti-CTIP2 (Abcam, 1:1000), -β-actin (Abcam, 1:4000).

Results and discussion

Expression of CTIP2 during epidermal morphogenesis

To characterize the expression profile of CTIP2 during mouse skin ontogenesis, we performed immunohistochemistry at different stages of development using an anti-CTIP2 monoclonal antibody, which has been previously described (Arlotta et al., 2005).

CTIP2 expression was detected in the ectoderm as early as embryonic day 10.5 (E10.5), where CTIP2-positive cells were found in the outermost layer of the cross-section of a developing fetus (Fig.3.1A, *a*). Some of these cells were already expressing the basal cell marker keratin 14 (K14) (Fig.3.1A, *b*), which signifies a commitment of these cells to give rise to stratified epithelia, (Byrne et al., 1994).

Expression of CTIP2 persisted at E12.5 (Fig.3.1A, *c*). This stage of skin development is marked by formation and stratification of the embryonic basal layer and all cells of that layer were found to be positive for CTIP2 expression (Fig.3.1A). CTIP2 expression precisely co-localized with basal cell marker K14 (Vassar et al., 1989) at E12.5 (Fig.3.1A, *d*).

Strong expression of CTIP2 was detected in the rapidly dividing basal cell layer at E14.5, and expression of CTIP2 appeared to be co-localized with that of K14 (Fig.3.1B, *a* and *b*). At this stage, the early differentiating layers started to form, and were identified using differentiation marker keratin 10 (K10) (Byrne et al., 1994). CTIP2 expression also extended to some cells in the differentiating suprabasal cell layer at E14.5, as seen by co-localization of CTIP2 and K10 staining (Fig.3.1B, *c*).

However, the level of CTIP2 expression in the suprabasal cell appeared to be lower than that of basal cells (Fig.3.1B, compare *b* and *c*). In addition, some cells of the future dermis were also found to express CTIP2 at this developmental stage (Fig.3.1B, *a*).

CTIP2 expression was further investigated at E16.5 and E18.5 (Fig. 3.1B, *d-i*). High levels of CTIP2 expression were consistently observed in the basal layer of the epidermis at these two stages (Fig.3.1B *d*, *e*, *g*, *h*). Some CTIP2 positive cells were observed in the suprabasal layers that expressed high levels of K10 at E16.5 (Fig.3.1B, *f*), whereas the suprabasal expression of CTIP2 at E18.5 was primarily restricted to a small number of K10-positive cells that were adjacent to the basal cells (Fig.3.1B, *I;* see supplemental Fig.3.1).

Later stages of skin morphogenesis were marked by the formation of hair follicles, and anti-CTIP2 antibody robustly stained hair bulbs and follicles at E16.5 and E18.5, respectively (Fig.3.1B, *d* and *g*). These stages were also characterized by expansion of the dermal compartment of the skin, and some of these dermal cells were also found to express CTIP2 (Fig.3.1B, *d* and *g,* and data not shown).

CTIP2 expression in proliferating cells

To evaluate the proliferation status of CTIP2-expressing cells we performed co-labeling studies using anti-CTIP2 and an antibody against the proliferation marker Ki67 (Schluter et al., 1993) at different stages during epidermal morphogenesis

(Fig.3.2). At early stages of development (E10.5), almost all cells of the fetus were positive for Ki67 expression (Fig.3.2, *b* and data not shown). This was expected as early stages of fetal development are marked by rapid and ubiquitous proliferation. All cells of the ectodermal compartment, as well as those of the underlying mesenchyme were found to express Ki67 (Fig.3.2, *b*). Two days later (at E12.5) virtually all cells of the ectoderm were positive for Ki67 expression (Fig.3.2, *e*). Most, but not all, cells of mesenchymal origin were negative for Ki67 staining at this developmental stage (Fig.3.2, *f*).

The basal cell layer of epidermis is highly proliferative at E14.5 (Mack et al., 2005), which is reflected in the presence of multiple Ki67-positive cells (Fig.3.2, *h-i*). A smaller fraction of cells of the future dermis were positive for Ki67 staining at this stage (Fig.3.2, *h-i*), and all layers of the developing skin became less proliferative with developmental progression. For example, only a fraction of basal cells, as well as those cells of the dermal compartment, were positive for Ki67 staining at E16.5 (Fig.3.2, *k-l*). By E18.5 only a few cells were still proliferating in the basal cell layer, and the dermis was mostly non-proliferative. Interestingly, epithelia of the developing hair follicles, which were invaginating into the dermis, still harbored a considerable number with Ki67-positive cells (Fig.3.2, *n*).

At early, highly proliferative stages of development (E10.5-E14.5) almost all of the CTIP2-positive epidermal cells were found to be dividing as indicated by co-localization of CTIP2 and Ki67 staining (Fig.3.2, *a-i*). The total number of Ki67- positive

cells was reduced in the epidermis at E16.5 but, in general, cells that were positive for Ki67 staining were also found to be positive for CTIP2 expression (Fig.3.2 *j-l*). By E18.5, the number of proliferating cells in fetal skin was comparatively reduced, but again a correspondence was observed between the Ki67 staining and that of CTIP2, indicating that majority of proliferating cells express CTIP2. Similarly, some CTIP2-positive cells were detected in the developing hair follicle epithelium, and these cells were also positive for Ki67 expression (Fig.3.2, *m-o*).

Expression of CTIP2 in adult skin

Immunohistochemistry was performed on 8-10-week old adult mouse skin using anti-CTIP2, -K14 and -K10 antibodies to evaluate the possibility that CTIP2 may be expressed in adult skin (Fig. 3.3). In the adult skin, CTIP2 expression was found in the majority, if not all cells of the basal layer (Fig. 3.3, *a* and *b*), hair follicles and some cells of the suprabasal K10-positive layers (Fig. 3.3, *c*), which is similar to the results that we obtained during embryogenesis (Fig. 3.1). In contrast to the developing dermis, CTIP2 expression was not detected in the dermal compartment of the adult skin (compare Fig. 3.3, *a* and Fig. 1B, *g*). Immunoblot analysis of CTIP2 in protein extracts from dorsal skin biopsies confirmed expression of CTIP2 in fetal (E18.5) and adult skin (Fig. 3.4, top panel).

Expression of CTIP2 in whole skin protein extracts of the E18.5 embryo was found to be significantly higher that that of the adult skin. This could be partially

explained by our observation that CTIP2 expression is maintained in the epidermal basal and suprabasal cells throughout development, and into the adulthood, whereas the adult dermal compartment, which is dramatically expanded relative to fetal skin, does not express significant amounts of CTIP2.

CTIP2 expression in stem cells present in the bulge of the adult hair follicle

The "bulge" in the outer root sheath (ORS) of the hair follicle is believed to be the site of keratinocyte epithelial stem cells that contributes to morphogenesis of the hair follicle, and adjacent interfollicular epidermis (Lavker and Sun, 2000; Khavari, 2004). Two markers of bulge stem cells are known to date: keratin 15 (K15) (Liu et al., 2003), and CD34 (Trempus et al., 2003), which is also a hematopoietic stem cell marker (Krause et al., 1996). As our immunohistochemistry data in the adult tissue revealed that CTIP2 was highly expressed in the hair follicle in adult skin, we performed co-staining of CTIP2 with K15 and CD34 to investigate if CTIP2 is expressed in stem cells of the hair bulge. As expected, K15 and CD34 specifically labeled keratinocytes in the bulge region of adult mouse hair follicle (Fig. 3.5A and B). CTIP2 was found to be co-expressed in some, but not all, of the keratinocytes in the bulge region with K15 and CD34 expression. In particular, keratinocytes of the outermost cell layer and those located in lower part of the "bulge" stained positively for CTIP2 (Fig. 3.5A and B, white arrows), while other $K15^{+}CD34^{+}$ cells located more medially within the hair bulge did not. Our findings support the idea that hair follicle "bulge" consists of a heterogeneous cell population of keratinocyte stem and/or progenitor

cells (Cotsarelis et al., 1990; Morris and Potten, 1994; Lavker and Sun, 2000). The positive staining of CTIP2 in the peripheral cells of the bulge suggests that CTIP2 might label the cells as they exit the stem/progenitor population. Further studies will be required to validate this hypothesis.

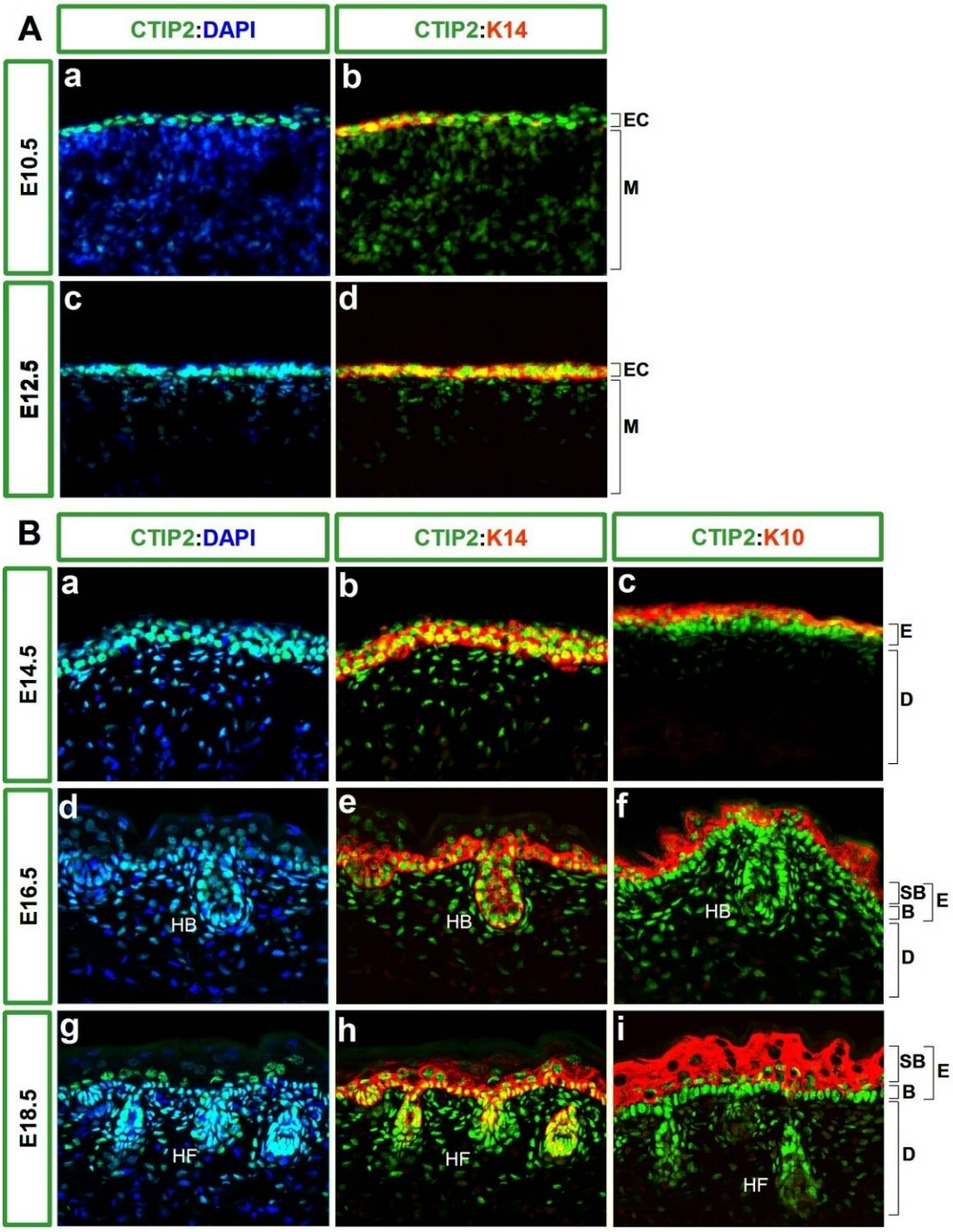
A
CTIP2:DAPI
CTIP2:K14
E10.5
a
b
EC
M
E12.5
c
d
EC
M
B
CTIP2:DAPI
CTIP2:K14
CTIP2:K10
E14.5
a
b
c
E
D
E16.5
d
e
f
HB
HB
HB
SB
B
E
D
E18.5
g
h
i
HF
HF
HF
SB
B
E
D

Figure 3.1. Expression of CTIP2 in the mouse fetal skin.

Immunohistochemistry was performed on 10 µm-thick frozen sections of wild type embryos using antibodies directed against CTIP2, K14 and K10.
A, CTIP2 (in green) is highly expressed in the ectoderm at E10.5 (upper panel) and E12.5 (lower panel) and is co-localized with the expression of K14 (in red).
B, high expression of CTIP2 was observed in the basal cells and upper layers of the epidermis of E14.5 (upper panel), E16.5 (middle panel) and E18.5 embryos (lower panel). K14 and K10 staining (in red) were used to label basal cells and suprabasal layers, respectively. E16.5 and E18.5 stages of development show high expression of CTIP2 in the basal layer of epidermis as well as in the dermis and hair follicles. All sections were counterstained with DAPI (in blue). Images were taken at 40X magnification. Abbreviation: ***EC***- *ectoderm,* ***M****-mesoderm,* ***E****-epidermis,* ***D****-dermis,* ***B****-basal cell layer,* ***SB****- suprabasal cell layers,* ***HB****-hair bulb,* ***HF****-hair follicle.*

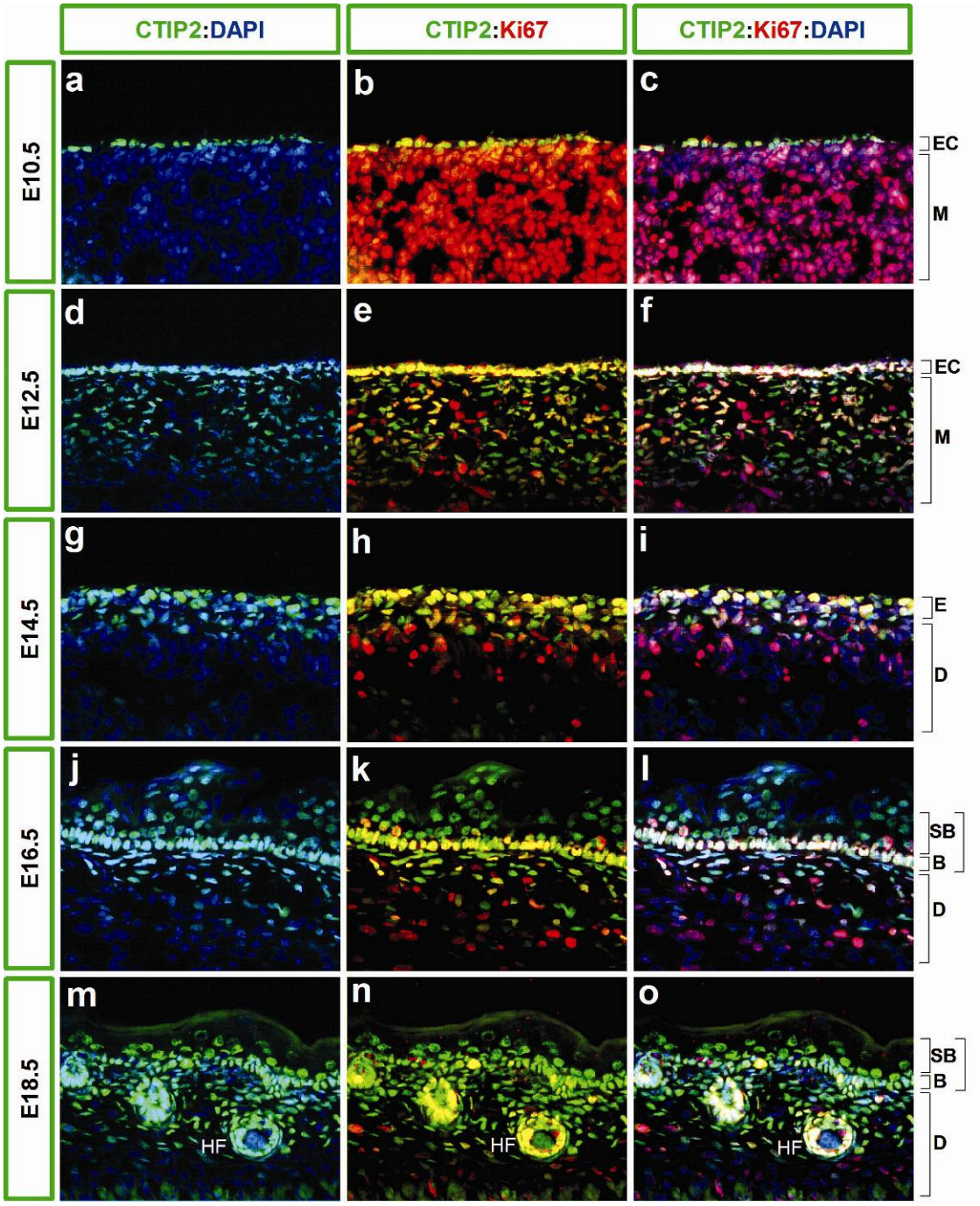
CTIP2:DAPI
CTIP2:Ki67
CTIP2:Ki67:DAPI
E10.5
E12.5
E14.5
E16.5
E18.5
a
b
c
d
e
f
g
h
i
j
k
l
m
n
o
EC
M
E
D
SB
B
HF

Figure 3.2. CTIP2 expression in proliferating cells.

10 µm-thick frozen section of wild type fetuses at different stages of development were analyzed immunohistochemically using antibodies directed against CTIP2 (green) and Ki67 (red) and counterstained with DAPI (blue). Images were taken at 40X magnification. Abbreviations are described in the legend of Fig. 3.1.

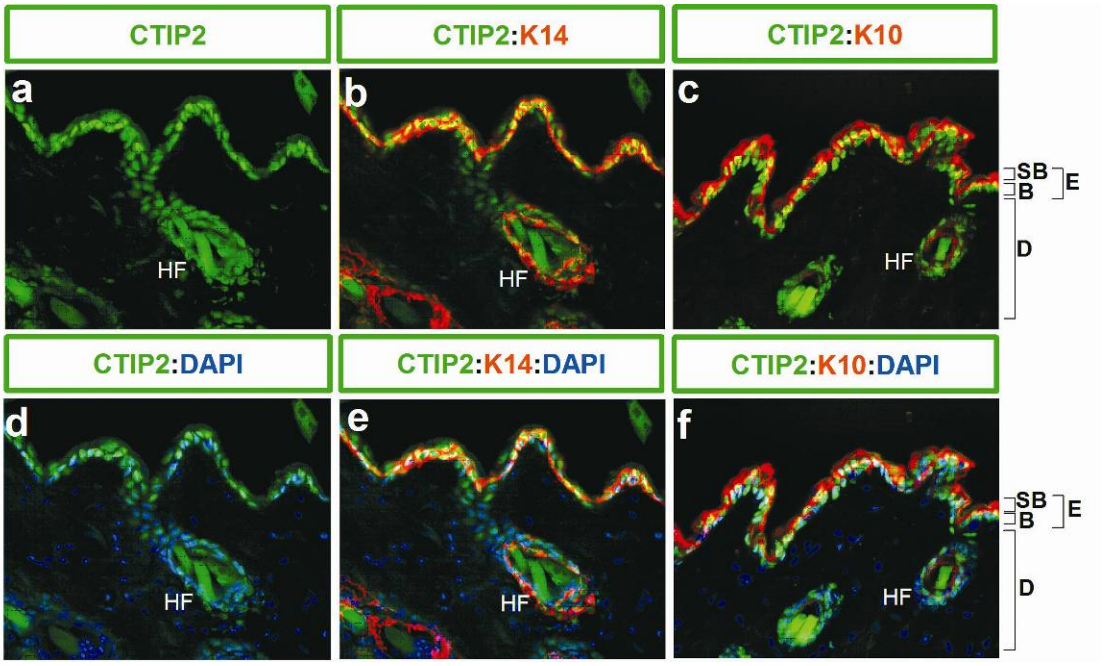

Figure 3.3. Expression of CTIP2 in the adult mouse skin.

10 µm-thick frozen skin sections obtained from dorsal skin biopsies of 8-10-week old C7/BL6 mice were stained with anti-CTIP2 (green), -K14 (red), -K10 (red) antibodies and counterstained with DAPI (blue), and photographed using 40X objective. Abbreviations are described in the legend of Fig. 3.1.

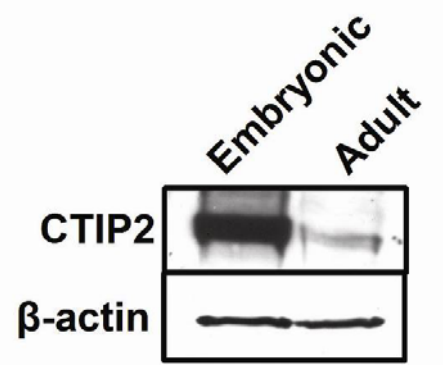

Figure 3.4. Immunoblot analysis of CTIP2 expression in fetal and adult skin.

Whole skin protein extracts were prepared from adult (8-week old) and fetal (E18.5) dorsal skin biopsies and analyzed using CTIP2-specific antibody (upper panel). β-actin was used as an internal loading control (lower panel).

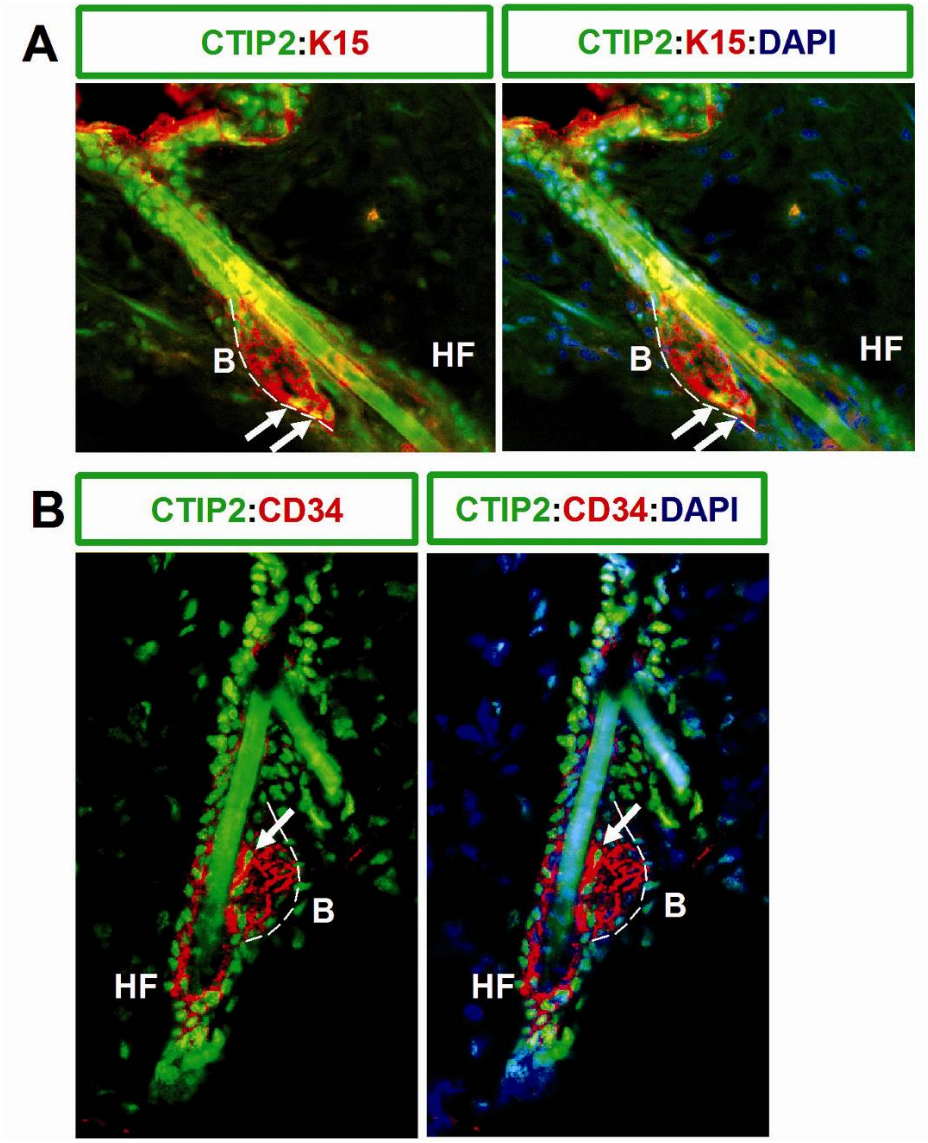

Figure 3.5. **Expression of CTIP2 in stem cells of the bulge region of the mouse hair follicle.**

10 µm-thick frozen skin sections obtained from dorsal skin biopsies 8-week old mice were co-stained with CTIP2 (green) and K15 (red: A) or CTIP2 (green) and CD34 (red: B) and images of hair follicles in the bulge region were taken at 40X magnification. Sections were counterstained with DAPI. White arrows indicate CTIP2 positive cells in the bulge region that are also positive for K15 or CD34. Abbreviation: ***B****-bulge,* ***HF****-hair follicle*.

CHAPTER 4

Dual Role of COUP-TF-interacting Protein 2 (CTIP2) in Regulating Epidermal Homeostasis and Skin Barrier Formation During Mouse Fetal Development

Olga Golonzhka, Xiaobo Liang, Nadia Messaddeq, Jean-Marc Bornert, Adam

Campbell, Daniel Metzger, Pierre Chambon, Gitali Indra, Mark Leid and Arup Indra

Prepared for submission to Development

Abstract

COUP-TF-interacting protein 2 (CTIP2; also known as Bcl11b) is a transcription factor that plays key roles in the development of the central nervous and immune systems. CTIP2 is also highly expressed in the developing epidermis, and at lower levels in the dermis, and in adult skin. Analyses of mice harboring a germline deletion of CTIP2 revealed that the protein plays critical roles in the skin, particularly in keratinocyte proliferation and late differentiation events, as well as in the development of the epidermal permeability barrier. At the core of all of these actions is a relatively large network of genes that is regulated directly or indirectly by CTIP2. The analysis of conditionally null mice, in which expression of CTIP2 was ablated specifically in epidermal keratinocytes, suggests that CTIP2 functions in both cell and non-cell autonomous contexts to exert regulatory influence over multiple phases of skin development including barrier establishment. Considered together, our results suggest that CTIP2 functions as a top-level regulator of skin morphogenesis.

Introduction

The development of the skin epidermis begins with the commitment of the primitive ectoderm to the keratinocyte cell fate. The subsequent processes of cellular proliferation, stratification and differentiation result in formation of the

multilayered structure of epidermis. During embryonic development, keratinocytes of the innermost layer of the epidermis, the proliferative, basal cell layer, undergo a program of the terminal differentiation, then exit the basal cell layer and migrate upward to the surface of the skin (Byrne et al., 2003; Mack et al., 2005). These cells initially differentiate into spinous, then granular cells, and finally into the tough, enucleated cells of the cornified layer, the corneocytes (Byrne et al., 2003).

The events of epidermal development are orchestrated by the concerted action of a number of transcription factors that regulate both the proliferative capacity and differentiative potential of epidermal keratinocytes (Segre, 2003; Segre, 2006). These include c-Myc, p63, Klf4, GATA3, AP-1 family transcription factors c-fos and c-jun, Id family of proteins and others (Segre et al., 1999; Langlands et al., 2000; Angel et al., 2001; Arnold and Watt, 2001; Shaulian and Karin, 2002; Koster et al., 2004; de Guzman Strong et al., 2006; Koster et al., 2007). The end product of epidermal development is the formation of the Epidermal Permeability Barrier (EPB), which provides a crucial physical and permeability barrier.

Formation of the epidermal barrier is a stepwise and orderly process (Segre, 2003; Segre, 2006). In the granular layer of epidermis, lipids are packaged inside lamellar bodies (LB), and structural proteins, such as keratins, loricrin and filaggrin, are assembled into macrofibrils. The cornified envelope (CE) is formed by deposition of precursor proteins on the inner surface of the plasma membrane (Elias, 2005). Transglutaminase (TGM) enzymes, then cross-link the cornified envelope proteins,

creating a tough sac that holds the keratin fibers (Candi et al., 2005). Finally, cellular organelles, including the nucleus are degraded and lipids from LB are extruded into the intercellular space and onto the CE scaffold forming a series of extracellular lipid membranes (lamellar bilayers) (Candi et al., 2005).

COUP-TF-interacting protein 2 (CTIP2; also known as Bcl11b) is a C_2H_2 zinc finger transcription factor (Avram et al., 2002; Senawong et al., 2003; Topark-Ngarm et al., 2006). CTIP2 is known to repress transcription of reporter genes in transiently transfected cells, either by tethering to other promoter-bound transcription factors (Avram et al., 2000) or by direct, sequence-specific DNA binding activity (Avram et al., 2002). The hypothesis that CTIP2 functions as a transcriptional repressor has been supported by transcriptome analyses in human neuroblastoma cells (Topark-Ngarm et al., 2006), and mouse thymocytes (Leid et al., submitted).

CTIP2 is expressed early during mouse development as well as in the adult animal, and in both cases, expression is most predominant in the CNS, thymus, and skin (Leid et al., 2004; Golonzhka et al., 2007). Mice null for expression of CTIP2 exhibit perinatal lethality and severe phenotypes in tissues that express the gene. In the CNS CTIP2 is required for proper axonal projection by corticospinal neurons and normal development of the medium spiny neurons (MSN) in the striatum (Arlotta et al., 2005; Arlotta et al., 2008). Germline disruption of CTIP2 results in an arrest of T cell development at the immature, $CD4^-CD8^-$ stage, with the complete absence of $\alpha\beta$ T cells (Wakabayashi et al., 2003b).

Here we report a novel function of CTIP2 in skin development. We show that CTIP2 controls epidermal proliferation/differentiation programs and EPB formation. CTIP2$^{-/-}$ mice, with a germline deletion for the CTIP2 gene, exhibit a hypoplastic epidermis, defects in EPB development, and increased transepidermal water loss (TEWL). These defects likely arose from large-scale disruption of gene expression in the mutant skin, including genes encoding structural protein and lipid modifying enzymes, as well as those involved in epidermal proliferation and differentiation, and EPB establishment. In the context of EPB development CTIP2 was found to function cell autonomously. However, the actions of CTIP2 in epidermal proliferation and early differentiation were found to be non-cell autonomous, most likely arising from CTIP2-dependent regulation of paracrine growth factor(s) expression in the dermis, including keratinocyte growth factor (KGF) and/or granulocyte/macrophage colony stimulating factor (GM-CSF) (Szabowski et al., 2000; Werner and Smola, 2001).

Materials and Methods

Generation of CTIP2$^{-/-}$ mice

14 kb of the mouse CTIP2 genomic locus (129SvPAS strain) was used to construct a CTIP2 targeting vector (Fig. 4.1B and C). After electroporation, five ES cell lines (out of 568) were verified to have undergone HR as judged by Southern analysis using 5' and 3' probes outside the targeting vector (Fig.4.1D and E). Two of these clones were

injected into blastocysts, and both gave rise to chimeric animals that were bred with C57BL/6 mice to allow germ line transmission (GLT) of the targeted L3 allele. These mice were bred with transgenic mice expressing the Flp recombinase under the control of the CMV promoter (Rodriguez et al., 2000) to excise the *neo* marker and generate L2 (floxed) *CTIP2* allele. Alternatively, mice harboring the L3 allele (LoxP-Exon 4-Frt-PGKneo-Frt-LoxP) were crossed with transgenic mice expressing Cre recombinase under the control of the CMV promoter (Dupe et al., 1997), to excise both the floxed CTIP2 exon 4 (and generate L- allele) as well as the neo marker. These mice were bred to homozygosity (CTIP2L-/L- , referred to as CTIP2-/- hereafter).

X-Gal permeability assay and Transepidermal Water Loss

X-Gal diffusion assays were performed as described previously (Hardman et al., 1998) with minor modifications. Transepidermal water loss was assessed using a vapometer (SWL4142, Delfin Technologies). Data was expressed in g/m^2h, and represents the mean ± S.E.M. from 3 independent animals (3 independent measurements per animal) of each genotype. Data were compared using an unpaired Student's t-test, with corrections for unequal variance.

Antibodies

The following antibodies and their dilutions were used for Immunohistochemistry: anti-CTIP2 (Abcam, 1:300), -K1 (Covance, 1:1000), -K14 (Covance, 1:1000), -K10 (Covance, 1:1000), -Ki67 (Abcam, 1:500), -Involucrin

(Covance, 1:1000), -Loricrin (Covance, 1:1000), Filaggrin (Covance, 1;1000). For Immunoblotting we used the dilutions mentioned above, except for anti-CTIP2 (1:1000 dilution), anti-CTIP1 (Bethyl) (1:500) and anti-ß-actin (1:4000).

Immunohistochemistry

Fetuses at E17.5 and E18.5 were collected, fixed with 4% paraformaldehyde, cryopreseved in 30% sucrose and frozen down in OCT. 10 µm cross sections were rinsed with PBS three times, permeabilized with ice-cold methanol for 3 min and blocked with blocking buffer (0.3% Boehringer Mannheim blocking reagent, 5% horse serum, 5% fetal calf serum, and 0.1% triton X-100 in PBS). Sections were then incubated with primary antibodies overnight, followed by three washes with PBST (PBS+0.01% Tween) and incubation with fluorescently-labeled secondary antibody (Cy2 (1:250) or Cy3 (1:500); Jackson ImmunoResearch) for 2 h at room temperature. Nuclei were visualized using DAPI. After final washes with PBST, sections were dehydrated through a series of ethanol washes, cleared in xylene and mounted with DPX mounting media. All images were captured at 40X magnification using Leica DMRA fluorescent microscope and Hamamatsu C4742-95 digital camera and processed using OpenLab software and Adobe Photoshop 7.0.

Histological analysis

Toluidine blue and H&E staining of 1.5 µm and 10 µm-thick skin sections, respectively, were performed as described (Indra et al., 2005a; Indra et al., 2005b).

For TEM analysis, 70-nm ultra-thin sections were processed as described (Indra et al., 2005b).

Nile red staining

Ten μm-thick frozen sections were stained with Nile Red and after 2 min examined with a Leitz fluorescence microscope (excitation 489 nm, emission 515 nm) (Indra et al., 2005a; Indra et al., 2005b)

RT-qPCR

RNA extraction and cDNA preparation were performed as described (Indra et al., 2005b). Real-time PCR was performed on an ABI 7500 Real-Time PCR system using SYBR green methodology as described (Indra et al., 2005a; Indra et al., 2005b). RT-PCR conditions and primers sequences for most of the genes have been previous described (Indra et al., 2005a; Indra et al., 2005b; Rodius et al., 2007). Other primer sequences are:

ΔNp63 (F): 5'-TTGTACCTGGAAAACAATG-3', (R) 5'-TCGAAGCTGTGT GGGCCCGGG-3';

p57 (F) 5'- GCCGGGTGATGAGCTGGGAA-3', (R):5'-AGAGAGGCTGGTCCTTCAGC-3';

Smpd3 (F): 5'-CAAATGTCTCAACAGCGGTCT-3', (R): 5'-CCAACAATTCTTTGGTCCTGA-3';

Gba2 (F): 5'- CACGAGTTTGCAGAGAAGAGG-3',(R): 5'- ATTGAGCATGTCGATGAAAGG-3';

Dgat2 (F): 5' AGCCCTCCAAGACATCTTCTC-3', (R): 5'- CCAGGTGAAGTAGAGCACAGC-3';

eLox3 (F): 5’- CAGTCGAATCTGTGTCACTGC-3’, (R): 5’- AGTTCCCGTTTCCTGTGGTC-3’;

Alox12b (F): 5’- GACTGCCGTGTCTACCACTTC-3’(R):5’- AGAAGTCCTTCTTGGCTCTGA-3’;

Elovl4 (F): 5’- CGCTCTATCTCCTGTTCGTGT-3’ (R): 5’- GCGTTGTATGATCCCATGAAT-3’;

KGF (F): 5’-GAAAGGGACCCAGGAGATGAA-3’ (R): 5’-TGATTGCCACAATTCCAACTG-3’;

GMCSF (F): 5’- AATTTCACCAAACTCAAGGGC-3’(R): 5’-GGGATATCAGTCAGAAAGGTT-3’;

HBEGF (F): 5’- GGACAGATCTGAACCTTTTCA-3’ (R): 5’- GCAGTAGTCCTTGTATTTCCT-3’.

Statistical analyses were conducted as described for TEWL measurements.

Microarray analysis

Total RNA was prepared from whole skin biopsies using Qiagen RNeasy Mini kit. Probe synthesis, hybridization and scanning were conducted by the Center for Genome Research and Biocomputing Core Laboratories at Oregon State University. The integrity and concentration of RNA was assessed using Bioanalyzer 2100 (Agilent Technologies) and RNA was used to probe the Affymetrix Mouse Genome 430 2.0 array. Results were analyzed using GeneSpring 7.2 (Silicon Genetics) software, and genes that differed from the control by at least 1.5-fold ($p < 0.05$ as determined by one-way analysis of variance) were further filtered by confidence level using Benjamini and Hochberg False Discovery Rate (< 20%).

Skin protein extraction

Whole skin biopsies were homogenized in RIPA buffer (50 mM Tris, pH 7.5, 1% NP-40, 0.5% sodium deoxycholate, 0.1% SDS, 150 mM NaCl, 5 mM EDTA, proteinase inhibitors) with tissue homogenizer and cleared by centrifugation. Supernatants were collected and equal amounts of protein were analyzed by immunoblotting. Where appropriate epidermis was separated form the underlying dermis by incubating the whole skin biopsies with the dispase solution (4mg/ml) for 4 h at room temperature. Epidermal protein extracts were prepared as described above.

Results

Generation of CTIP2$^{-/-}$ mice

CTIP2$^{-/-}$ mice were generated by floxing exon 4 of the CTIP2 locus, which encodes ~ 75% of the CTIP2 open reading frame and six zinc finger motifs (Fig. 4.1A). The targeting vector used to modify CTIP2 locus by homologous recombination (HR) is schematically depicted in Figs. 4.1B and C, and HR was confirmed by Southern analysis (Fig.4.1D and E). The heterozygous off-spring from this cross, which harbored one wild-type (+) and one mutant *CTIP2* allele (L-), did not show an overt phenotype, and were viable and fertile. CTIP2$^{+/-}$ mice were bred to generate the CTIP2$^{-/-}$ mouse, and the lack of CTIP2 protein in these mice was confirmed by immunoblotting in skin (Fig. 4.1F). CTIP2$^{-/-}$ mice were born at the expected Mendelian ratio and without obvious abnormalities, with the exception of an open eye phenotype (Fig. 4.2A,

arrow; compare Figs. 2B and C), as previously described by Kominami and co-workers (Wakabayashi et al., 2003b). CTIP2$^{-/-}$ mice did not feed and died within the first day after birth. These phenotypic characteristics, together with severe thymic hypocellularity and complete loss of $\alpha\beta$ T lymphocytes (data not shown), recapitulated previously reported observations of CTIP2-null mice (Wakabayashi et al., 2003b).

Loss of CTIP2 results in compromised barrier function, epidermal hypoplasia and increased transepidermal water loss

CTIP2 is highly expressed in mouse ectoderm during development, beginning around embryonic day E10.5 (Golonzhka et al., 2007). To examine whether the germline deletion of CTIP2 resulted in epidermal defects we investigated permeability barrier function in these mice by performing X-gal permeability assays at E17.5 and E18.5. Control embryos showed very little X-gal staining at either E17.5 or E18.5 (Fig. 4.2A). In contrast, CTIP2$^{-/-}$ fetuses stained strongly with X-gal at E17.5, particularly on the ventral surface and the head, while the heterozygous CTIP2$^{-/+}$ displayed an intermediate level of staining (Fig. 4.2A, left panel). The dorsal surface of CTIP2$^{-/-}$ mice did not take up appreciable amounts of X-gal, signifying that barrier establishment has commenced in this region. Similar studies conducted at E18.5 (Fig. 4.2A, right panel) revealed no difference in the EPB function between CTIP2$^{-/-}$ and wt mice, with the exception of blue staining around the eyelids of the CTIP2$^{-/-}$ mice (Fig. 4.2A, arrow).

We also performed transepidermal water loss (TEWL) studies in CTIP2$^{-/-}$ mice to assess the rate of water evaporation rate from the skin at E17.5 and E18.5. At E17.5, TEWL from the CTIP2$^{-/-}$ dorsal skin averaged ~ 12 g/m^{2}h, which is about six-fold higher than that of wt controls (Fig. 4.2D, left panel). The rate of water loss on the ventral side of E17.5 CTIP2$^{-/-}$ mice was approximately two-fold greater than that of wt mice (Fig. 4.2D). Although there was no difference in dorsal water loss between wt and CTIP2$^{-/-}$ mice at E18.5, the ventral surface of the mutants continued to lose water at a greater rate than wt controls (Fig. 4.2D, right panel). Together, these results indicate that skin barrier establishment is disrupted in CTIP2$^{-/-}$ mice and suggest the novel role of CTIP2 in skin barrier formation.

Histological analysis of dorsal skin at E17.5 and E18.5 revealed that CTIP2$^{-/-}$ epidermis is hypoplastic with decreased number of differentiating and cornified cell layers and profound loss of the normal cornified layer with the typical “basket weave” appearance (Fig. 4.2E). These findings indicate that CTIP2$^{-/-}$ mice might have epidermal proliferation and/or differentiation defects.

CTIP2$^{-/-}$ mice exhibit altered expression of markers of epidermal proliferation and early differentiation

Reduced epidermal thickness of the CTIP2$^{-/-}$ mutant fetuses could be due to an alteration in epidermal proliferation and differentiation. To test this, we performed immunohistochemical analyses (IHC) to assess the expression of a proliferation

marker Ki67, (Schluter et al., 1993), markers of keratinocyte basal cells (Keratin 14; K14) (Byrne et al., 1994), and the early differentiation markers (Keratin 10; K10, (Fuchs and Green, 1980; Roop et al., 1983)). Reduced number of Ki67 positive cells and reduced K14 staining were observed in the skin of the CTIP2$^{-/-}$ mutant mice (compare Figs. 4.3A and 3D; 3B and E). Similarly, the expression of K10 was strongly reduced (Fig. 4.3C and F). Immunoblot analyses of skin protein extracts further confirmed the decrease in the expression of K10 as well as K14, in the mutant fetuses (Fig. 4.3M). Altogether, these results suggest that reduced epidermal thickness of the CTIP2$^{-/-}$ fetuses may be due to reduced proliferation and/or altered differentiation in the skin of the mutant mice.

CTIP2$^{-/-}$ mice exhibit alterations in expression of terminal epidermal differentiation markers and genes implicated in epidermal homeostasis and permeability barrier formation

Altered (delayed) barrier formation in the CTIP2$^{-/-}$ mutant fetuses could be due to an alteration in epidermal terminal differentiation program. We performed IHC analyses of late epidermal differentiation markers loricrin, involucrin and filaggrin. The expression levels of involucrin and filaggrin, but not that of loricrin, was altered in the E18.5 CTIP2$^{-/-}$ skin (compare Figs. 4.3G and J, 3H and K, I and L), and this was further confirmed by immunoblotting (Fig. 4.3M). These data suggest that impaired barrier formation in the CTIP2 null mice may be due to altered terminal differentiation in the developing skin.

We performed RT-qPCR analyses of several genes implicated in the control of the epidermal early- and late-differentiation, and barrier formation using E18.5 wt and mutant skin. Interestingly, while *Id2* and *p57* expression was upregulated or derepressed in the mutant skin, consistent with the previously demonstrated repressor activity of CTIP2 (Topark-Ngarm et al., 2006), expression of both *c-Myc* and *p63* was downregulated at E18.5 (Fig. 4.3N), suggesting that CTIP2 may directly or indirectly activate expression of the latter two genes. RT-qPCR analyses for genes encoding structural proteins and transcription factors involved in late terminal differentiation and barrier formation, such as transglutaminase-1 (*Tgase1*), *GATA3*, *Klf4*, and *caspase-14* revealed that all were down-regulated at both E17.5 and E18.5 in the mutant mice (Fig. 4.3N and data not shown). We also observed significant downregulation of *c-Fos*, but not *c-Jun*, suggesting that altered gene expression in CTIP2 mutant skin may be mediated, at least in part, by certain members of AP-1 family of transcription factors (Shaulian and Karin, 2002; Zenz and Wagner, 2006). Altogether, our data suggest that CTIP2 directly or indirectly regulates expression of most of the known structural proteins and transcription factors implicated in the epidermal homeostasis and EPB formation.

CTIP2$^{-/-}$ mice exhibit defects in surface lipid distribution and decreased expression of lipid-metabolizing enzymes.

To determine if the observed barrier defect in the CTIP2$^{-/-}$ mutants was due to the altered distribution of polar and neutral lipids, we analyzed the surface lipid

distribution of mutant and wt epidermis by Nile Red staining. These studies revealed that neutral lipids were unevenly distributed along the cornified layer of the mutant epidermis, while forming a yellow-colored dense, continuous ribbon on top of the cornified layer in control fetuses (compare Figs. 4.4A and B). No significant changes were observed in the distribution of polar lipids between the wt and mutant epidermis (Figs. 4.4A and B, red-orange color). Altogether, these results suggest a possible alteration in the composition of the neutral lipids in the mutant skin.

Ultrastructural analysis of the epidermis from E17.5 fetuses did not reveal differences in the basal or spinous cell populations between control and CTIP2 mutants (data not shown). Likewise, similar numbers of desmosomes (D), keratohyaline granules (KG), keratin filaments (KF) and lamellar granules (LG; also called keratinosomes) were present in the granular cells of both control and CTIP2$^{-/-}$ mice (Fig. 4.4C and D, and data not shown). In the control fetuses, at the interface of granular and cornified cells, lipid discs that were extruded from the LGs were uniformly aligned and formed lipid lamellar membranes (Fig.4. 4E). In contrast, in mutant epidermis, the lipid discs were replaced by large vesicles (marked by arrows in Fig. 4.4F), and the intercellular (lipid) lamellar membranes (LL) in cornified layers were disorganised and highly variable in thickness (compare Fig. 4.4G to H, and I to J). Similar numbers of corneodesmosomes (CD) were present between the cornified cells in both control and mutant skin, however, the mutant CDs were smaller in size than the controls, and the mutant corneocytes were loosely packed (Fig. 4.4H and J).

These results suggest that impaired barrier formation in the CTIP2 mutant fetuses could be, at least in part, due to altered lipid metabolism in the developing skin.

The results of Nile red staining and TEM studies prompted us to perform RT-qPCR analyses for genes encoding proteins that are implicated in the lipid homeostasis in the developing skin (Fig. 4.4K). RT-qPCR revealed dysregulated expression of *Smpd3* (Mao-Qiang et al., 1996; Gurrieri et al., 2003), *Dgat2* (Stone et al., 2004), *Elovl4* (Cameron et al., 2007; Li et al., 2007; Vasireddy et al., 2007), *eLox3* (Furstenberger et al., 2007) and *Alox12b* (Moran et al., 2007), but not of *Gba2* (Holleran et al., 1994) or *Pla2gV* in the skin of CTIP2 mutants compared to wt controls (Fig. 4K). These results suggest that CTIP2 might directly or indirectly regulate genes implicated in lipid metabolism and in the formation of extracellular lipid matrix.

Generation of epidermis-specific CTIP2 knockout mice

To determine whether the observed defects in EPB formation in $CTIP2^{-/-}$ mice were a result of the cell-autonomous function of CTIP2 we generated an epidermis-specific CTIP2 knockout by crossing CTIP2 floxed mice ($CTIP2^{L2/L2}$, see Fig.1) with a K14-Cre transgenic mouse (Indra et al., 2000) to obtain a mouse line in which CTIP2 gene was specifically ablated in keratinocytes ($CTIP2^{ep-/-}$). To confirm the excision of the floxed CTIP2 allele in $CTIP2^{ep-/-}$ mice, we separated epidermis and dermis and genotyped both tissues for L- (excised) and L2 (floxed) alleles. L-, but not L2, alleles were detected in the epidermis of E17.5 $CTIP2^{ep-/-}$ fetuses (Fig. 4.5A, top), whereas

only L2 alleles were present in the dermis of these mice (Fig. 4.5A, bottom), thus demonstrating that CTIP2 was efficiently and selectively ablated in the keratinocytes of the developing epidermis. In agreement with this result CTIP2 protein was not detected in epidermal extracts from CTIP2$^{ep-/-}$ fetuses by immunoblotting, thus validating the CTIP2$^{ep-/-}$ mouse model (Fig. 4.5B). A modest up-regulation of the highly related CTIP1 (Avram et al., 2002) was observed in the mutant epidermis (Fig. 4.5B), which may be a compensatory response to the lack of CTIP2. Newborn litters were of the expected size and Mendelian ratios. CTIP2$^{ep-/-}$ mice were born without any apparent abnormalities, fed normally, survived into adulthood and were fertile.

CTIP2$^{ep-/-}$ mice exhibit compromised barrier function and increased transepidermal water loss during development

To determine if CTIP2 regulates EPB establishment in a cell-autonomous manner, we performed X-gal permeability assays on CTIP2$^{L2/L2}$ (as a control) and CTIP2$^{ep-/-}$ mice at E17.5 and E18.5 (Fig. 4.5C). Similar to CTIP2$^{-/-}$, CTIP2$^{ep-/-}$ mice exhibited a delay in barrier establishment. CTIP2$^{ep-/-}$ mice showed extensive blue staining on the ventral side of the body, limbs and the head at E17.5, and residual X-gal staining at E18.5, whereas control embryos showed very little coloration at either E17.5 or E18.5 (Fig. 4.5C). These results demonstrate that CTIP2, in a cell-autonomous manner, regulates EPB formation during fetal development. We further investigated this in the TEWL experiments. The rate of water evaporation from the dorsal skin of E17.5 CTIP2$^{ep-/-}$ mice was about three-fold higher than that of the control mice (Fig.

5D, left panel) but at E18.5 the difference in water loss on the dorsal side was not significant (Fig. 4.5D, right panel). Transepidermal water loss from the ventral side of the body of CTIP2$^{ep-/-}$ mice only slightly exceeded that of the control mice at E17.5, however was still 2.5-fold higher at E18.5. These findings suggest that CTIP2$^{ep-/-}$ mice exhibit considerable permeability barrier defects and recapitulate the barrier phenotype of CTIP2$^{-/-}$ mice.

CTIP2$^{ep-/-}$ mice develop histologically normal epidermis

The X-gal diffusion assay and TEWL measurements demonstrated that CTIP2$^{ep-/-}$ mice exhibited epidermal barrier defects in the late stages of development, which prompted us to examine the epidermis of these mice at the histological level at E17.5 and E18.5 (Fig. 4.5E). Unexpectedly, histological analyses revealed that the skin thickness and architecture of CTIP2$^{ep-/-}$ mice was indistinguishable from that of wt mice. All the epidermal layers were present and the cornified layer appeared relatively normal at both stages. Immunohistochemical and Immunoblot analyses did not reveal any significant changes in levels of expression of epidermal markers K1, K10, K14, involucrin, filaggrin and loricrin (data not shown).

Microarray analysis of CTIP2$^{ep-/-}$ skin revealed downregulation of enzymes involved in lipid metabolism and alterations in the epidermal differentiation complex (EDC)

To gain insights into the molecular mechanisms of permeability barrier defects in the conditional CTIP2$^{ep-/-}$ mice, we performed expression profiling of dorsal skin RNA from E17.5 CTIP2$^{ep-/-}$ and CTIP2$^{L2/L2}$ mice (Fig. 4.6). We found that out of the total 45,000 probe sets, only 1688 probe sets, corresponding to 750 unique genes were significantly altered (up- or down-regulated), indicating that epidermal-specific deletion of CTIP2 leads to a highly selective (< 1%) alteration in gene expression (Fig. 4.6A).

The transcriptome analyses revealed that genes implicated in lipid homeostasis were also down-regulated in CTIP2$^{ep-/-}$ epidermis (data not shown). Indeed, Nile Red staining performed on E17.5 CTIP2$^{ep-/-}$ skin confirmed that the surface distribution of neutral lipids was impaired as it appeared uneven in CTIP2$^{ep-/-}$ skin, signifying that lipid metabolism is defective in mutant skin (compare Fig. 4.6C and D). Several of these differentially expressed genes involved in lipid metabolism (*Smpd3*, *Dgat2*, *Elovl4*, *eLox3*, *Alox12b*) as well as *Tgase1* and *Caspase14* were analyzed by RT-qPCR analyses (Fig. 4.6E). We confirmed that the expression of most of these lipid-metabolizing enzymes was downregulated in CTIP2$^{ep-/-}$ skin.

Most interestingly, approximately half of the genes within the epidermal differentiation complex (EDC), which is located in two adjacent bands on chromosome 3 (3qF1 and 3qF2.1; see Fig. 4.6B) and encodes structural proteins of the cornified envelope, were found to be dysregulated in CTIP2$^{ep-/-}$ mice, and the majority of those were down-regulated in mutant skin. This finding suggests that

CTIP2 directly or indirectly activates expression of many genes of the EDC complex in the developing epidermis. Altogether, these findings suggest that CTIP2 is involved in cell-autonomous regulation of lipid metabolism and barrier establishment in skin.

CTIP2 is involved in controlling the mesenchymal-epithelial crosstalk through regulation of KGF expression in the dermis

To test our hypothesis that CTIP2 may non-cell autonomously regulate proliferation of epidermis we analyzed expression of several diffusible factors known to be involved in the control of keratinocyte proliferation by RT-qPCR. We compared the levels of expression of KGF, GM-CSF and HBEGF in whole-skin RNA extracts from wt, CTIP2$^{-/-}$ and CTIP2$^{ep-/-}$ fetuses (Fig. 4.7A). KGF was down-regulated by almost 60% in the CTIP2$^{-/-}$ mice; however the expression level of KGF was similar to wt levels in the skin of the CTIP2$^{ep-/-}$ mice. Reduced expression of KGF in the dermis of the total knockout mice could be (at least partially) responsible for the observed hypoplasticity of the CTIP2$^{-/-}$ epidermis (Fig. 4.2F). In skin of CTIP2$^{ep-/-}$ mice, CTIP2 expression is preserved in the dermis and the levels of KGF are normal, which could explain, at least in part, the development of morphologically normal epidermis (Fig. 4.5E), and underlie the non-cell autonomous role of CTIP2 in epidermal development. We also observed about 25% downregulation of GM-CSF and HBEGF in the skin of the CTIP2$^{-/-}$ mice, although the levels of these transcripts remained the same in the conditional skin.

Discussion

We identify herein a novel regulator of gene expression and the developmental program responsible for establishment of the epidermal protective barrier during skin organogenesis. In the absence of CTIP2, the epidermal developmental program is perturbed leading to the thinning of the epidermis with a corresponding reduction in a number of differentiated cell layers. Terminal keratinocyte differentiation is also impaired, most likely owing to disrupted gene expression in CTIP2$^{-/-}$ mice, contributing to a delay in EPB establishment and increased transepidermal water loss. Thus, CTIP2 appears to be a key regulator of skin developmental processes, in which it functions in both cell and non-cell autonomous contexts.

CTIP2 is required for epidermal barrier establishment

The results of X-gal diffusion assays indicated that barrier formation was severely disrupted in CTIP2$^{-/-}$ mice at E17.5 but this defect was largely overcome by E18.5, suggesting that barrier formation was most likely delayed in CTIP2$^{-/-}$ mice. However, a substantial degree of epidermal hypocellularity was observed in CTIP2$^{-/-}$ mice at E18.5, which led us to conclude that EPB formation and/or function remained disrupted in CTIP2$^{-/-}$ mice at this developmental stage. Indeed, TEWL measurement taken at E18.5 demonstrated an increased rate of water loss in CTIP2$^{-/-}$ mice as compared to wt controls, demonstrating that barrier defects persisted at E18.5 in the

mutants. The apparent disparity between results of X-gal and TEWL assays in the mutant mice at E18.5 may be due to the relatively impreciseness of the former assay. Nonetheless, it is unquestionably true that the barrier defect is less severe at E18.5 than at E17.5 in CTIP2$^{-/-}$ mice, and this may be explained by compensatory mechanisms. The highly related CTIP1 is expressed in skin (see Fig. 5.5B) and shares many functional properties with CTIP2. For example, both CTIP1 and CTIP2 interact with COUP-TF family members (Avram et al., 2000), exhibit identical sequence-specific DNA binding activity (Avram et al., 2002), and repress transcription via similar mechanisms (Senawong et al., 2003; Cismasiu et al., 2005; Senawong et al., 2005). Although the distribution and function of CTIP1 in skin are unknown, CTIP1 could, in principle, compensate for the lack of CTIP2, which may explain the "recovery" of the barrier defect that we observe at E18.5 in CTIP2$^{-/-}$ and CTIP2$^{ep-/-}$ mice. Consistent with this hypothesis we detected a modest up-regulation of CTIP1 expression in the epidermal extracts of CTIP2$^{ep-/-}$ mice as compared to those prepared from wild-type animals.

Barrier defects can be caused by inappropriate expression of proteins involved in the assembly and crosslinking of the cornified envelope, and/or inadequate lipid processing in the granular and cornified layers, which can result in defective lipid lamellae formation. Gene expression profiling performed on CTIP2$^{ep-/-}$ mice confirmed the involvement of CTIP2 in control of epidermal differentiation and barrier formation as around 50% of the genes of the epidermal differentiation complex (EDC)

were downregulated together with altered expression of most of the lipid metabolizing enzymes in the skin.

The irregular distribution of neutral surface lipids (and increased water loss through the breached areas), abnormal lipid discs and lipid lamellar structures in the mutant mice may be a consequence of the relative deficiency in lipid-metabolizing enzymes in CTIP2 mutant mice. Mutations in and inhibition of these enzymes, such as *Elovl4, Dgat2*, *Gba2*, *Smpd3*, *Alox12b*, *eLox3*, *Pla2gV*, and *Pla2gVI* have been linked to alteration in barrier integrity (Mao-Qiang et al., 1996; Gurrieri et al., 2003; Stone et al., 2004; Cameron et al., 2007; Epp et al., 2007; Furstenberger et al., 2007; Vasireddy et al., 2007). Keratinocyte terminal differentiation and EPB formation were similarly affected in skin from both CTIP2 null mice and mice that lacked CTIP2 only in the epidermis ($CTIP2^{ep-/-}$), suggesting a cell autonomous effect of CTIP2 in the keratinocyte lineage.

CTIP2 is involved in epidermal homeostasis and control of keratinocyte proliferation and differentiation

The hypoplasticity of $CTIP2^{-/-}$ epidermis is most likely the result of insufficient proliferation and/or altered differentiation. CTIP2 is expressed in all basal cells, some suprabasal cells, and the $K15^{+}CD34^{-}$ population of stem cells (Golonzhka et al., 2007). We observed significant reduction in epidermal proliferation and early differentiation in the skin of $CTIP2^{-/-}$ mice compared to the control mice. In the same line, expression

of several factors that are implicated in the control of epidermal proliferation and differentiation, including *p63*, *c-Myc*, *GATA3*, *c-fos*, *Klf4*, *KGF* (Byrne et al., 1994; Mills et al., 1999; Pelengaris et al., 1999; Waikel et al., 1999; Yang et al., 1999; Yokota et al., 1999; Grachtchouk et al., 2000; Langlands et al., 2000; Arnold and Watt, 2001; Mill et al., 2003; Koster et al., 2004; Simbulan-Rosenthal et al., 2005; de Guzman Strong et al., 2006; Yu et al., 2006; Koster et al., 2007) was down-regulated in CTIP2$^{-/-}$ mice, suggesting that CTIP2 directly or indirectly regulates the corresponding promoters. Interestingly, expression of *Id2* and *p57* was up-regulated in CTIP2$^{-/-}$ epidermis. *p57* (Topark-Ngarm et al., 2006) and *Id2* (Leid, et al., submitted) are known, direct targets of CTIP2 in neuroblastoma cells and thymocytes, respectively, and is very likely that CTIP2 directly regulates expression of p57 in keratinocytes as well.

As was observed in CTIP2$^{-/-}$ mice, conditional ablation of CTIP2 in keratinocytes resulted in delayed EPB formation in the CTIP2$^{ep-/-}$ mice. However, conditional ablation of CTIP2 in keratinocytes did not significantly alter the proliferation or differentiation programs of these cells and the epidermis of CTIP2$^{ep-/-}$ mice was indistinguishable from that of wt mice. This demonstrates that CTIP2 is dispensable for keratinocyte proliferation and early differentiation events. In that case it would appear that CTIP2 is acting non-cell autonomously, possibly by controlling the expression of dermal factors that regulate epidermal morphogenic events in a paracrine fashion. Indeed, we observed down-regulation of keratinocyte

growth factor (KGF), a dermal fibroblast-derived growth factor in CTIP2$^{-/-}$, but not in CTIP2$^{ep-/-}$ mice, suggesting that KGF may play a role in the non-cell autonomous effects of CTIP2 in keratinocytes. Interactions between mesenchymal and epithelial cells play an important role in regulating tissue development and homeostasis (Ronnov-Jessen et al., 1996; Angel et al., 2001; Angel and Szabowski, 2002). Similar, non-cell autonomous effects in skin have been reported for c-Jun and IKK1 (Gareus et al., 2007; Szabowski et al., 2000). KGF and granulocyte macrophage colony stimulating factor (GM-CSF), whose expressions were positively controlled by c-Jun, were identified as key regulators of the paracrine loop responsible for fine tuned balance of keratinocyte proliferation and differentiation (Szabowski et al., 2000). c-Jun also regulates expression of HBEGF and EGFR in keratinocytes in a cell autonomous manner and mice lacking c-Jun specifically in epidermis do not display obvious skin phenotype (Li et al., 2003; Gareus et al., 2007). Interestingly, we did not observe any significant change in c-Jun expression in skin of CTIP2$^{-/-}$ or CTIP2$^{ep-/-}$ mice, suggesting an alternative mechanism of regulating expression of KGF or GMCSF. Mice harboring a germline deletion of IKK1 exhibit severe defects in epidermal differentiation, defective EPB function and increased TEWL, much like CTIP2$^{-/-}$ mice (Li et al., 1999). However, the epidermis in keratinocyte-specific IKK1 knockout mice develops normally in a histological/morphological sense, but this mouse still displays the impaired barrier and increased TEWL (Gareus et al., 2007). Further analysis of IKK1 total knockouts revealed that IKK1 may influence epidermal development in a

non-cell autonomous fashion thorough the regulation of expression/release of yet unidentified diffusible factor(s) from the dermis (Gareus et al., 2007). Nonetheless, the parallels between the cell and non-cell autonomous actions of CTIP2 and IKK1 in the epidermis are striking, and suggest a convergence in the two pathways within dermal fibroblasts.

Conclusion and future directions

In the present study, epidermal keratinocyte specific ablation of CTIP2 gene revealed that CTIP2 cell-autonomously controls barrier establishment in a multifaceted fashion, affecting all stages of that process. It is possible that CTIP2 plays specific role(s) in suprabasal cells of the epidermis, and this can be further addressed by deleting CTIP2 in those cells using a K10-Cre-ERT2 transgenic mouse line (Calleja et al., 2006). Similarly, the role of CTIP2 in maintaining the adult skin homeostasis can be further clarified by analyzing the effects of the acute loss of CTIP2 in adult skin by using an inducible Cre system (Indra et al., 2005a; Indra et al., 2005b; Rodius et al., 2007).

CTIP2 is also involved in controlling epidermal proliferation and morphogenesis, in a non-cell-autonomous fashion, through control of expression of diffusible factors in dermal cells. To gain insights into the function of "mesenchymal" CTIP2 and its role in controlling the epidermal proliferation/differentiation program, a

mouse line lacking CTIP2 specifically in the dermis, using fibroblast-specific Cre transgenic lines, will need to be generated and analyzed (Florin et al., 2004).

CTIP2 was originally identified as a transcriptional repressor (Avram et al., 2000), and we would predict that ablation of CTIP2 would result in de-repression of its transcriptional targets. However, majority of the genes identified in expression profiling analyses of mutant mice were downregulated in absence of CTIP2. That could represent an indirect effect of CTIP2 ablation or perhaps a direct effect of the absence of CTIP2 on the promoters of the corresponding genes. While transcriptional repression mechanisms of CTIP2 have been well studied (Senawong et al., 2003, Topark-Ngarm et al., 2006, Cismasiu et al., 2006), the mechanistic basis for CTIP2 acting as a transcriptional activator has not, but may involve recruitment of the coactivators p300 and/or CBP to the target promoter template (Cismasiu et al., 2006). Further analyses will be required to unravel the mechanism(s) of transcriptional regulation mediated by CTIP2 in the skin in health and disease.

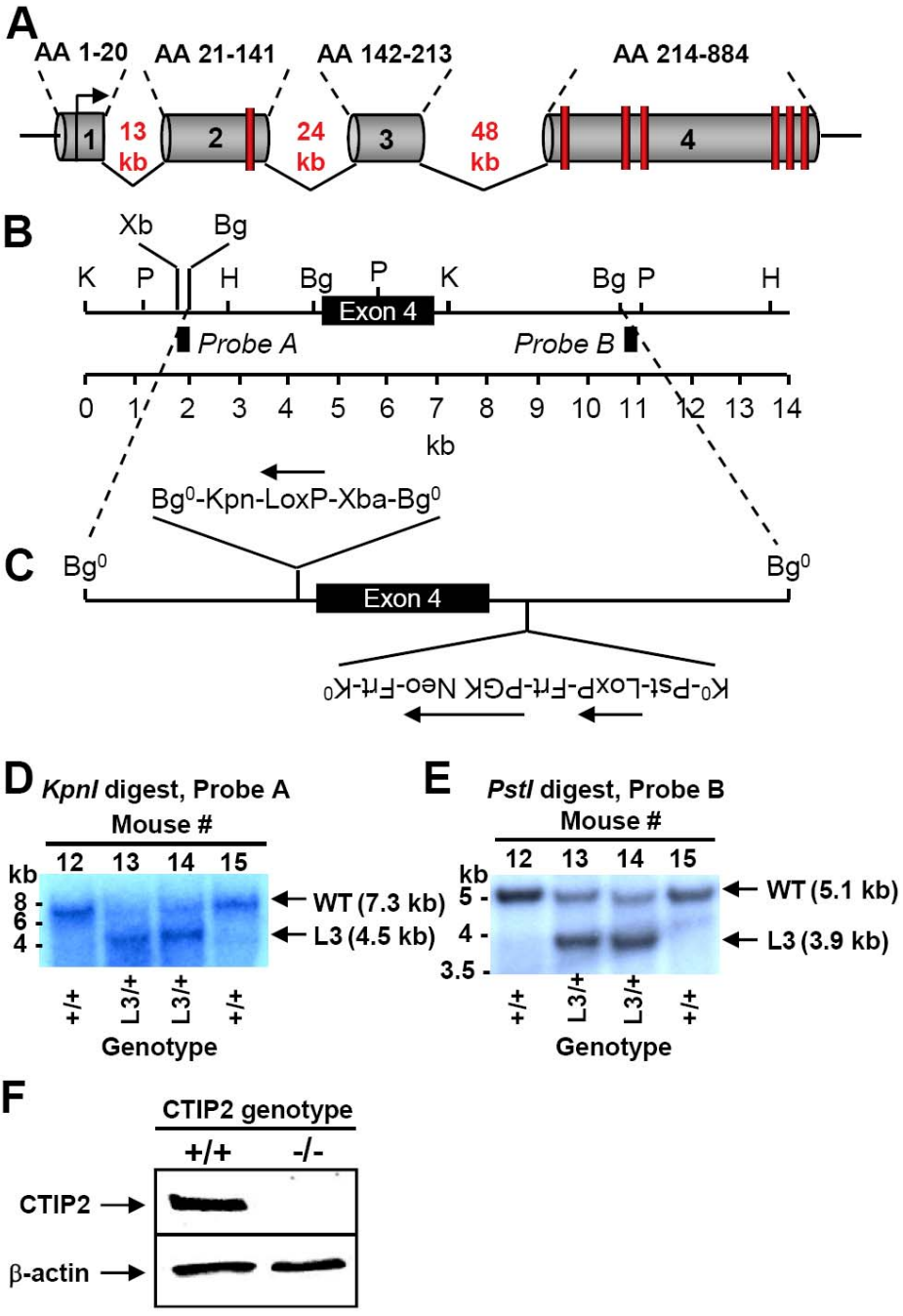
A
AA 1-20
AA 21-141
AA 142-213
AA 214-884
1
13 kb
2
24 kb
3
48 kb
4
B
Xb
Bg
K
P
H
Bg
P
K
Bg
P
H
Exon 4
Probe A
Probe B
0 1 2 3 4 5 6 7 8 9 10 11 12 13 14
kb
Bg0-Kpn-LoxP-Xba-Bg0
C
Bg0
Exon 4
Bg0
K0-PSt-LoxP-Frt-PGK Neo-Frt-K0
D
KpnI digest, Probe A
Mouse #
12 13 14 15
kb
8
6
4
WT (7.3 kb)
L3 (4.5 kb)
+/+ L3/+ L3/+ +/+
Genotype
E
PstI digest, Probe B
Mouse #
12 13 14 15
kb
5
4
3.5
WT (5.1 kb)
L3 (3.9 kb)
+/+ L3/+ L3/+ +/+
Genotype
F
CTIP2 genotype
+/+ -/-
CTIP2
β-actin

Figure 4.1. Floxing the CTIP2 locus.

A, Schematic representation of the mouse CTIP2 locus with exons 1-4 and corresponding amino acids (top). The vertical red bars represent C_2HC (exon 2) or C_2H_2 zinc finger motifs (exon 4).
B, Magnification of exon 4 and flanking sequences with selected restriction sites and location of Southern probes.
C, Schematic representation of the CTIP2 targeting vector indicating the direction of upstream and downstream LoxP sites and PGK-neo. PGK-neo was flanked by Frt sites for excision by Flp recombinase. Restriction sites were introduced into both the upstream and downstream LoxP sites to facilitate analyses of HR at the CTIP2 locus.
D-E,Southern analyses of HR at the CTIP2 locus using 5' (Probe A in panel A) and 3' (Probe B in panel A) probes, respectively. The L3 genotype refers to presence of the entire targeting vector, including the PGK-neo, into the CTIP2 locus by HR.
F, Immunoblot of whole cell extracts prepared from E18.5 skin from $CTIP2^{+/+}$ and $CTIP2^{-/-}$ mice using an anti-CTIP2 monoclonal antibody.

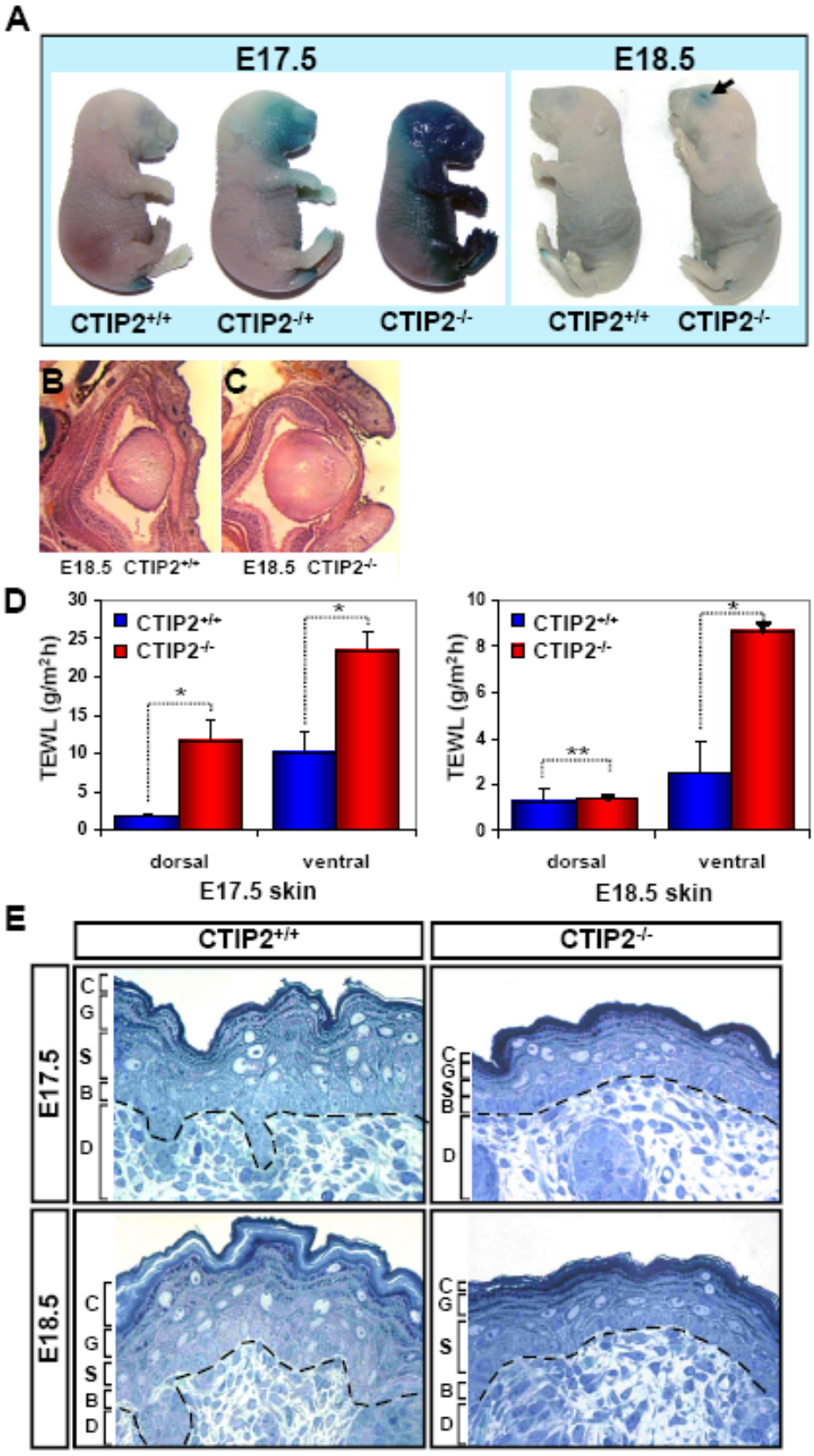
A
E17.5
E18.5
CTIP2+/+
CTIP2-/+
CTIP2-/-
CTIP2+/+
CTIP2-/-
B
C
E18.5 CTIP2+/+
E18.5 CTIP2-/-
D
TEWL (g/m²h)
CTIP2+/+
CTIP2-/-
dorsal
ventral
E17.5 skin
E18.5 skin
E
CTIP2+/+
CTIP2-/-
E17.5
E18.5
C
G
S
B
D

Figure 4.2. CTIP2$^{-/-}$ mice exhibit permeability barrier defects and epidermal hypoplasia.

A, X-gal diffusion assay performed on CTIP2$^{+/+}$ and CTIP2$^{-/-}$ fetuses at E17.5 and E18.5.
B-C, H & E staining of coronal section of the eye in CTIP2$^{+/+}$ (C) and CTIP2$^{-/-}$ (D) mice at E18.5.
D, Transepidermal water loss measurements from dorsal and ventral skin of CTIP2$^{+/+}$ and CTIP2$^{-/-}$ mice at E17.5 and E18.5. (Plotted are mean measurements of three independent mice per genotype ± S.E.M.). * - $p<0.05$, ** - not statistically significant.
F, Histology of toluidine blue stained dorsal skin biopsies of CTIP2$^{+/+}$ and CTIP2$^{-/-}$ mice at E17.5 and E18.5. Marked epidermal hypoplasia was observed in CTIP2$^{-/-}$ mice. D-dermis, B- basal layer, S-spinous layer, G-granular layer, c-cornified layer

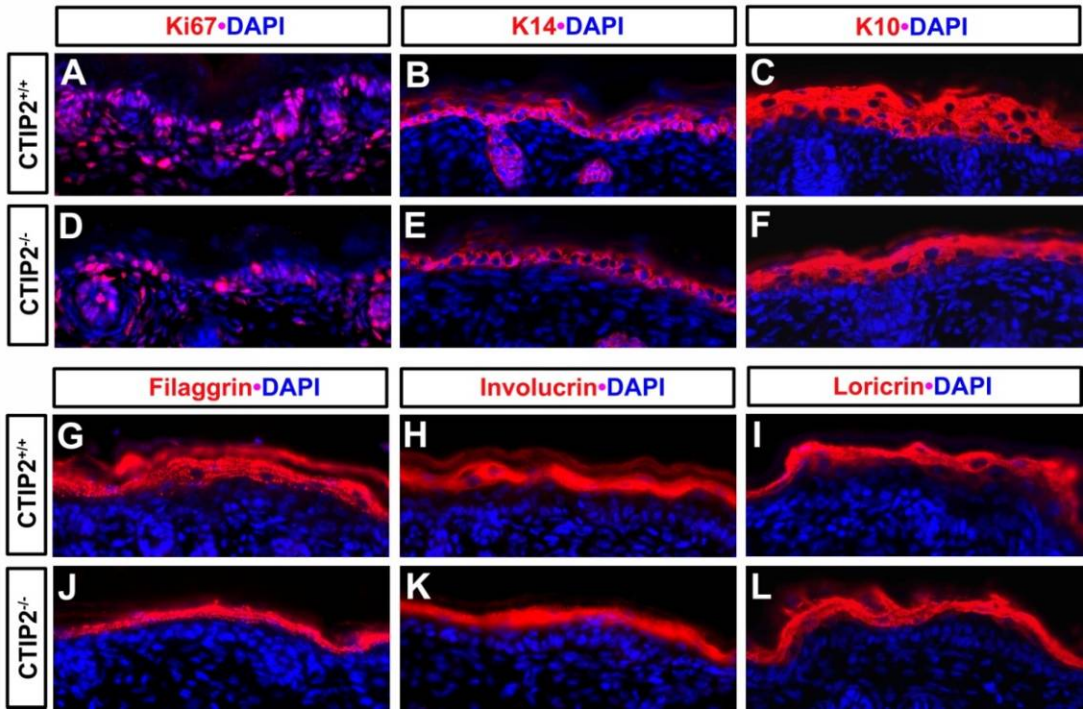
Ki67•DAPI
K14•DAPI
K10•DAPI
CTIP2+/+
CTIP2-/-
A
B
C
D
E
F
Filaggrin•DAPI
Involucrin•DAPI
Loricrin•DAPI
G
H
I
J
K
L

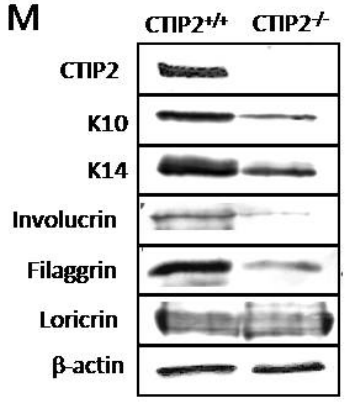
M
CTIP2+/+
CTIP2-/-
CTIP2
K10
K14
Involucrin
Filaggrin
Loricrin
β-actin

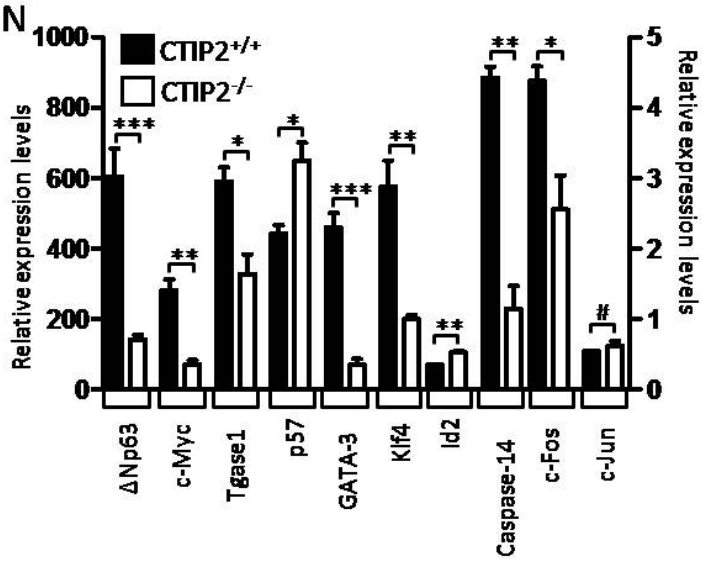
N
CTIP2+/+
CTIP2-/-
Relative expression levels
1000
800
600
400
200
0
5
4
3
2
1
0
***
**
*
*
***
**
**
**
*
#
ΔNp63
c-Myc
Tgase1
p57
GATA-3
Klf4
Id2
Caspase-14
c-Fos
c-Jun

Figure 4.3. Decreased expression of epidermal markers and genes involved in epidermal barrier establishment in CTIP2$^{-/-}$ mice.

A-H, Immunohistochemistry of dorsal skin of CTIP2$^{+/+}$ and CTIP2$^{-/-}$ mice at E18.5. Genotypes and antibodies (red staining) used are indicated, and all sections were counterstained with DAPI (blue). SB-suprabasal layers, B- basal layer, D-dermis.
G-L, Immunohistochemistry of dorsal skin with late differentiation markers loricrin, involucrin and filaggrin (all in red) in CTIP2$^{+/+}$ and CTIP2$^{-/-}$ mice at E18.5. All sections were counterstained with DAPI (blue). Abbreviations are as in A-H.
M, Immunoblot of dorsal skin extracts from CTIP2$^{+/+}$ and CTIP2$^{-/-}$ mice at E18.5 using indicated antibodies.
N, RT-qPCR analysis of dorsal skin from CTIP2$^{+/+}$ and CTIP2$^{-/-}$ mice at E18.5. Relative expression levels for all genes are shown on Y-axis to the left, except for c-Fos and c-Jun, which are plotted on the right Y-axis. Statistical significance denotations: * - $p < 0.05$; ** - $p < 0.01$; *** - $p < 0.001$; # - no statistically significant difference between wt and mutant mice.

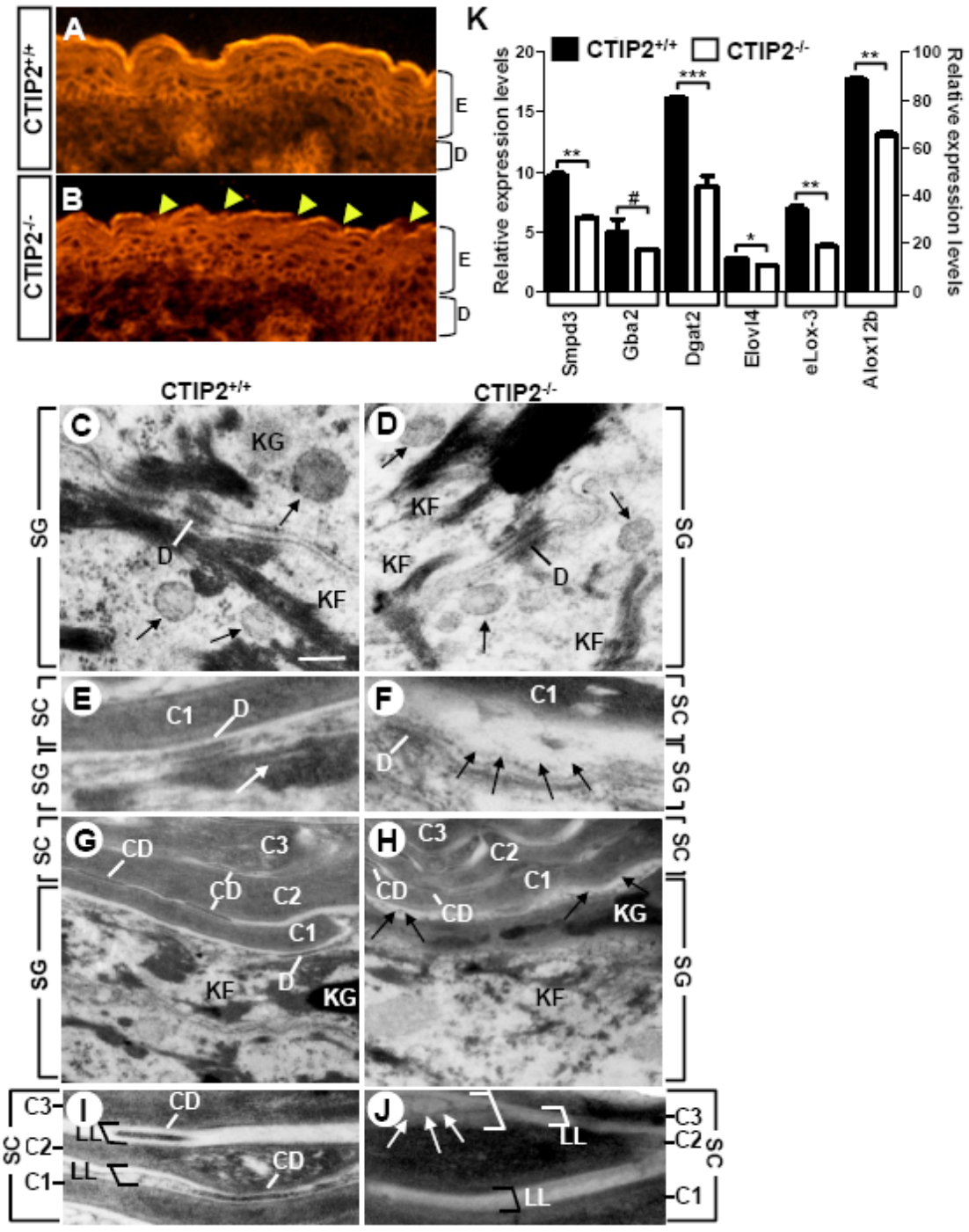
A
B
CTIP2+/+
CTIP2-/-
E
D
K
CTIP2+/+
CTIP2-/-
Relative expression levels
Relative expression levels
Smpd3
Gba2
Dgat2
Elovl4
eLox-3
Alox12b
CTIP2+/+
CTIP2-/-
C
D
KG
KF
D
SG
SC
E
F
C1
G
H
CD
C3
C2
C1
I
J
LL
C3
C2
C1
SC

Figure 4.4. Defects in lipid distribution and expression of lipid-processing enzymes in CTIP2$^{-/-}$ mice.

A-B, Nile red staining of skin from CTIP2$^{+/+}$ and CTIP2$^{-/-}$ mice at E18.5. Arrowheads indicate an absence of neutral lipids on the skin surface of the mutant mice. E-epidermis, D-dermis.

C-J, Transmission electron microscopy of dorsal skin from CTIP2$^{+/+}$ and CTIP2$^{-/-}$ mice at E17.5 as indicated. SG-Stratum granulosum, SC-stratum corneum, D-desmosomes, CD-corneodesmosomes, KF-keratin filaments, KG- keratohyalin granules. C1, C2 and C3- cornified
cell layers, LL–lipid lamellae. Large white arrows in E point towards the lamellar granules (LG) at the SG-SC interface. White and black lines in E, F, G and H indicate desmosomes (D) and corneodesmosomes, respectively; black arrows in F and H indicate vesicles at the interface of SG and SC. White arrows in J point towards vesicles. Black and white brackets in I and J indicate LL. Scale bar in C: 0.2 µm for C-F; 0.4 µm for G and H; and 0.25 µm for I and J.

K, RT-qPCR analyses for expression of selected genes involved in lipid homeostasis in dorsal skin from CTIP2$^{+/+}$ and CTIP2$^{-/-}$ mice at E18.5. Relative expression levels for all genes are shown on Y-axis to the right, except for eLox3 and Alox12b, which are plotted on the right Y-axis. Statistical significance denotations: *- $p < 0.05$; **- $p < 0.01$; ***- $p < 0.001$; #: no statistically significant difference between wt and mutant mice.

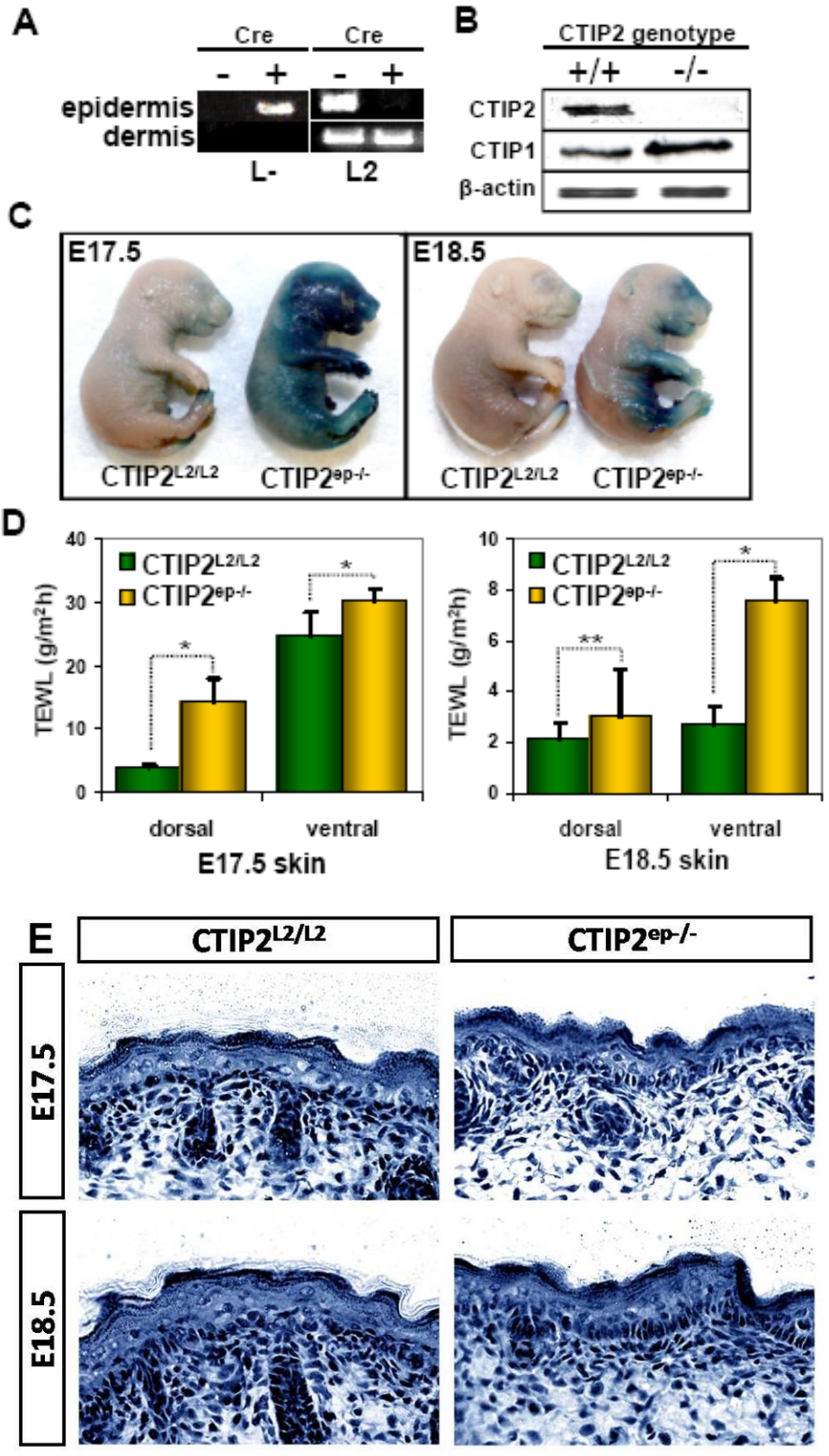
A
Cre
Cre
- + - +
epidermis
dermis
L- L2
B
CTIP2 genotype
+/+ -/-
CTIP2
CTIP1
β-actin
C
E17.5
E18.5
CTIP2L2/L2
CTIP2ep-/-
CTIP2L2/L2
CTIP2ep-/-
D
CTIP2L2/L2
CTIP2ep-/-
TEWL (g/m2h)
dorsal
ventral
E17.5 skin
CTIP2L2/L2
CTIP2ep-/-
TEWL (g/m2h)
dorsal
ventral
E18.5 skin
E
CTIP2L2/L2
CTIP2ep-/-
E17.5
E18.5

Figure 4.5. CTIP2$^{ep-/-}$ mice exhibit barrier defects, increased water loss and normal epidermis.

A, PCR detection of the CTIP2 L- and L2 alleles in the epidermis and mesenchyme at E17.5. Note that the L- allele is detected only in the epidermis in the presence of the Cre transgene (+ cre).
B, Immunoblot analysis for CTIP2 and CTIP1 proteins in epidermal protein extracts from CTIP2$^{L2/L2}$ and CTIP2$^{ep-/-}$ fetuses at E17.5.
C, X-gal diffusion assay performed on CTIP2$^{L2/L2}$ and CTIP2ep$^{-/-}$ fetuses at E17.5 and E18.5, as indicated.
D, TEWL measurements from dorsal and ventral skin of CTIP2$^{L2/L2}$ and CTIP2$^{ep-/-}$ fetuses at E17.5 and E18.5. Mean measurements of three independent mice per genotype ± S.E.M. are shown.
E, Histology of dorsal skin biopsies from CTIP2$^{L2/L2}$ and CTIP2$^{ep-/-}$ mice at E17.5 and E18.5. D-dermis, B- basal layer, S-spinous layer, G-granular layer, C-cornified layer.

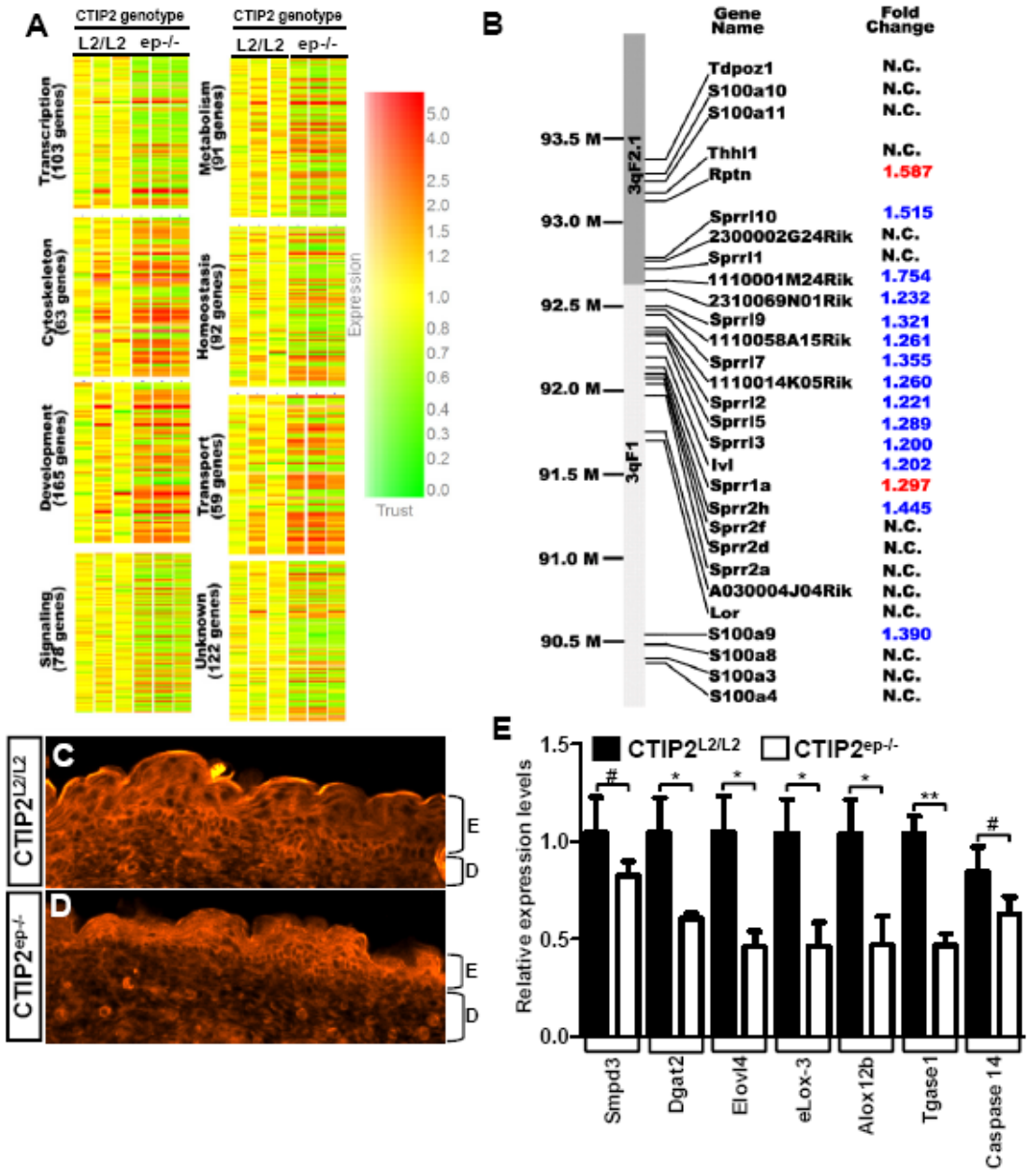
A
CTIP2 genotype
L2/L2
ep-/-
Transcription (103 genes)
Metabolism (91 genes)
Cytoskeleton (63 genes)
Homeostasis (92 genes)
Development (165 genes)
Transport (59 genes)
Signaling (78 genes)
Unknown (122 genes)
Expression
Trust
5.0
4.0
2.5
2.0
1.5
1.2
1.0
0.8
0.7
0.6
0.4
0.3
0.2
0.0
B
Gene Name
Fold Change
3qF2.1
3qF1
93.5 M
93.0 M
92.5 M
92.0 M
91.5 M
91.0 M
90.5 M
Tdpoz1 N.C.
S100a10 N.C.
S100a11 N.C.
Thhl1 N.C.
Rptn 1.587
Sprrl10 1.515
2300002G24Rik N.C.
Sprrl1 N.C.
1110001M24Rik 1.754
2310069N01Rik 1.232
Sprrl9 1.321
1110058A15Rik 1.261
Sprrl7 1.355
1110014K05Rik 1.260
Sprrl2 1.221
Sprrl5 1.289
Sprrl3 1.200
Ivl 1.202
Sprr1a 1.297
Sprr2h 1.445
Sprr2f N.C.
Sprr2d N.C.
Sprr2a N.C.
A030004J04Rik N.C.
Lor N.C.
S100a9 1.390
S100a8 N.C.
S100a3 N.C.
S100a4 N.C.
C
D
CTIP2L2/L2
CTIP2ep-/-
E
D
E
CTIP2L2/L2
CTIP2ep-/-
Relative expression levels
1.5
1.0
0.5
0.0
#
*
*
*
*
**
#
Smpd3
Dgat2
Elovl4
eLox-3
Alox12b
Tgase1
Caspase 14

Figure 4.6. Microarray analyses of CTIP2$^{ep-/-}$ mice indicate that CTIP2 is a top-level transcription factor in skin development.

A, Cluster analysis of individual skin samples taken from three CTIP2$^{L2/L2}$ and three CTIP2$^{ep-/-}$ mice. Results were filtered by expression level (threshold was set for a 1.5-fold change) and t-test using Benjamini and Hochberg False Discovery Rate (< 20%). Genes that met both requirements were sorted according to their function. The color code used for the fold changes are: red = up-regulated; green = down-regulated, yellow = no change.
B, Epidermal differentiation complex (EDC) genes mapped onto mouse chromosome 3. Fold changes in gene expression for all genes of the EDC complex in CTIP2$^{ep-/-}$ skin mice are represented. Genes up- or down-regulated are shown in “red” and “blue”, respectively; N.C.-no change.
C-D, Nile red staining of CTIP2$^{L2/L2}$ (C) and CTIP2$^{ep-/-}$ (E) mouse skin at E17.5. E-epidermis, D-dermis.
E, RT-qPCR validation of CTIP2 target genes involved in lipid metabolism and barrier establishment. Statistical denotations: * - $p < 0.05$; ** - $p < 0.01$; *** - $p < 0.001$; # - no statistically significant difference between CTIP2L2/L2 and CTIP2ep-/- mice.

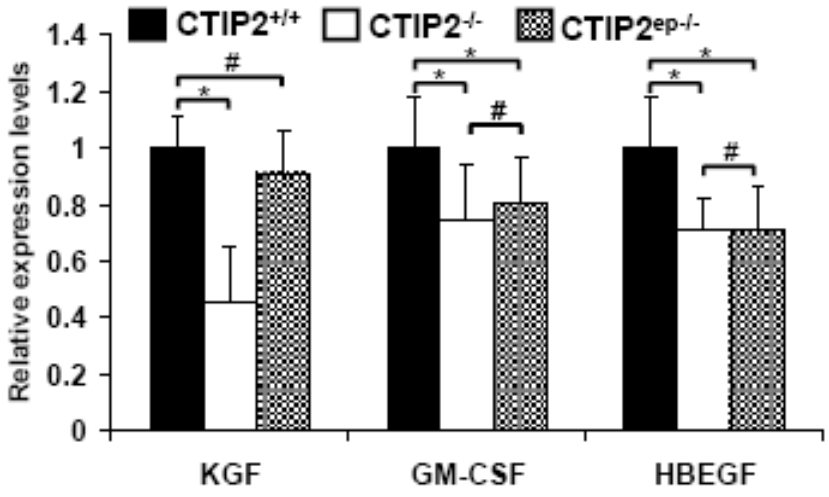

Figure 4.7. CTIP2 regulates expression of growth factors involved in mesenchymal-epithelial crosstalk for maintaining epidermal homeostasis.

RT-qPCR analysis of genes encoding growth factors KGF, GM-CSF and HBEGF in the skin of E18.5 CTIP2$^{+/+}$, CTIP2$^{-/-}$ and CTIP2$^{ep-/-}$ fetuses. Statistical denotations: * - $p < 0.05$; # - no statistically significant difference between different groups.

CHAPTER 5

CTIP2 Controls the Terminal Differentiation of Ameloblasts

Olga Golonzhka, Chrissa Kioussi, Mark Leid

Prepared for submission to Development

Abstract

CTIP2 (also known as Bcl11b) is a transcription factor that plays an essential role in the development of the skin, central nervous and immune systems. Here we show that CTIP2 is also highly expressed in the developing tooth and plays an important role in development of the craniofacial complex. CTIP2 is preferentially expressed in the ectodermal organs of the tooth, including inner and outer enamel epithelia, stellate reticulum, stratum intermedium and ameloblast cell lineage. CTIP2 is also present, although at much lower levels, in the mesenchyme at the very early stages of the tooth development however CTIP2 expression was not detected in the dental papilla or odontoblasts.

Analyses of the tooth development in mice with a germline deletion of CTIP2 revealed that this protein plays and important role in late stages of the tooth development. Mutant tooth germs developed normally through the cap stage, however, multiple defects were observed at the bell stage. The sizes of the incisors and molars were reduced in the CTIP2 mutants, the stellate reticulum structure was found to be hypoplastic and the lower incisors developed an ectopic ameloblast cell population on the lingual aspect of the tooth. CTIP2 ablation also severely affected the terminal differentiation of the ameloblasts, cells responsible for enamel production. Ameloblast morphology, polarization and adhesion were also severely disrupted in CTIP2 mutants. Finally, large-scale perturbation of gene expression was observed in the oral cavity of CTIP2 mutant mice. For example, the expression of

several ameloblast markers, including amelogenin, ameloblastin and enamelin was downregulated in CTIP2$^{-/-}$ mice, as was expression of MSX2 and epiprofin, both of which have been implicated in the tooth development and ameloblast differentiation. Moreover, the two latter genes appear to be direct targets of CTIP2, as demonstrated by chromatin immunoprecipitation (ChIP) analyses.

Together, our results suggest that CTIP2 functions as a critical regulator of the epithelial cell fate, differentiation, and tooth morphogenesis.

Introduction

Teeth develop as a result of the coordinated molecular interactions between the ectoderm of the first branchial arch and the underlying neural crest-derived mesenchyme (Mina and Kollar, 1987; Lumsden, 1988). Oral ectoderm induces the odontogenic potential of the mesenchyme and initiates tooth development (Lumsden, 1988). Around embryonic day 10.5 (E10.5), a thickening of the oral ectoderm occurs at the sites of the future tooth resulting in a formation of the dental lamina. Subsequent expansion of the dental lamina into an underlying mesenchyme leads to the formation of the tooth bud (bud stage, E12.5). Bud stage is followed by the cap stage (E14.5) as a result of expansion and folding of the dental ectoderm (Miletich and Sharpe, 2003; Thesleff, 2003). Transition from the bud to cap stage is regulated by the transient signaling center – the primary enamel knot – which forms

at the tip of the epithelial tooth bud. The enamel knot expresses numerous signaling molecules belonging to FGF, BMP, Wnt and Hh pathways and stimulates proliferation of the surrounding epithelial cells as well as the mesenchyme (Vaahtokari et al., 1996; Thesleff and Sharpe, 1997; Thesleff et al., 2001; Tucker and Sharpe, 2004). Epithelium continues to expand and differentiates into the inner enamel epithelium (IEE) and outer enamel epithelilum (OEE), stratum intermedium and stellate reticulum (Lumsden, 1988). The junctions between IEE and OEE called cervical loops grow and engulf the mesenchyme (dental papilla) (bell stage, E16). The secondary enamel knots form in the molar teeth and trough secretion of various signaling molecules instruct formation of the future cusps and late tooth differentiation (Thesleff et al., 2001) .

Two tooth-specific cell types are formed at the bell stage of odontogenesis: ameloblasts – enamel secreting cells, which differentiate from the inner enamel epithelium, and odontoblasts – dentin-secreting cells, which are derived from the dental mesenchyme (Ruch et al., 1995; Zeichner-David et al., 1995; Thesleff and Sharpe, 1997). Odontoblast differentiation starts at the tips of the cusps and is induced by the secondary enamel knots. Odontoblasts secrete the dentin matrix, which then induces the terminal differentiation program of ameloblasts (Ruch et al., 1995).

The terminal differentiation of ameloblast starts during the late bell stage of tooth development and consists of presecretory, secretory and maturation stages

(Zeichner-David et al., 1995; Fukumoto et al., 2004). Presecretory ameloblasts start to express proteins of the enamel matrix. Secretory ameloblasts still actively synthesize and start to secrete the enamel matrix proteins. Enamel matrix proteins include two main classes: amelogenins and non-amelogenins. The group of amelogenins is the most abundant, comprises about 80 to 90% of the total enemal protein content and is essential for the enamel formation. The non-amelogenin proteins include enamelin, tuftelins, ameloblastin as well as sulfated proteins (Zeichner-David et al., 1997; Moradian-Oldak, 2001) Secreted amelogenin gets assembled into a structural framework (nanospheres). Ameloblasts then transport calcium and phosphate ions into the extracellular matrix, which results in a nucleation and growth of the hydroxyapatite crystals. During maturation stage crystals harden, proteins get degraded and inorganic crystals almost entirely replace the protein component (Fincham et al., 1999).

Mouse incisors are unique as they continue to grow throughout the life of the animal. This growth is balanced by the abrasion by means of the contact with the upper incisors during feeding. The lingual side of the incisors (facing the tongue) is enamel-free, which makes such filing possible and generates a sharp tip. The lack of the enamel on the lingual side is a result of the absence of the ameloblasts on that side, as mouse incisors develop ameloblasts only on the labial side (facing the lip) (Tummers and Thesleff, 2003).

Despite the advancement in the understating of the molecular events involved in the tooth initiation, the knowledge of the mechanisms and players involved in regulating late tooth morphogenesis and cytodifferentiation of the dental cells, particularly ameloblasts, is limited.

CTIP2, also known as Bcl11b, is a transcription factor that plays an essential, yet poorly understood role in developmental processes. CTIP2 is a member of a C_2H_2 zinc finger family and was first identified as a COUP-TF-interacting protein that could potentiate COUP-TF-mediated repression in transient transfection assays (Avram et al., 2000). Later it was shown that CTIP2 can act as a *bona fide* transcription regulator and can bind to DNA directly (Avram et al., 2002). Germline deletion of CTIP2 in mice ($CTIP2^{-/-}$) results in perinatal lethality (Wakabayashi et al., 2003b). Closer analyses of $CTIP2^{-/-}$ mice revealed abnormalities in the developing immune and nervous systems. Thymuses of $CTIP2^{-/-}$ mice were significantly reduced in size and their T-cell count was only 10% of that of the normal, due to the profound apoptosis and incomplete rearrangement of the TCRβ locus (Wakabayashi et al., 2003b). Abnormalities in the nervous system of $CTIP2^{-/-}$ mice include defects in the path-finding and fasciculation of the cortical projection neurons, as well as defects in the differentiation and aggregation of the striatal medium spiny neurons (Arlotta et al., 2005; Arlotta et al., 2008). We have also reported high expression of CTIP2 in skin and determined that CTIP2 is involved in regulating keratinocyte differentiation and the epidermal barrier establishment (submitted).

Herein, we analyzed the spatial and temporal expression patterns of CTIP2 during tooth organogenesis. We demonstrate that CTIP2 is highly expressed in the oral ectoderm of the developing tooth throughout all the stages. We report high expression of CTIP2 in all of the dental tissues of ectodermal origin, including the inner and outer enamel epithelia, enamel knot, stratum intermidium and stellate reticulum. CTIP2 appears to be the only known transcription factor to be expressed exclusively in the epithelial tissues at later stages of the tooth development.

In CTIP2$^{-/-}$ mice tooth development proceeds normally through bud and cap stage, however at later stages molar teeth are characterized by hypoplastic stellate reticulum and poorly developed cusps. The incisors develop ameloblast-like cells on the lingual side of the tooth. We show that CTIP2 is highly expressed in ameloblast cell lineage (presecretory and secretory stages) and is essential for its terminal differentiation. Ameloblasts are formed, but are significantly smaller in size, disorganized and unpolarized. CTIP2$^{-/-}$ ameloblast exhibit a down-regulation of ameloblast-specific genes such as amelogenin, ameloblastin and enamelin and exhibit defects in cell adhesion. We have also observed a down-regulation in expression of MSX2, a homeobox transcription factor, which has been previously reported to be expressed in ameloblasts and control their terminal differentiation. We show by chromatin immunoprecipitation that MSX2 and epiprofin are direct targets of CTIP2. CTIP2 also directly controls expression of amelogenin, enamel and

laminin 5-3a. We conclude that CTIP2 is a novel transcription factor that is essential for the terminal differentiation of ameloblasts.

Materials and methods

Immunohistochemistry and histology

Embryos were collected from matings of $CTIP^{+/-}$ mice. The day of the plug was considered 0.5 d.p.c. Mouse embryos at different developmental stages were dissected, washed with PBS and fixed with 4% paraformaldehyde solution in PBS at 4˚C. After fixation, embryos were rinsed with PBS, cryopreserved in 25% sucrose and embedded in the OCT (Optimal Cutting Temperature, Tissue Tek). Tissue sections were cut at 16µm, air-dried, rinsed with PBS (3 times for 5 min) and treated with ice-cold methanol for 3 min to permeabilize the tissue. After 1h incubation with the blocking buffer (0.3% blocking reagent (Roche), 5% heat inactivated bovine serum, 5% heat inactivated donkey serum, 0.1% Triton X-100 in PBS) sections were incubated overnight at 4°C with the appropriate combination of the primary antibodies. Following the primary antibody incubation, sections were washed three times for 10 min with PBST (0.1% Tween 20 in PBS) and incubated with the secondary antibodies conjugated to the Cy2 or Cy3 fluorescent dyes (Jackson Immunochemicals) for 2 hours at room temperature. Sections were then washed 3 times for 10 min with PBST, dehydrated through a series of graded ethanol, cleared with xylene and

mounted for microscopy. Images were taken using Zeiss Imager.Z1 fluorescent microscope equipped with the Zeiss AxioCam HRm camera.

For histological analysis sections were stained with hematoxylin, counterstained with eosin, dehydrated and mounted with DPX as described above. Sections were photographed using the system described above. Images were processed and artificially colored using Adobe Photoshop.

Antibodies and dilutions

Antibodies against CTIP2 (1:300, Abcam), Amelogenin (1:250, Santa Cruz), Ameloblastin (1:250, Santa Cruz), Enamelin (1:250, Santa Cruz), Tuftelin (1:250, Santa Cruz), DSP (1:250, Santa Cruz), MSX2 (1:200, Affinity Bioreagents), β-tubulin (1:200, Sigma) were used.

Whole mount in situ hybridization

Digoxigenin (DIG)-labeled CTIP2 probe was generated according to the protocol of the DIG RNA labeling kit (Sp6/T7) (Roche). Briefly, linearized BlueScript plasmid containing CTIP2 cDNA fragment 343-2439 bp was transcribed using T7 polymerase in the reaction mix containing DIG-labeled UTPs.

For whole mount in situ hybridization, embryos were collected at E9.5, fixed with 4% paraformaldehyde in PBS for 3 hours at 4°C, dehydrated with methanol and stored in methanol at -20°C for future use. After genotyping, embryos were

rehydrated with the graded methanol, treated with proteinase K (10µg/ml) for 10 min and postfixed with a 4% paraformaldehyde/0.1% glutaraldehyde solution for 20 min. Embryos were then prehybridized in the Hybridization Buffer (50% Formamide, 5XSSC, pH4.5, 1% SDS, 50 µg/ml yeast tRNA, 50 µg/ml heparin) at 65˚C for 30 min and subjected to the overnight hybridization at 65˚C with the CTIP2 probe. Following the hybridization, embryos were washed twice with the hybridization buffer and then twice with the maleic acid buffer (0.1 M maleic acid, 0.15 M NaCl, 0.1% Tween). Embryos were then incubated with the blocking buffer (1X maleic acid buffer, 2% blocking reagent (Roche), 20% sheep serum), followed by the 2h incubation with the anti- DIG antibody coupled to the alkaline phosphatase. After subsequent washes with the maleic acid buffer, the colorimetric reaction was developed using the BCIP-NBT substrate (Roche). Reactions were stopped with PBS.

Real Time quantitative PCR

Lower jaws were dissected from E18.5 embryos and stored in RNAlater reagent (Qiagen) at 4˚C for future processing. Total RNA was extracted using RNAeasy kit (Qiagen), and first stand was synthesized using oligo(dT) primers and reverse transcriptase Supersript III (Invitrogen). cDNA was amplified using gene-specific primers using ABI 7500 Real-Time PCR system and SYBR green methodology. Forward (F) and reverse (R) primer sequences used were:

Amelogenin:

(F) 5’-TTCAGCCTCATCACCACCTT-3’; (R) 5’-AGGGATGTTTGGCTGATGGT-3’

Ameloblastin:

(F) 5’-ACAACGCATGGCGTTTCCAA-3’; (R) 5’-ACCTTCACTGCGGAAGGATA-3’

Enamelin:

(F) 5’-TGCAGAAAGCCCAAACCCAAGT-3’; (R) 5’-TTTGGCTGAGAAGAGCTGGCTT-3’

Laminin 5-3a:

(F) 5’-CACAGGATGGTTGTGGATCTTT-3’; (R) 5’-TGATTTTGACTTGGTCGCTGAAG-3’

MSX2:

(F) 5’-TTCACCACATCCCAGCTTCTA-3’; (R) 5’-TTGCAGTCTTTTCGCCTTAGC-3’

SP3:

(F) 5’-TTAGGAGGAGCACCAAACCGA-3’; (R) 5’-TAGCAGCACCTGGAATCTGTA-3’

Epiprofin:

(F) 5’-GGCAAGGCATACGCTAAGAC-3’; (R) 5’-CACAGGGGAACTTCTTGGT-3’

ChIP analyses

Lower jaws from E16.5 embryos were dissected, minced with scissors and trypsinized for 30 min at 37˚C. The cell suspension was then washed twice with cold

PBS and cross-linked with 1% formaldehyde (in PBS) for 10 min at 4˚C. The crosslinking reaction was quenched using 2.5 M glycine, and cells were then washed with cold PBS, pelleted and flash-frozen in liquid nitrogen for future processing. After genotyping, wt and CTIP2$^{-/-}$ jaws were used for immunoprecipitation reactions (CTIP2$^{-/-}$ jaws were used as a control). After thawing, cells were lysed with the ChIP lysis buffer (1% SDS, 10 mM EDTA, 50 mM Tris-Hcl, pH8.1) and sonicated until the DNA fragment size range was between 500 bp and 1.5 kb. Lysates were then diluted 3.5 times with the ChIP dilution buffer (1% Triton X-100, 2 mM EDTA, 150 mM NaCl, 20 mM Tris-Hcl, pH 8.1) and 10% of the diluted lysates was saved as an input sample for subsequent normalization procedures. The remaining lysate was subjected to the immunoprecipitation reaction using 5 µg of the anti-CTIP2 antibody that was coupled to magnetic beads (Dynabeads, Invitrogen). After overnight incubation, the beads were washed eight times with the RIPA buffer (50 mM HEPES, pH 8, 1 mM EDTA pH 8, 1% NP40, 0.7% deoxycolate, 0.5M LiCl), and once with Tris-EDTA buffer. Immune complexes were then eluted using 10% SDS solution in Tris-EDTA buffer at 65˚C for 10 min. DNA-protein complexes were subjected to the reversal of the crosslinking by overnight incubation at 65˚C. Samples were then digested with proteinase K, and DNA was purified using a PCR purification kit (Qiagen). Immunoprecipitated DNA was analyzed by quantitative PCR (as described above) and primers specific for the proximal and distal promoter regions of the genes of interest. Results were expressed as a fold-change of enrichment of the template amplicon relative to the CTIP2$^{-/-}$

controls. Amplification conditions were as follows: 15 min at 95˚C, 30s at 95˚C, 30 sec at 58˚C, 30 sec at 72˚C. Primer sequences were:

MSX2

Distal: (F) 5’-AGGGTGGCTCACCTCCTATT-3’; (R) 5’-ACTGCAGGCGGAGACTGTAT-3’

Proximal: (F) 5’-TGCTGGTGCACACCTACACT-3’; (R) 5’-TCTCCAGCTCTGGCTAGCTT-3’

Epiprofin

Proximal: (F) 5’-GCCCCACTGTTTAGCTCTGA-3’; (R)5’-AGACCCCTCCTCCTTAACCA-3’

Distal: (F) 5’-AGCTGCCTCTTCCAGATGAA-3’; (R) 5’-CCAGGAAGTAGTGGCCTGAT-3’

Laminin 5-3a

Distal: (F) 5’-CCCTTTGAACCTCATGTTCCT-3’; (R) 5’-CTCAGCTCAGCACCAATGAA-3’

Proximal: (F) 5’-AACCCATAAACCAGGGAACC-3’; (R) 5’-TGATCCCAGACAGACCTTGA-3’

Enamelin

Distal: (F) 5’-CAAGACTTTGGGCTGGAGAG-3’; (R) 5’-CACCACAGATGGTTGTGAGC-3’

Proximal: (F) 5’-AAGGGATTTGTGAGGGTGTG-3’; (R) 5’-AGTGCCAAAAGCTGTCTCCT-3’

Amelogenin

Distal: (F) 5’-AGGGTGGCTCACCTCCTATT-3’; (R) 5’-ACTGCAGGCGGAGACTGTAT-3’

Proximal: (F) 5’-TGCTGGTGCACACCTACACT-3’; (R) 5’-TCTCCAGCTCTGGCTAGCTT-3’

Ameloblastin

Distal: (F) 5’-GCGGATTTCTGAGTTTGAGG-3’; (R) 5’-GGTTTTTCGAGACAGGGTTTC-3’

Proximal: (F) 5’-CGCTCTTATCTGCTCATGGA-3’; (R) 5’-GCATCAGTGTCAAGCCAGAT-3’

Results

CTIP2 is expressed in developing mandible and tooth

CTIP2 expression was examined in detail throughout all the stages of mouse odontogenesis. CTIP2 was first detected at E9.5 by in situ hybridization in the first branchial arch (Fig.5.1A, white arrows), and appeared to be more pronounced in the mandibular component of the arch (Fig. 5.1A, black arrows). Antibody staining against CTIP2 at E10.5 revealed a high level of expression of CTIP2 in the oral ectoderm, and lower levels in the surrounding mesenchyme (Fig. 5.1B). At E12.5, CTIP2 expression was detected in the thickening of the oral ectoderm, representing the dental epithelium of the future incisor (Figs. 5.1C and E) and molar (Fig. 5.1D). Prominent CTIP2 expression was also observed in the mesenchyme of the future jaw (Figs. 5.1C and E), and much lower levels of CTIP2 were also present in the condensing dental mesenchyme, which will give rise to the future dental papilla (Fig. 5.1D).

CTIP2 was highly expressed in all of the cells of the dental epithelium as well as the enamel knot At cap stage (around E14.5) (Fig. 5.1F). By E16.5, the dental epithelium has already differentiated into the inner and outer epithelia, and both of these structures, as well as cervical loop region and stellate reticulum, expressed high levels of CTIP2, which persisted at E18.5 (Fig. 5.1G and H). Expression of CTIP2 in the oral ectoderm persisted throughout all the embryogenesis (Fig. 5.1), but expression of CTIP2 was not detected in the dental papilla at later stages of tooth development.

CTIP2 is expressed in ameloblasts

CTIP2 was highly expressed in the inner enamel epithelium (Figs. 5.1G and H), which gives rise to ameloblasts at later stages of tooth morphogenesis. We performed double-labeling immunohistochemistry of CTIP2 and ameloblast-specific products to analyze the expression of CTIP2 at the late bell stage (Figs. 5.1I-N). CTIP2 was highly expressed in the ameloblast cell lineage as judged by co-localization with amelogenin, ameloblastin, and enamelin (Figs. 5.1I, K and M). Ameloblasts at bell stage of tooth development are characterized by lengthened cell shape and elongated nuclei and CTIP2 expression was robust in the ameloblastic nuclei as visualized by co-staining with DAPI (Fig 5.1. J, L and N). Additionally, it is evident that all cells of the inner enamel epithelium and stratum intermedium express high levels of CTIP2.

CTIP2-null mice exhibit defects in tooth development

Approximately 25% of CTIP2$^{-/+}$ mice in our colony exhibit malocclusion (Fig. 5.2), accompanied by chalky enamel, the latter of which may suggest enamelization and/or mineralization defects (Fig. 5.2B). This observation together with the spatiotemporal pattern of CTIP2 expression during odontogenesis suggested that CTIP2 may play a role in tooth development and/or physiology. To test this hypothesis we examined tooth development in CTIP2-null mice.

Analyses of the dentition of CTIP2$^{-/-}$ mice revealed that tooth initiation occurred normally (data not shown), however later stages exhibited several defects. Molars of CTIP2$^{-/-}$ mice were slightly smaller than those of a wt at the bud stage (E14.5; compare Figs. 5.3A and B). The enamel knot was present in mutant developing molars at E14.5, but the dental cord was slightly elongated as compared to the wt. By E16.5, molars of CTIP2$^{-/-}$ mice appeared smaller and underdeveloped, the enamel knot was not well-defined and the stellate reticulum was somewhat hypoplastic (compare Figs. 5.3C and D). By E18.5 the molars of CTIP2$^{-/-}$ mice had developed relatively normally but were slightly reduced in size and exhibited a reduced stellate reticulum structure and underdeveloped cusps (compare Figs. 5.4E and F).

Mutant developing incisors exhibited a more severe phenotype as compared to molars. The bud of the future incisor was smaller with the slightly elongated dental cord (Figs. 5.3G and H). Coronal sectioning of the head at E16.5 confirmed a slight reduction in size of the lower incisors (compare Figs. 5.3I and J). The stellate

reticulum on the labial side of the incisor was largely reduced and indiscernible (compare Figs. 5.3K and L). This resulted in a close association between outer enamel epithelium, inner enamel epithelium, and stratum intermedium, making these structures difficult to identify in the mutants (asterisk in Fig. 5.3L). In contrast, we observed an expansion of a stellate reticulum-like structure on the lingual side, which was not present in wt littermates (black asterisks in Fig. 5.3J). The expansion of stellate reticulum in CTIP2 mutants was accompanied by the large expansion of the lingual outer enamel epithelium (yellow asterisk in Fig. 5.3J). Incisorial ameloblasts from wild-type mice began to differentiate, acquired a characteristic elongated shape, and became polarized at E16.5 (Figs. 5.3I and K). In contrast, CTIP2$^{-/-}$ ameloblasts appeared disorganized and were not well polarized at this developmental stage (compare Figs. 5.3I and J, and 5.3K and L). Furthermore, while wild-type ameloblasts developed only on the labial side of the incisors and the lingual aspect was populated mostly by epithelial cells (see Fig. 5.3I), cells resembling ameloblasts were found on both the labial and lingual aspects of the developing incisors in CTIP2 mutants (Fig. 5.3J, red asterisk). The inappropriate presence of ameloblasts on the lingual aspect of the incisors in CTIP2 mutants persisted at E18.5 (Fig. 5.3N, yellow asterisk), at which the mutant incisors were also found to be smaller with a reduction in enamel matrix formation (Fig. 5.3N, red asterisk). Thus, it would appear that loss of CTIP2 disrupted ameloblastogenesis, the boundary of the ameloblast domain, and/or ameloblast specification in the mutants, with a

corresponding effect on incisorial symmetry and enamelization. Odontoblasts in CTIP2$^{-/-}$ mice did not exhibit obvious morphological defects (Figs. 5.3K and L).

CTIP2 controls terminal cytodifferentiation and polarization of ameloblasts

Given high expression of CTIP2 in the ameloblast lineage we next examined ameloblast differentiation at E16.5 and E18.5 CTIP2$^{-/-}$ mice using the markers of ameloblast differentiation amelogenin and ameloblastin and enamelin (Fig. 5.4). At E16.5 wt ameloblasts had already begun to differentiate and expressed high levels of amelogenin (Fig. 5.4A). In addition they have undergone polarization by E16.5 and exhibited elongated cell bodies. In contrast, no expression of amelogenin was detected in CTIP2$^{-/-}$ ameloblasts at E16.5 (Fig. 5.4B, yellow asterisk) and mutant ameloblasts appeared disorganized and non-polarized (compare Figs. 5.4A and B). The polarization of ameloblasts is characterized by accumulation of microtubules. Strong β-tubulin expression was detected in the well-defined ameloblast processes at the apical surface of ameloblasts (Fig. 5.4C, white arrows) and around the basement membrane region (Fig. 5.4C, white asterisk) at E16.5. The nuclei of wt ameloblasts have already elongated along the apical-basal axis and were positioned primarily on the side adjacent to the stratum intermedium (Fig. 5.4C). Nuclei of the mutant ameloblasts, on the other hand, were round and located indiscriminately throughout the ameloblast layer (Fig. 5.4D). The apical processes did not form (Fig. 5.4D, white arrows) and cells appeared smaller that wt. CTIP2-null ameloblasts were expressing β-tubulin, however, the overall levels of its expression appeared slightly lower that in

a wt due to the decreased size and disorganization of the ameloblast cell layer (compare Figs. 5.4C and D).

At E18.5, expression of amelogenin, ameloblastin and enamelin could be detected in CTIP2$^{-/-}$ ameloblasts, however, levels of expression of these proteins were lower than those in wt cells (compare Figs. 5.4E and F, and G and H, and I and J white arrows). Even though CTIP2$^{-/-}$ ameloblasts appeared elongated, their cell bodies were still significantly shorter than wt ameloblasts and their nuclei appeared smaller and some of them were still detected in the apical region of the cell. We evaluated the expression levels of ameloblast-specific genes by RT-qPCR and found that amelogenin, ameloblastin and enamelin were down-regulated 5- to 15-fold in CTIP2$^{-/-}$ mice (Fig. 5.4K).

Ameloblasts form strong cell adhesion-based contacts involving numerous adhesion molecules, such as laminins, cadherins and integrins, which contribute to the structural integrity of ameloblast cell layer. However, cell of the ameloblast layer in CTIP2 mutants exhibited decreased cell-cell adhesion, especially in the apical regions (yellow asterisks in Figs. 5.4F, H and J) and we have observed a striking down-regulation of laminin 5-3a (Fig. 5.4K). Laminin 5-3a is highly expressed in ameloblasts and is involved in controlling their adhesion, differentiation and integrity.

We have also performed immunostaining with antibodies against tuftelin and DSP to assess the development of odontoblasts in CTIP2$^{-/-}$ mice (Fig. 5.5).

Odontoblasts develop from the dental papilla, which is derived from the migratory neural crest cells that populate the first branchial arch early in development. CTIP2 expression was not detected in odonoblatsts (Fig. 5.1) and CTIP2-null odontoblasts appeared to be structurally normal and well-polarized (compare Figs. 5.3I and J, and K and L). Expression of tuftelin was detected in the odontoblastic processes and the levels of tuftelin expression were similar in wt and mutant odontoblasts (Figs. 5.5A and B, white arrows). Tuftelin was also found to be expressed in ameloblasts and the overall levels of tuftelin expression in ameloblasts were not very different between wt and mutant. However, due to the disorganization of the cell layer, the cellular distribution of tuftelin appeared perturbed.

We have observed a slight down-regulation of DSP in mutant odontoblasts (compare Figs. 5.5C and D, however, this could be secondary to impaired epithelium differentiation and secretion of enamel by ameloblasts. DSP is also transiently expressed in pre-ameloblast and we were able to detect considerable amounts of DSP in wt ameloblast (Fig. 5.5C), Interestingly, DSP expression was largely reduced in CTIP2$^{-/-}$ ameloblasts.

Together, these results suggest that tooth defects in CTIP2-null mice arise from the intrinsic defect in the ameloblast lineage and that CTIP2 cell-autonomously regulated ameloblast terminal differentiation and therefore enamel production.

CTIP2 controls the expression of a network of genes implicated in ameloblastogenesis

CTIP2 and a limited number of other transcription factors are known to be expressed in ectodermal tissues of the oral cavity and participate in the later stages of ameloblastogenesis. For example, epiprofin (also known as KLF14 or SP6), which controls proliferation and differentiation of the dental epithelium, is expressed in both developing ameloblasts and in differentiated odontoblasts (Nakamura et al., 2008). Additionally, Sp3 controls enamel production through regulation of expression of ameloblast-specific genes (Bouwman et al., 2000). The homoeobox gene MSX2 regulates terminal differentiation of ameloblasts, and the ameloblast phenotype of $MSX2^{-/-}$ mice (Bei et al., 2004) strongly resembles that of CTIP2-null mice described herein. Therefore, we analyzed the expression of these transcription factors in the oral cavity of CTIP2-null mice at E18.5 and found that expression of both MSX2 and epiprofin was down-regulated by approximately two-fold (Fig. 5.6A), while that of Sp3 was unchanged in the mutants.

We hypothesized that CTIP2 may control terminal differentiation of ameloblasts through regulation of MSX2 expression. MSX2 is expressed in both dental epithelium and mesenchyme (Fig. 5.6C and F), and in the latter is co-expressed with CTIP2 at both E14.5 and E16.5 (Fig. 5.6D and G). We performed chromatin immunoprecipitation (ChIP) experiments in isolated oral cavities from E16.5 mice to determine if the regulation of MSX2 expression by CTIP2 was due to the interaction of CTIP2 with the MSX2 promoter. Because CTIP2 is expressed predominantly in the oral epithelium at this developmental stage (Fig. 5.1), we reasoned that the

immunoprecipitated chromatin prepared in this way would be predominantly of epithelial origin, and that of mesenchymal cells would be mostly eliminated.

We examined both proximal and distal promoter regions of MSX2 and epiprofin, as well as laminin 5-3a, enamelin, amelogenin and ameloblastin (Fig. 5.7). We found that CTIP2 interacted preferentially with the proximal promoter of epiprofin (Fig. 5.7A) and with the distal region of the amelogenin promoter (Fig. 5.7B). CTIP2 was present on both proximal and distal promoter regions of MSX2, laminin 5-3a and enamelin (Fig. 5.7A and B) however, we did not detect CTIP2 on either proximal or distal promoter region of ameloblastin gene. Our findings suggest that MSX2, laminin5-3a, enamelin and amelogenin may be direct targets of CTIP2 in the developing tooth. Moreover, CTIP2 appears likely to control ameloblast differentiation in a multifaceted manner through control of MSX2 expression, and also by direct regulation of expression of ameloblast-specific genes.

Discussion

Herein, we provide evidence that CTIP2 is highly expressed the developing tooth and plays an essential role in the tooth development and ameloblast differentiation. CTIP2-null ameloblasts exhibit structural abnormalities, such as reduced size and poor polarization. Mutant ameloblasts fail to synthesize appropriate amounts of amelogenin and non-amelogenin proteins that are required for enamel

formation. CTIP2 directly regulates the transcription of these genes and in the absence of CTIP2 the expression of these transcripts is severely compromised. In addition, CTIP2 affects other pathways that are implicated in the regulation of the ameloblast differentiation and enamel formation (see model, Fig. 5.8). We found that CTIP2 binds to the promoters of MSX2 and epiprofin and positively regulates their expression in the ectoderm of the tooth, as in the absence of CTIP2 the expression of these genes was diminished.

CTIP2 controls expression of enamel proteins and therefore enamel formation

CTIP2-null ameloblasts exhibit approximately a 10-fold reduction in the expression of three main secretory stage proteins: amelogenin, ameloblastin and enamelin. Amelogenin has been shown to be critical for the normal enamel formation and amelogenin-null mice develop abnormal teeth characterized by the chalky white color and disorganized hypoplastic enamel (Gibson et al., 2001). It was suggested that amelogenin is not required for the enamel crystal formation but rather for its organization. Enamelin on the other hand, promotes and catalyzes the growth of the enamel crystals and is important for establishing the mineralization front at the ameloblast surface (Hu et al., 2008). Ameloblastin is a cell adhesion molecule that is required for the maintenance of the differentiated state of ameloblasts. Ameloblastin-null mice develop severe enamel hypoplasia, as their ameloblasts detach from the matrix, lose polarity and reenter the cell cycle

(Fukumoto et al., 2004). From this we can conclude that CTIP2 governs enamel formation and mineralization through regulation of the terminal differentiation of ameloblasts. It is also feasible that CTIP2 plays a role in maintaining the differentiated state of ameloblasts, perhaps through sustaining ameloblastin expression. However, it is not known whether CTIP2 is expressed in the adult tooth and the perinatal death of the CTIP2-null mice renders the analysis of an adult tooth impossible.

CTIP2 cell-autonomously regulated development of tooth structures

The histomorphological structure and polarization of ameloblasts appeared to be perturbed in mutant ameloblast, suggesting that CTIP2 may play a role in controlling the cell structure and tissue organization. Mutant ameloblasts were not polarized and lacked the characteristic ameloblast processes and showed a reduction in cell-cell adhesion.

The ameloblast phenotype we observed suggests a cell-autonomous function of CTIP2 in these cells and that CTIP2 might exhibit multiple temporally controlled functions during the formation of the tooth. In addition to the defects in the ameloblast lineage, mutant teeth were characterized by the blunted cusps and reduced stellate reticulum. CTIP2 expression was detected in the enamel knots (primary and secondary), which would be consistent with the observed cusp defects. Perhaps CTIP2 is involved in regulated signaling or apoptotic events in the enamel knot, which lead to the demarcation of the future cusp. CTIP2 is expressed in the

stellate reticulum and ablation of CTIP2 resulted in the hypoplasticity of this structure, perhaps due to the insufficient proliferation. Conversely, CTIP2 was not present in the dental papilla and odontoblasts and the phenotype we observed in the odontoblasts was milder as compared to the other tooth structures. Morphologically, CTIP2-null odontoblasts appeared normal; however, they expressed reduced levels of DSP. The reciprocal interaction between ameloblast and odontoblasts is critical for their normal differentiation and neither cell type can develop independent of the other. Thus, the abnormalities in odontoblasts may be a consequence of the altered signaling originating from the epithelium. Interestingly, we did detect very low (compared to the epithelium) expression of CTIP2 in the condensing mesenchyme at E12.5 and E14.5 and perhaps such transient pulse of expression is necessary for the normal odontoblast differentiation program. This subject can be directly addressed by analyzing ameloblast and odontoblast differentiation in a conditional mouse line (K14-cre-CTIP2), where CTIP2 is specifically ablated from the epithelium.

Interestingly, CTIP2 is highly expressed in the stratum intermedium. The function of this structure is unknown and the function of CTIP2 in this structure remains to be elucidated. Nevertheless, we observed a disorganization of the stratum intermedium layer in the mutant incisors.

CTIP2 controls a network of genes involved in tooth morphogenesis

Multiple lines of evidence suggest that MSX2 and CTIP2 function in modulating tooth development through the same pathway. MSX2 was proposed to control ameloblast terminal differentiation through control of laminin 5-3a expression and MSX2-null ameloblast phenotypically resemble those of CTIP2 mutants (Bei et al., 2004). MSX2-null mice also exhibit defects in cusp morphogenesis as a result of a reduced proliferation in the enamel organ. We show that CTIP2 positively controls MSX2 expression and may act upstream of MSX2 during ameloblastogenesis. How MSX2 regulates laminin 5-3a expression is not known, however, it has been shown that MSX2 can repress the promoter activity of amelogenin-promoter reporter construct (Zhou et al., 2000). Such regulation is independent of MSX2 DNA binding and is antagonistic of that of C/EBPα, which was recently identified as an activator of the amelogenin promoter (Zhou et al., 2000). It is not known whether this reflects the factual events in the mouse ameloblasts but the relationship between CTIP2-mediated regulation of MSX2 and amelogenin needs to be determined.

The phenotype of dentition of Sp3 mutant mice was milder that of CTIP2-null mice. The ameloblasts were born and did not exhibit significant structural abnormalities, however showed a reduction in amelogenin and ameloblastin transcripts and enamel structure (Bouwman et al., 2000). Sp3 expression did not change significantly in CTIP2-null mice raising the possibility that CTIP2 and Sp3 control cytodifferentiation of ameloblasts independently.

CTIP2 positively regulates expression of target genes in the ameloblast cell lineage

Previous reports provided evidence that CTIP2 can repress transcription through the association with the NuRD co-repressor complex. This was demonstrated in T lymphocytes (Cismasiu et al., 2005) as well as in neuroblastoma cells (Topark-Ngarm et al., 2006). Yet another report indicated that CTIP2 represses HIV-1 transcription through the recruitment of the deacetylases HDAC1 and HDAC2 as well as the methyltransferase SUV39H1 with subsequent heterochromatin formation in the microglial cells (Marban et al., 2007). Interestingly, it has also been shown that CTIP2 can activate transcription of target genes in T cells and does so by recruiting p300 co-activator complex (Cismasiu et al., 2006). The genes we identified herein as direct targets of CTIP2 appear to be activated by it as their expression is reduced in the absence of CTIP2. The mechanisms of CTIP2–mediated gene activation in the tooth still need to be elucidated. p300 is a probable potential co-activator complex recruited by CTIP2 for several reasons: it has been shown previously in T cells, and it is recruited by C/EBPα protein, which is known to regulate the amelogenin promoter activity.

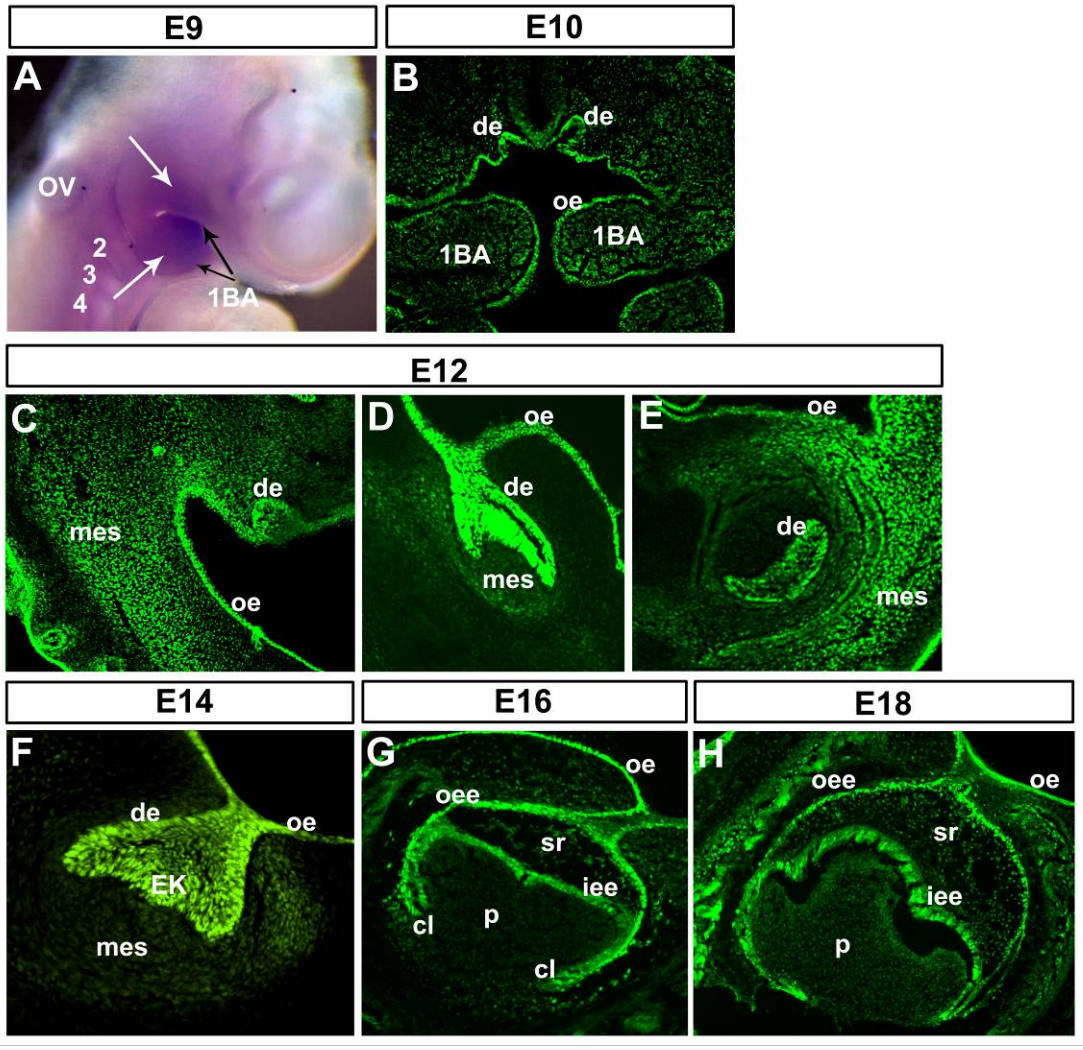
E9
E10
A
OV
2
3
4
1BA
B
de
de
oe
1BA
1BA
E12
C
de
mes
oe
D
oe
de
mes
E
oe
de
mes
E14
E16
E18
F
de
oe
EK
mes
G
oe
oee
sr
iee
cl
p
cl
H
oee
oe
sr
iee
p

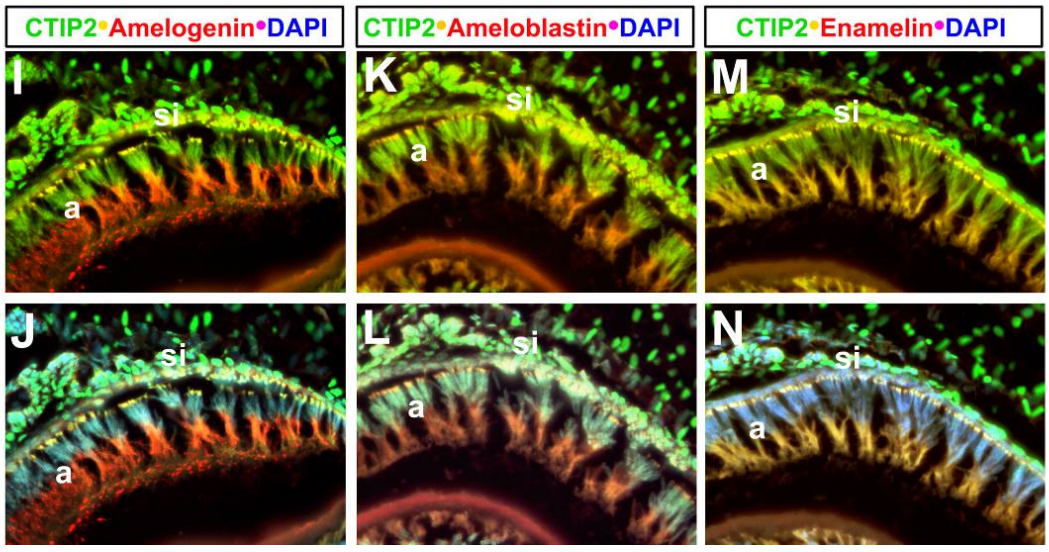
CTIP2•Amelogenin•DAPI
CTIP2•Ameloblastin•DAPI
CTIP2•Enamelin•DAPI
I
si
a
K
si
a
M
si
a
J
si
a
L
si
a
N
si
a

Figure 5.1. CTIP2 is expressed in the developing tooth.

A, E 9.5 whole mount in situ hybridization with the CTIP2 *in situ* probe. White arrows indicate the mandibular and maxillary components of the 1st branchial arch where CTIP2 expression is detected. Black arrows indicate the regions of the 1st bracnshial arch where CTIP2 expression is the highest.
B-H, Immunohistochemistry (IHC) of the coronal sections of the head of the embryos at different developmental stages using anti-CTIP2 antibody (green).
B, section of the E10.5 head across 1st branchial arch.
C, the jaw region of the E12.5 wt embryo, showing high expression of CTIP2 in the mesenchyme, oral ectoderm and the thickening of the dental epithelium of the future upper incisor.
D, E12.5, the lower molar.
E, E12.5, the lower incisor.
F, the lower molar of the E14.5 embryo (cap stage).
G, E16.5 lower molar.
H, E18.5 lower molar.
I, K and M, double Immunohistochemistry of the ameloblasts of the lower incisor at E18.5 using antibodies directed against CTIP2 (in green) and ameloblast specific genes (in red): ameloblastin (I), Amelogenin (K), Enamelin (M)
J, L and N, same as I, K and M counterstained with DAPI (in blue).
Abbreviations: OV –otic vesicle,1BA – 1st branchial arch, 2, 3 and 4, - numbers of the corresponding branchial arches, de – dental epithelium, oe-oral epithelium, mes – mesenchyme, EK – enamel knot, p – papilla, cl – cervical loop, sr – stellate reticulum, oee – outer enamel epithelium , iee – inner enamel epithelium, si - stratum intermedium, a - ameloblasts.

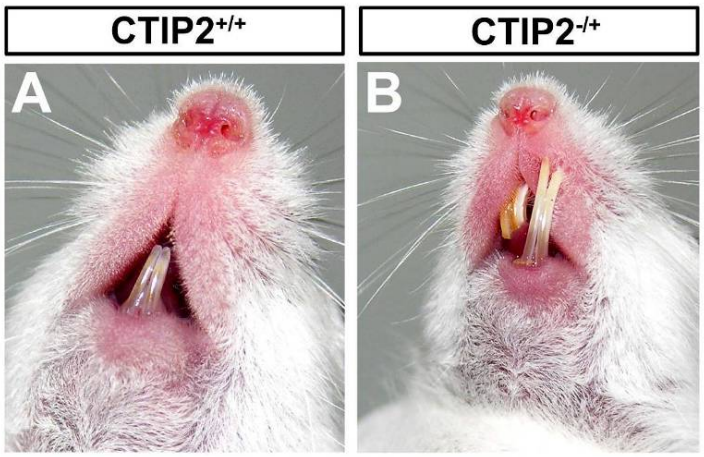

Figure 5.2. CTIP2$^{-/+}$ mice experience malocclusion.

A, incisors of the 5-week old wt mouse.
B, incisors of the 5-week old CTIP2$^{-/+}$ mouse, showing overgrown and misaligned teeth (malocclusion). Malocclusion is observed in 25% of the CTIP2$^{-/+}$ mice.

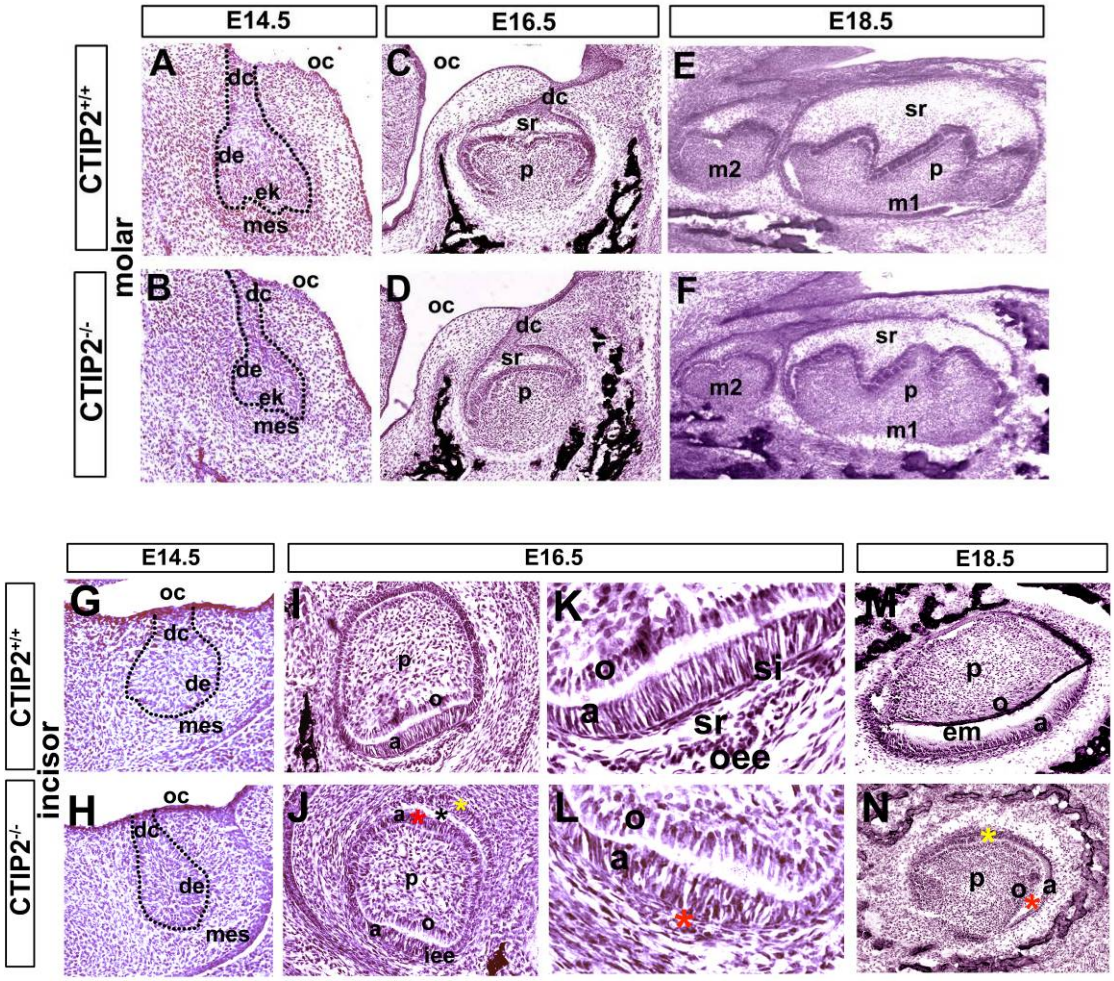
E14.5
E16.5
E18.5
CTIP2+/+
CTIP2-/-
molar
incisor
A
B
C
D
E
F
G
H
I
J
K
L
M
N
oc
dc
de
ek
mes
sr
p
m2
m1
o
a
si
oee
iee
em

Figure 5.3. CTIP2 mice exhibit defects in tooth development.

A-D and **G-L** – H&E staining of the coronal head sections at different developmental stages.
E-F and **M-N** – H&E staining of the saggital head sections at E18.5.
A, C, E- histology of the wt lower molar at E14.5 (A) (black dotted line outlines the tooth bud), E16.5 (C) and E18.5 (E).
B, D, F –histology of the CTIP2-null molar at E14.5 (B) (black dotted line outline dthe tooth bud), E16.5 (D) and E18.5 (F).
G and H - lower incisor bud of the wt (G) and CTIP2-null (H) mice at E14.5.
I and J – lower incisor of the wt (I) and CTIP2-null (J) mice at E16.5. In J: red asterisk indicates the ectopic ameloblast-like cells, black asterisk – expanded stellate reticulum, yellow asterisk – expanded outer enamel epithelium.
K and L – higher magnification of the developing incisors of the wt (K) and CTIP2-null (L) mice at E16.5. In K: red asterisk indicates the reduced stellate reticulum.
M-N – lower incisor of the wt and CTIP2- null mice at E18.5. In N: red asterisk indicates the reduced enamel matrix, yellow asterisk – ectopic ameloblast-like cells.
Abbreviations: de – dental epithelium, oc-oral cavity, dc – dental cord, mes – mesenchyme, ek – enamel knot, p – papilla, cl – cervical loop, sr – stellate reticulum, oee – outer enamel epithelium , iee – inner enamel epithyelium, si - stratum intermedium, a - ameloblasts, o-odontoblasts, em – enamel matrix, m1 – first molar, m2 - second molar.

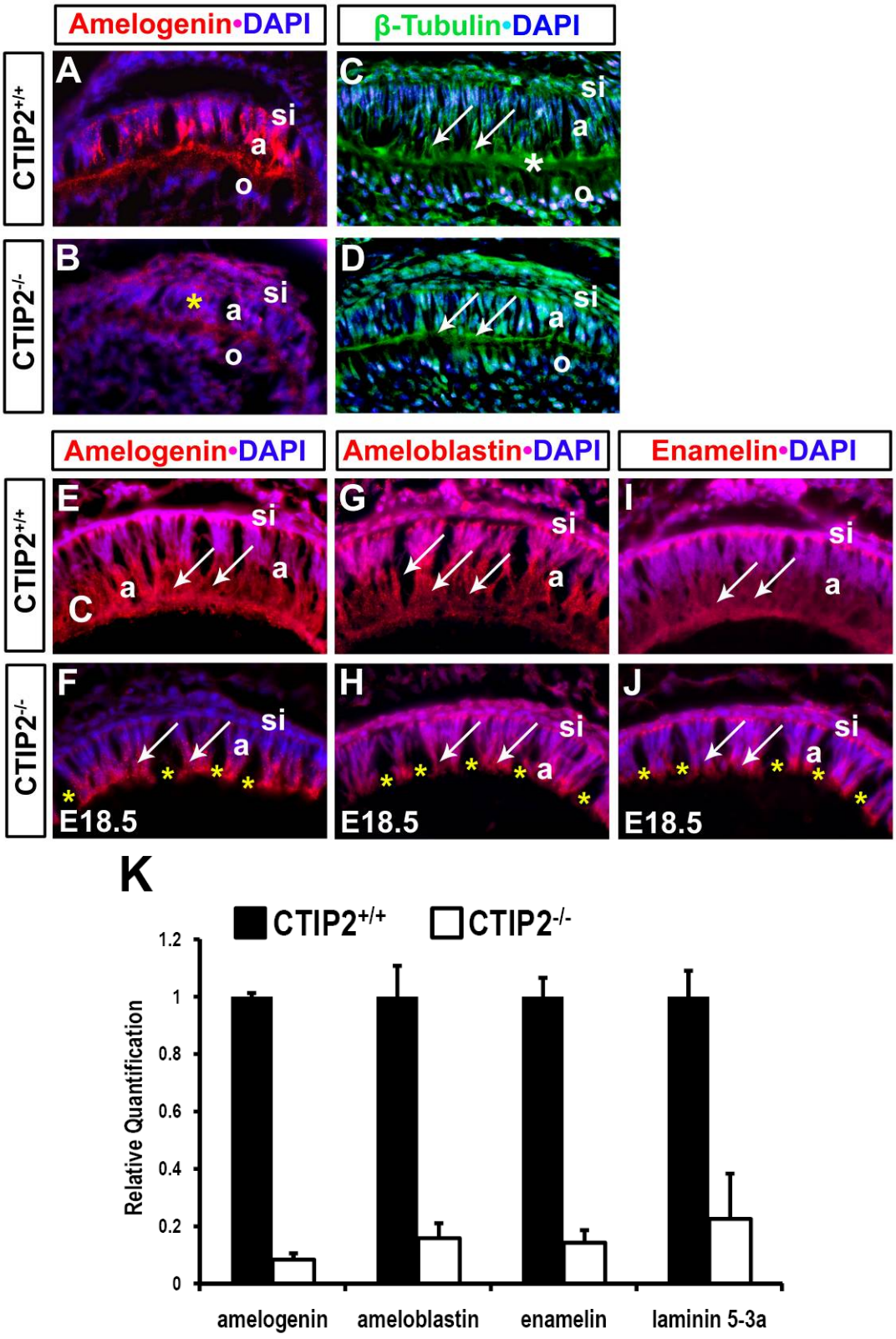
Amelogenin•DAPI
β-Tubulin•DAPI
CTIP2+/+
CTIP2-/-
A
B
C
D
si
a
o
Amelogenin•DAPI
Ameloblastin•DAPI
Enamelin•DAPI
E
F
G
H
I
J
E18.5
K
CTIP2+/+
CTIP2-/-
Relative Quantification
1.2
1
0.8
0.6
0.4
0.2
0
amelogenin
ameloblastin
enamelin
laminin 5-3a

Figure 5.4. CTIP2-null mice exhibit defects in the terminal differentiation of the ameloblast cell lineage.

A-B, IHC of the coronal sections of the ameloblasts of the lower incisors of the wt (A) and CTIP2-null (B) mice at E16.5 using antibodies against amelogenin (in red). Yellow asterisk in B shows the absence of amelogenin expression in the CTIP2-null ameloblasts.
C-D, IHC of the coronal sections of the ameloblasts of the lower incisors of the wt (C) and CTIP2-null (D) mice at E16.5 using antibodies against β-tubulin (in green). White arrows in C point to the elongated ameloblast processes which are present only in the well-polarized wt ameloblasts, white asterisk indicates the areas of accumulation of the β-tubulin. CTIP2-null ameloblasts lack processes and are not polarized (white arrows in D).
E-J, IHC of the E18.5 ameloblasts of the lower incisors of the wt (E, G, I) and CTIP2-null (F, H, J) mice using antibodies against ameloblast-specific proteins (in red) amelogenin (E-F), Amleoblatsin (G-H) and enamelin (I-J). White arrows point to the ameloblast processes. Yellow asterisks mark the spaces between ameloblasts, which form as a result of the reduced adhesion.
All section were counterstained with DAPI.
K, RT-qPCR comparing levels of the amelogenin, ameloblastin, enamelin and lamin 5-3a expression in the wt (black bars) and CTIP2-null (white bars) jaws. All differences in the expression levels were statistically significant.
Abbreviations: si - stratum intermedium, a - ameloblasts, o-odontoblasts.

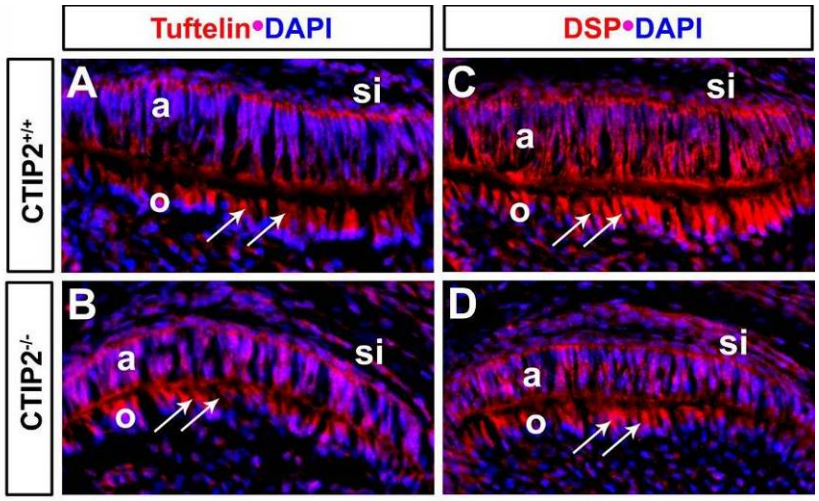

Figure 5.5. CTIP2-null odontoblast display minor defects.

A-D, IHC of the coronal sections of the ameloblasts of the lower incisors of the wt (A and C) and CTIP2-null (B and D) mice at E16.5 using antibodies against tuftelin (A and B) and DSP (C and D) (in red). White arrows point to the odontoblast processes. All sections were counterstained with DAPI.
Abbreviations: si - stratum intermedium, a - ameloblasts, o-odontoblasts.

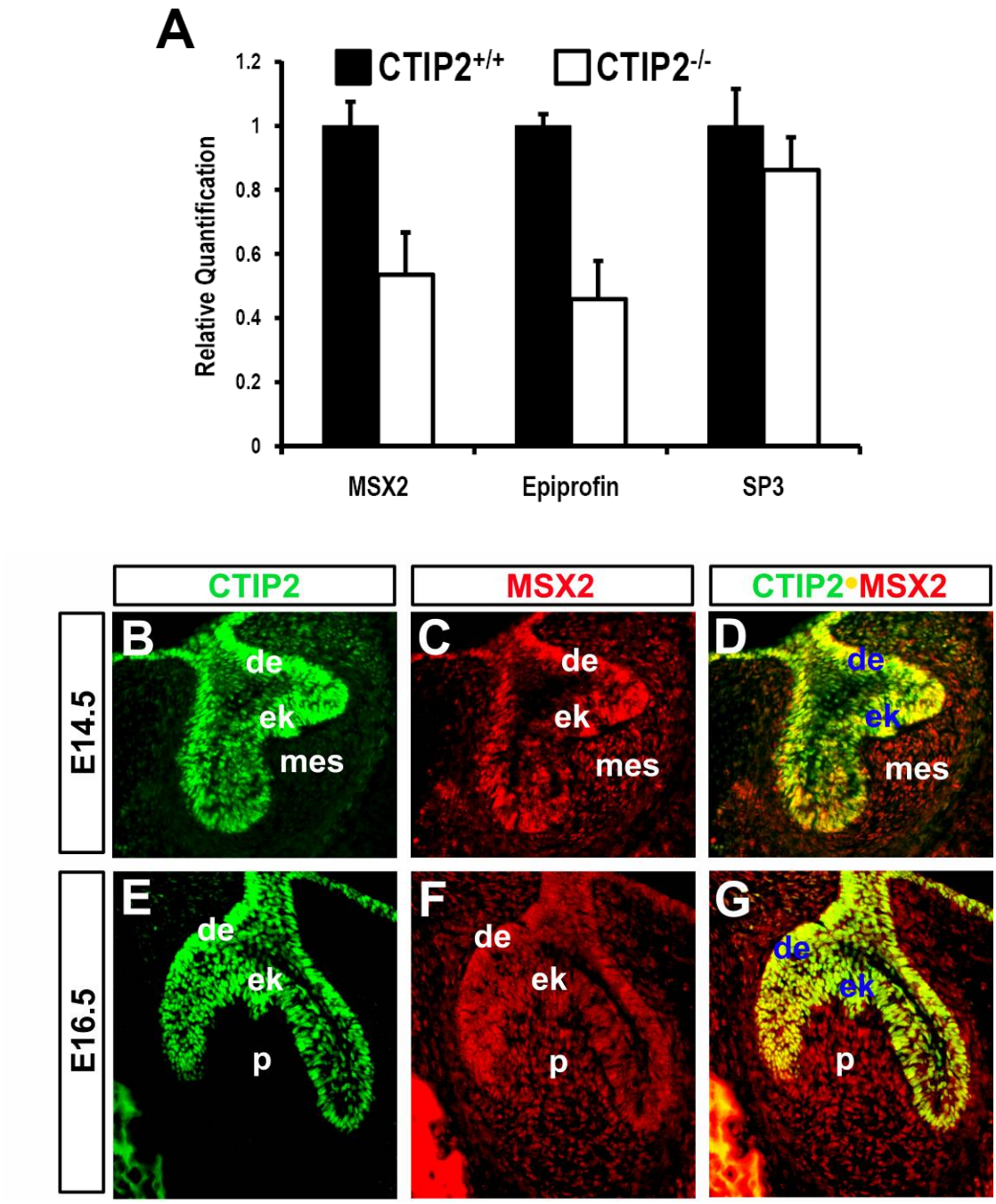
A
CTIP2+/+
CTIP2-/-
Relative Quantification
1.2
1
0.8
0.6
0.4
0.2
0
MSX2
Epiprofin
SP3
CTIP2
MSX2
CTIP2•MSX2
E14.5
E16.5
B
C
D
E
F
G
de
ek
mes
p

Figure 5.6. CTIP2 regulates expression of other transcription factor involved in the ameloblast differentation.

A, RT-qPCR comparing levels of expression of MSX2, epiprofin and Sp3 in the wt (black bars) and CTIP2-null (white bars) jaws. The difference in Sp3 expression between wt and CTIP2-null mice was not statistically significant.
B-G, IHC of the E14.5 (B-D) and E16.5 (E-G) wt teeth using antibodies against MSX2 (red, C and F) and CTIP2 (green, B and E), showing their co-localization in the dental epithelium (yellow, D and G).
Abbreviations: de – dental epithelium, ek - enamel knot, mes – mesenchyme, p-dental papilla.

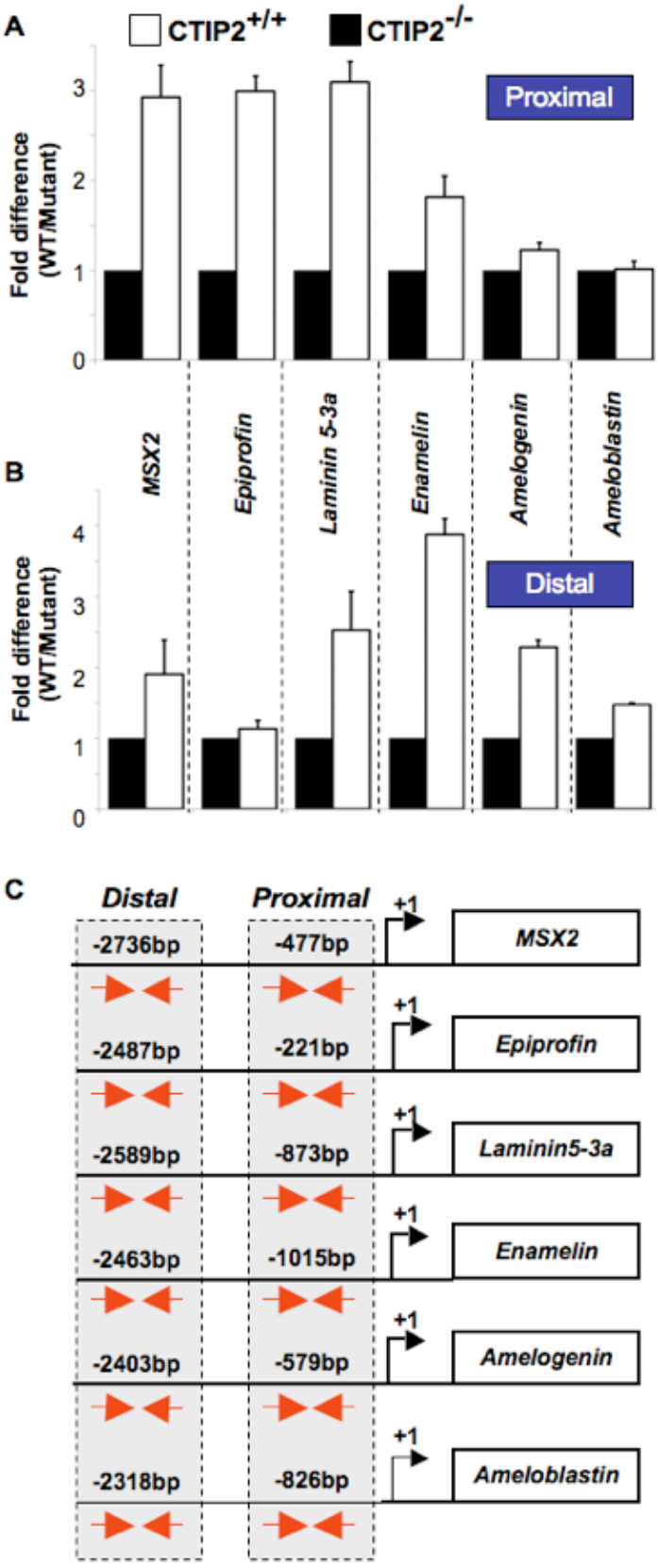
A
CTIP2+/+
CTIP2-/-
Proximal
Fold difference (WT/Mutant)
0
1
2
3
MSX2
Epiprofin
Laminin 5-3a
Enamelin
Amelogenin
Ameloblastin
B
Distal
Fold difference (WT/Mutant)
0
1
2
3
4
C
Distal
Proximal
-2736bp
-477bp
MSX2
-2487bp
-221bp
Epiprofin
-2589bp
-873bp
Laminin5-3a
-2463bp
-1015bp
Enamelin
-2403bp
-579bp
Amelogenin
-2318bp
-826bp
Ameloblastin
+1

Figure 5.7. CTIP2 interacts with promoter regions of several ameloblast-related genes.

A, ChIP studies on the proximal promoter regions of the indicated genes.
qPCR was used to amplify indicated promoter regions that were coimmunoprecipitated with the anti-CTIP2 antibody in extracts from wt (white bars) and CTIP2-null (black bars) oral cavities from E16 mice. The ratio of amplification products present in immunoprecipitates from wt and mutant mice was calculated to give an indication of the specificity of the ChIP signal in wt mice.
B, ChIP studies on the distal promoter regions of the same genes.
C, schematic representation of the location of proximal and distal primer sets used for qPCR of the indicated genes in A and B. PCR amplification of all promoter regions of all genes generated amplicons of 100 bp or less.

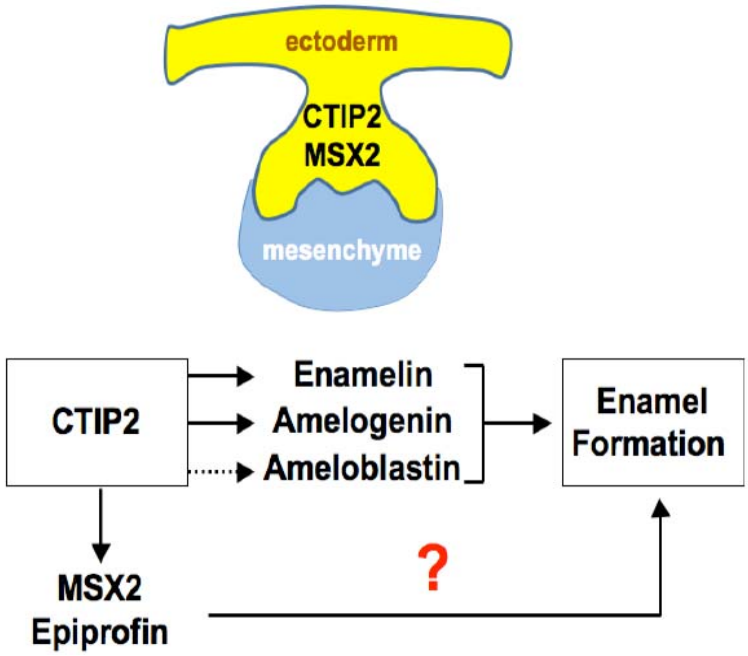

Figure 5.8. The model for the action of CTIP2 during tooth morphogenesis.

CTIP2 appears to directly regulate expression of several genes known to be important in ameloblastogenesis and/or ameloblast maintenance. Solid arrows imply direct regulation, whereas the dashed arrow indicates an indirect relationship. To our knowledge, target genes for MSX2 and epiprofin in the oral epithelium have not been identified, and this is denoted by the question mark. The net output of this network is enamelization of the developing tooth as indicated.

CHAPTER 6

CONCLUSION

Information is rapidly accumulating regarding the role of the protein known as CTIP2. Several years ago our knowledge about CTIP2 function was limited to its role in T cell survival. Our lab has contributed substantially to the understanding of the mechanisms of CTIP2 action and recently to its indispensable role in the mouse developmental processes.

We have documented several novel observations concerning the domains of CTIP2 expression. We demonstrated that CTIP2 is highly expressed in the developing skin and the craniofacial complex. Epidermis, oral epithelium, dental epithelium and nervous system all originate from the ectodermal germ layer of the embryo and all express very high levels of CTIP2. We have also observed that CTIP2 is expressed in the fibroblasts of the skin dermis and the mesenchyme of the oral cavity during tooth development. These tissues, as well as T lymphocytes, which are known to express high levels of CTIP2, arise from the mesoderm germ layer. The expression pattern of CTIP2 in the endodermal tissues is not known at this point of time and this aspect needs further examination.

CTIP2 plays an important role in all the tissues in which the protein has been detected. We have shown that CTIP2 controls the terminal differentiation of keratinocytes and the establishment of the epidermal permeability barrier. Disruption of the CTIP2 locus by homologous recombination resulted in a great reduction in the synthesis of the structural and metabolic proteins that are required for the normal development and/or function of skin. In addition, we found that

expression of CTIP2 in the dermis complements the cell-autonomous function in the epidermis through regulation of the production and/or secretion of diffusible, paracrine factors that affect keratinocyte proliferation.

We also demonstrated that CTIP2 is required for normal tooth development, and once again we showed that CTIP2 was involved in controlling the terminal differentiation of a specific cell type – the ameloblasts. In the absence of CTIP2, ameloblasts failed to differentiate properly and did not express the proteins necessary for ameloblast function, which would probably ultimately affect the production of the essential enamel layer of the tooth.

Our studies also identified CTIP2 as a bifunctional transcriptional regulatory protein that can act as both a repressor and an activator of transcription, perhaps depending on the cell type or promoter context. To date, most of the mechanistic studies have been performed using cell culture systems and transiently transfected cells, in which CTIP2 functions as a transcriptional repressor. However, our in vivo studies clearly demonstrated that CTIP2 functions as an activator of transcription of critical target genes in both the developing skin and oral ectoderm. Numerous genes in CTIP2-null mouse skin and developing tooth were found to be down-regulated, which provides further evidence that CTIP2 may function as a transcriptional activator in a promoter-specific manner. CTIP2-mediated transcriptional activation appeared to be direct, as we found that CTIP2 was bound to the promoter regions of many of these genes. Our next step will be to identify the mechanism underlying

CTIP2-mediated transcriptional activation, which is currently being pursued in the Leid laboratory. It seems likely that these studies will reveal that the transcriptional regulatory activity of CTIP2 is both cell type- and promoter context-dependent.

CTIP2 is highly expressed in specific neuronal populations. To characterize the mechanism of CTIP2-mediated transcriptional repression in the neuronal context we performed a series of analyses in the neuroblastoma cells. We identified a direct target of CTIP2 in SK-N-MC neuroblastoma cells, p57Kip2, and showed that CTIP2 exerted its repressive regulation through the recruitment of the NuRD co-repressor complex to the p57Kip2 promoter template. We similarly identified p57Kip2 as a CTIP2 target gene in the skin. Identification of p57Kip2 as a CTIP2 target gene suggests that CTIP2 may be a positive regulator of the cell cycle, and this appears to be consistent with reduced proliferation in the developing skin in the absence of CTIP2. This finding may be confirmed in follow-up studies, designed to determine the mechanistic basis of CTIP2-mediated repression of p57Kip2 in keratinocytes.

Bibliography

Albin, R.L., Young, A.B., and Penney, J.B. (1989). The functional anatomy of basal ganglia disorders. *Trends in neurosciences 12*, 366-375.

Albu, D.I., Feng, D., Bhattacharya, D., Jenkins, N.A., Copeland, N.G., Liu, P., and Avram, D. (2007). BCL11B is required for positive selection and survival of double-positive thymocytes. *The Journal of experimental medicine 204*, 3003-3015.

Angel, P., and Szabowski, A. (2002). Function of AP-1 target genes in mesenchymal-epithelial cross-talk in skin. *Biochemical pharmacology 64*, 949-956.

Angel, P., Szabowski, A., and Schorpp-Kistner, M. (2001). Function and regulation of AP-1 subunits in skin physiology and pathology. *Oncogene 20*, 2413-2423.

Arlotta, P., Molyneaux, B.J., Chen, J., Inoue, J., Kominami, R., and Macklis, J.D. (2005). Neuronal subtype-specific genes that control corticospinal motor neuron development in vivo. *Neuron 45*, 207-221.

Arlotta, P., Molyneaux, B.J., Jabaudon, D., Yoshida, Y., and Macklis, J.D. (2008). Ctip2 controls the differentiation of medium spiny neurons and the establishment of the cellular architecture of the striatum. *J Neurosci 28*, 622-632.

Arnold, I., and Watt, F.M. (2001). c-Myc activation in transgenic mouse epidermis results in mobilization of stem cells and differentiation of their progeny. *Curr Biol 11*, 558-568.

Avram, D., Fields, A., Pretty On Top, K., Nevrivy, D.J., Ishmael, J.E., and Leid, M. (2000). Isolation of a novel family of C(2)H(2) zinc finger proteins implicated in transcriptional repression mediated by chicken ovalbumin upstream promoter transcription factor (COUP-TF) orphan nuclear receptors. *The Journal of biological chemistry 275*, 10315-10322.

Avram, D., Fields, A., Senawong, T., Topark-Ngarm, A., and Leid, M. (2002). COUP-TF (chicken ovalbumin upstream promoter transcription factor)-interacting protein 1 (CTIP1) is a sequence-specific DNA binding protein. *Biochem J 368*, 555-563.

Bei, M., Stowell, S., and Maas, R. (2004). Msx2 controls ameloblast terminal differentiation. *Dev Dyn 231*, 758-765.

Berg, J.M., and Godwin, H.A. (1997). Lessons from zinc-binding peptides. *Annual review of biophysics and biomolecular structure 26*, 357-371.

Berg, J.M., and Shi, Y. (1996). The galvanization of biology: a growing appreciation for the roles of zinc. *Science* (New York, NY) *271*, 1081-1085.

Bezrookove, V., van Zelderen-Bhola, S.L., Brink, A., Szuhai, K., Raap, A.K., Barge, R., Beverstock, G.C., and Rosenberg, C. (2004). A novel t(6;14)(q25-q27;q32) in acute myelocytic leukemia involves the BCL11B gene. *Cancer Genet Cytogenet 149*, 72-76.

Bitterman, K.J., Anderson, R.M., Cohen, H.Y., Latorre-Esteves, M., and Sinclair, D.A. (2002). Inhibition of silencing and accelerated aging by nicotinamide, a putative negative regulator of yeast sir2 and human SIRT1. *J Biol Chem 277*, 45099-45107.

Blander, G., and Guarente, L. (2004). The Sir2 family of protein deacetylases. *Annu Rev Biochem 73*, 417-435.

Bouwman, P., Gollner, H., Elsasser, H.P., Eckhoff, G., Karis, A., Grosveld, F., Philipsen, S., and Suske, G. (2000). Transcription factor Sp3 is essential for post-natal survival and late tooth development. *The EMBO journal 19*, 655-661.

Byrne, C., Hardman, M., and Nield, K. (2003). Covering the limb--formation of the integument. *Journal of anatomy 202*, 113-123.

Byrne, C., Tainsky, M., and Fuchs, E. (1994). Programming gene expression in developing epidermis. *Development* (Cambridge, England) *120*, 2369-2383.

Calleja, C., Messaddeq, N., Chapellier, B., Yang, H., Krezel, W., Li, M., Metzger, D., Mascrez, B., Ohta, K., Kagechika, H*., et al.* (2006). Genetic and pharmacological evidence that a retinoic acid cannot be the RXR-activating ligand in mouse epidermis keratinocytes. *Genes & development 20*, 1525-1538.

Cameron, D.J., Tong, Z., Yang, Z., Kaminoh, J., Kamiyah, S., Chen, H., Zeng, J., Chen, Y., Luo, L., and Zhang, K. (2007). Essential role of Elovl4 in very long chain fatty acid synthesis, skin permeability barrier function, and neonatal survival. *Int J Biol Sci 3*, 111-119.

Candi, E., Schmidt, R., and Melino, G. (2005). The cornified envelope: a model of cell death in the skin. *Nature reviews 6*, 328-340.

Chen, B., Schaevitz, L.R., and McConnell, S.K. (2005). Fezl regulates the differentiation and axon targeting of layer 5 subcortical projection neurons in cerebral cortex. *Proc Natl Acad Sci* U S A *102*, 17184-17189.

Christian, M., Tullet, J.M., and Parker, M.G. (2004). Characterization of four autonomous repression domains in the corepressor receptor interacting protein 140. *J Biol Chem 279*, 15645-15651.

Cismasiu, V.B., Adamo, K., Gecewicz, J., Duque, J., Lin, Q., and Avram, D. (2005). BCL11B functionally associates with the NuRD complex in T lymphocytes to repress targeted promoter. *Oncogene 24*, 6753-6764.

Cismasiu, V.B., Ghanta, S., Duque, J., Albu, D.I., Chen, H.M., Kasturi, R., and Avram, D. (2006). BCL11B participates in the activation of IL2 gene expression in CD4+ T lymphocytes. *Blood 108*, 2695-2702.

Coleman, J.E. (1992). Zinc proteins: enzymes, storage proteins, transcription factors, and replication proteins. *Annual review of biochemistry 61*, 897-946.

Cotsarelis, G., Sun, T.T., and Lavker, R.M. (1990). Label-retaining cells reside in the bulge area of pilosebaceous unit: implications for follicular stem cells, hair cycle, and skin carcinogenesis. *Cell 61*, 1329-1337.

Cunningham, J.J., and Roussel, M.F. (2001). Cyclin-dependent kinase inhibitors in the development of the central nervous system. *Cell Growth Differ 12*, 387-396.

de Guzman Strong, C., Wertz, P.W., Wang, C., Yang, F., Meltzer, P.S., Andl, T., Millar, S.E., Ho, I.C., Pai, S.Y., and Segre, J.A. (2006). Lipid defect underlies selective skin barrier impairment of an epidermal-specific deletion of Gata-3. *J Cell Biol 175*, 661-670.

De, S., Nguyen, A.Q., Shuler, C.F., and Turman, J.E., Jr. (2005). Mesencephalic trigeminal nucleus development is dependent on Krox-20 expression. *Developmental neuroscience 27*, 49-58.

Dignam, J.D., Lebovitz, R.M., and Roeder, R.G. (1983). Accurate transcription initiation by RNA polymerase II in a soluble extract from isolated mammalian nuclei. *Nucleic Acids Res 11*, 1475-1489.

Dowell, P., Peterson, V.J., Zabriskie, T.M., and Leid, M. (1997). Ligand-induced peroxisome proliferator-activated receptor alpha conformational change. *J Biol Chem 272*, 2013-2020.

Dupe, V., Davenne, M., Brocard, J., Dolle, P., Mark, M., Dierich, A., Chambon, P., and Rijli, F.M. (1997). In vivo functional analysis of the Hoxa-1 3' retinoic acid response element (3'RARE). *Development* (Cambridge, England) *124*, 399-410.

Dyer, M.A., and Cepko, C.L. (2000). p57(Kip2) regulates progenitor cell proliferation and amacrine interneuron development in the mouse retina. *Development 127*, 3593-3605.

Elias, P.M. (2005). Stratum corneum defensive functions: an integrated view. *The Journal of investigative dermatology 125*, 183-200.

Epp, N., Furstenberger, G., Muller, K., de Juanes, S., Leitges, M., Hausser, I., Thieme, F., Liebisch, G., Schmitz, G., and Krieg, P. (2007). 12R-lipoxygenase deficiency disrupts epidermal barrier function. *The Journal of cell biology 177*, 173-182.

Fincham, A.G., Moradian-Oldak, J., and Simmer, J.P. (1999). The structural biology of the developing dental enamel matrix. *Journal of structural biology 126*, 270-299.

Florin, L., Alter, H., Grone, H.J., Szabowski, A., Schutz, G., and Angel, P. (2004). Cre recombinase-mediated gene targeting of mesenchymal cells. *Genesis 38*, 139-144.

Franco, C.B., Scripture-Adams, D.D., Proekt, I., Taghon, T., Weiss, A.H., Yui, M.A., Adams, S.L., Diamond, R.A., and Rothenberg, E.V. (2006). Notch/Delta signaling constrains reengineering of pro-T cells by PU.1. *Proc Natl Acad Sci* U S A *103*, 11993-11998.

Fuchs, E., and Green, H. (1980). Changes in keratin gene expression during terminal differentiation of the keratinocyte. *Cell 19*, 1033-1042.

Fujita, N., Jaye, D.L., Geigerman, C., Akyildiz, A., Mooney, M.R., Boss, J.M., and Wade, P.A. (2004). MTA3 and the Mi-2/NuRD complex regulate cell fate during B lymphocyte differentiation. *Cell 119*, 75-86.

Fukumoto, S., Kiba, T., Hall, B., Iehara, N., Nakamura, T., Longenecker, G., Krebsbach, P.H., Nanci, A., Kulkarni, A.B., and Yamada, Y. (2004). Ameloblastin is a cell adhesion molecule required for maintaining the differentiation state of ameloblasts. *The Journal of cell biology 167*, 973-983.

Furstenberger, G., Epp, N., Eckl, K.M., Hennies, H.C., Jorgensen, C., Hallenborg, P., Kristiansen, K., and Krieg, P. (2007). Role of epidermis-type lipoxygenases for skin barrier function and adipocyte differentiation. *Prostaglandins Other Lipid Mediat 82*, 128-134.

Ganss, B., and Jheon, A. (2004). Zinc finger transcription factors in skeletal development. *Crit Rev Oral Biol Med 15*, 282-297.

Ganss, B., and Kobayashi, H. (2002). The zinc finger transcription factor Zfp60 is a negative regulator of cartilage differentiation. *J Bone Miner Res 17*, 2151-2160.

Ganss, B., Teo, W., Chen, H., and Poon, T. (2002). Krox-26 is a novel C2H2 zinc finger transcription factor expressed in developing dental and osteogenic tissues. *Connective tissue research 43*, 161-166.

Gareus, R., Huth, M., Breiden, B., Nenci, A., Rosch, N., Haase, I., Bloch, W., Sandhoff, K., and Pasparakis, M. (2007). Normal epidermal differentiation but impaired skin-barrier formation upon keratinocyte-restricted IKK1 ablation. *Nature cell biology 9*, 461-469.

Gerfen, C.R. (1992). The neostriatal mosaic: multiple levels of compartmental organization in the basal ganglia. *Annual review of neuroscience 15*, 285-320.

Gibson, C.W., Yuan, Z.A., Hall, B., Longenecker, G., Chen, E., Thyagarajan, T., Sreenath, T., Wright, J.T., Decker, S., Piddington, R*., et al.* (2001). Amelogenin-deficient mice display an amelogenesis imperfecta phenotype. *The Journal of biological chemistry 276*, 31871-31875.

Golonzhka, O., Leid, M., Indra, G., and Indra, A.K. (2007). Expression of COUP-TF-interacting protein 2 (CTIP2) in mouse skin during development and in adulthood. *Gene Expr Patterns 7*, 754-760.

Grabarczyk, P., Przybylski, G.K., Depke, M., Volker, U., Bahr, J., Assmus, K., Broker, B.M., Walther, R., and Schmidt, C.A. (2007). Inhibition of BCL11B expression leads to apoptosis of malignant but not normal mature T cells. *Oncogene 26*, 3797-3810.

Grachtchouk, M., Mo, R., Yu, S., Zhang, X., Sasaki, H., Hui, C.C., and Dlugosz, A.A. (2000). Basal cell carcinomas in mice overexpressing Gli2 in skin. *Nat Genet 24*, 216-217.

Graybiel, A.M. (2005). The basal ganglia: learning new tricks and loving it. *Current opinion in neurobiology 15*, 638-644.

Gurrieri, S., Furstenberger, G., Schadow, A., Haas, U., Singer, A.G., Ghomashchi, F., Pfeilschifter, J., Lambeau, G., Gelb, M.H., and Kaszkin, M. (2003). Differentiation-dependent regulation of secreted phospholipases A2 in murine epidermis. *J Invest Dermatol 121*, 156-164.

Hardman, M.J., Sisi, P., Banbury, D.N., and Byrne, C. (1998). Patterned acquisition of skin barrier function during development. *Development* (Cambridge, England) *125*, 1541-1552.

Hendrich, B., Guy, J., Ramsahoye, B., Wilson, V.A., and Bird, A. (2001). Closely related proteins MBD2 and MBD3 play distinctive but interacting roles in mouse development. *Genes Dev 15*, 710-723.

Herman, G.E., and El-Hodiri, H.M. (2002). The role of ZIC3 in vertebrate development. *Cytogenetic and genome research 99*, 229-235.

Hohl, M., and Thiel, G. (2005). Cell type-specific regulation of RE-1 silencing transcription factor (REST) target genes. *Eur J Neurosci 22*, 2216-2230.

Holleran, W.M., Ginns, E.I., Menon, G.K., Grundmann, J.U., Fartasch, M., McKinney, C.E., Elias, P.M., and Sidransky, E. (1994). Consequences of beta-glucocerebrosidase deficiency in epidermis. Ultrastructure and permeability barrier alterations in Gaucher disease. *J Clin Invest 93*, 1756-1764.

Hong, W., Nakazawa, M., Chen, Y.Y., Kori, R., Vakoc, C.R., Rakowski, C., and Blobel, G.A. (2005). FOG-1 recruits the NuRD repressor complex to mediate transcriptional repression by GATA-1. *Embo J 24*, 2367-2378.

Hu, J.C., Hu, Y., Smith, C.E., McKee, M.D., Wright, J.T., Yamakoshi, Y., Papagerakis, P., Hunter, G.K., Feng, J.Q., Yamakoshi, F.*, et al.* (2008). Enamel defects and ameloblast-specific expression in Enam knock-out/lacz knock-in mice. *The Journal of biological chemistry 283*, 10858-10871.

Indra, A.K., Dupe, V., Bornert, J.M., Messaddeq, N., Yaniv, M., Mark, M., Chambon, P., and Metzger, D. (2005a). Temporally controlled targeted somatic mutagenesis in embryonic surface ectoderm and fetal epidermal keratinocytes unveils two distinct developmental functions of BRG1 in limb morphogenesis and skin barrier formation. *Development 132*, 4533-4544.

Indra, A.K., Li, M., Brocard, J., Warot, X., Bornert, J.M., Gerard, C., Messaddeq, N., Chambon, P., and Metzger, D. (2000). Targeted somatic mutagenesis in mouse epidermis. *Hormone research 54*, 296-300.

Indra, A.K., Mohan, W.S., 2nd, Frontini, M., Scheer, E., Messaddeq, N., Metzger, D., and Tora, L. (2005b). TAF10 is required for the establishment of skin barrier function in foetal, but not in adult mouse epidermis. *Dev Biol 285*, 28-37.

Joseph, B., Wallen-Mackenzie, A., Benoit, G., Murata, T., Joodmardi, E., Okret, S., and Perlmann, T. (2003). p57(Kip2) cooperates with Nurr1 in developing dopamine cells. *Proc Natl Acad Sci* U S A *100*, 15619-15624.

Kamimura, K., Ohi, H., Kubota, T., Okazuka, K., Yoshikai, Y., Wakabayashi, Y., Aoyagi, Y., Mishima, Y., and Kominami, R. (2007). Haploinsufficiency of Bcl11b for suppression of lymphomagenesis and thymocyte development. B*iochemical and biophysical research communications 355*, 538-542.

Kantor, B., Makedonski, K., Shemer, R., and Razin, A. (2003). Expression and localization of components of the histone deacetylases multiprotein repressory complexes in the mouse preimplantation embryo. *Gene Expr Patterns 3*, 697-702.

Kehle, J., Beuchle, D., Treuheit, S., Christen, B., Kennison, J.A., Bienz, M., and Muller, J. (1998). dMi-2, a hunchback-interacting protein that functions in polycomb repression. *Science 282*, 1897-1900.

Khavari, P.A. (2004). Profiling epithelial stem cells. *Nature biotechnology 22*, 393-394.

Kim, J., Sif, S., Jones, B., Jackson, A., Koipally, J., Heller, E., Winandy, S., Viel, A., Sawyer, A., Ikeda, T.*, et al.* (1999). Ikaros DNA-binding proteins direct formation of chromatin remodeling complexes in lymphocytes. *Immunity 10*, 345-355.

Koster, M.I., Dai, D., Marinari, B., Sano, Y., Costanzo, A., Karin, M., and Roop, D.R. (2007). p63 induces key target genes required for epidermal morphogenesis. *Proc Natl Acad Sci* U S A *104*, 3255-3260.

Koster, M.I., Kim, S., Mills, A.A., DeMayo, F.J., and Roop, D.R. (2004). p63 is the molecular switch for initiation of an epithelial stratification program. *Genes & development 18*, 126-131.

Krause, D.S., Fackler, M.J., Civin, C.I., and May, W.S. (1996). CD34: structure, biology, and clinical utility. *Blood 87*, 1-13.

Kuppers, R., Sonoki, T., Satterwhite, E., Gesk, S., Harder, L., Oscier, D.G., Tucker, P.W., Dyer, M.J., and Siebert, R. (2002). Lack of somatic hypermutation of IG V(H) genes in lymphoid malignancies with t(2;14)(p13;q32) translocation involving the BCL11A gene. *Leukemia 16*, 937-939.

Langlands, K., Down, G.A., and Kealey, T. (2000). Id proteins are dynamically expressed in normal epidermis and dysregulated in squamous cell carcinoma. *Cancer Res 60*, 5929-5933.

Lavker, R.M., Miller, S., Wilson, C., Cotsarelis, G., Wei, Z.G., Yang, J.S., and Sun, T.T. (1993). Hair follicle stem cells: their location, role in hair cycle, and involvement in skin tumor formation. *The Journal of investigative dermatology 101*, 16S-26S.

Lavker, R.M., and Sun, T.T. (2000). Epidermal stem cells: properties, markers, and location. *Proceedings of the National Academy of Sciences of the United States of America 97*, 13473-13475.

Lee, M.S., Gippert, G.P., Soman, K.V., Case, D.A., and Wright, P.E. (1989). Three-dimensional solution structure of a single zinc finger DNA-binding domain. *Science* (New York, NY) *245*, 635-637.

Leid, M., Ishmael, J.E., Avram, D., Shepherd, D., Fraulob, V., and Dolle, P. (2004). CTIP1 and CTIP2 are differentially expressed during mouse embryogenesis. *Gene Expr Patterns 4*, 733-739.

Li, G., Gustafson-Brown, C., Hanks, S.K., Nason, K., Arbeit, J.M., Pogliano, K., Wisdom, R.M., and Johnson, R.S. (2003). c-Jun is essential for organization of the epidermal leading edge. *Developmental cell 4*, 865-877.

Li, Q., Lu, Q., Hwang, J.Y., Buscher, D., Lee, K.F., Izpisua-Belmonte, J.C., and Verma, I.M. (1999). IKK1-deficient mice exhibit abnormal development of skin and skeleton. *Genes & development 13*, 1322-1328.

Li, W., Sandhoff, R., Kono, M., Zerfas, P., Hoffmann, V., Ding, B.C., Proia, R.L., and Deng, C.X. (2007). Depletion of ceramides with very long chain fatty acids causes defective skin permeability barrier function, and neonatal lethality in ELOVL4 deficient mice. *Int J Biol Sci 3*, 120-128.

Liu, Y., Lyle, S., Yang, Z., and Cotsarelis, G. (2003). Keratin 15 promoter targets putative epithelial stem cells in the hair follicle bulge. *The Journal of investigative dermatology 121*, 963-968.

Lumsden, A.G. (1988). Spatial organization of the epithelium and the role of neural crest cells in the initiation of the mammalian tooth germ. *Development* (Cambridge, England) *103 Suppl*, 155-169.

Luo, J., Su, F., Chen, D., Shiloh, A., and Gu, W. (2000). Deacetylation of p53 modulates its effect on cell growth and apoptosis. *Nature 408*, 377-381.

Mack, J.A., Anand, S., and Maytin, E.V. (2005). Proliferation and cornification during development of the mammalian epidermis. *Birth Defects Res C Embryo Today 75*, 314-329.

Mackay, J.P., and Crossley, M. (1998). Zinc fingers are sticking together. *Trends in biochemical sciences 23*, 1-4.

MacLeod, R.A., Nagel, S., and Drexler, H.G. (2004). BCL11B rearrangements probably target T-cell neoplasia rather than acute myelocytic leukemia. *Cancer Genet Cytogenet 153*, 88-89.

MacLeod, R.A., Nagel, S., Kaufmann, M., Janssen, J.W., and Drexler, H.G. (2003). Activation of HOX11L2 by juxtaposition with 3'-BCL11B in an acute lymphoblastic leukemia cell line (HPB-ALL) with t(5;14)(q35;q32.2). *Genes Chromosomes Cancer 37*, 84-91.

Mao-Qiang, M., Jain, M., Feingold, K.R., and Elias, P.M. (1996). Secretory phospholipase A2 activity is required for permeability barrier homeostasis. T*he Journal of investigative dermatology 106*, 57-63.

Marban, C., Suzanne, S., Dequiedt, F., de Walque, S., Redel, L., Van Lint, C., Aunis, D., and Rohr, O. (2007). Recruitment of chromatin-modifying enzymes by CTIP2 promotes HIV-1 transcriptional silencing. *The EMBO journal 26*, 412-423.

Martin-Subero, J.I., Gesk, S., Harder, L., Sonoki, T., Tucker, P.W., Schlegelberger, B., Grote, W., Novo, F.J., Calasanz, M.J., Hansmann, M.L*., et al.* (2002). Recurrent involvement of the REL and BCL11A loci in classical Hodgkin lymphoma. *Blood 99*, 1474-1477.

Martinez-Climent, J.A., Alizadeh, A.A., Segraves, R., Blesa, D., Rubio-Moscardo, F., Albertson, D.G., Garcia-Conde, J., Dyer, M.J., Levy, R., Pinkel, D*., et al.* (2003). Transformation of follicular lymphoma to diffuse large cell lymphoma is associated with a heterogeneous set of DNA copy number and gene expression alterations. *Blood 101*, 3109-3117.

Matsuoka, S., Edwards, M.C., Bai, C., Parker, S., Zhang, P., Baldini, A., Harper, J.W., and Elledge, S.J. (1995). p57KIP2, a structurally distinct member of the p21CIP1 Cdk inhibitor family, is a candidate tumor suppressor gene. *Genes Dev 9*, 650-662.

Miletich, I., and Sharpe, P.T. (2003). Normal and abnormal dental development. *Human molecular genetics 12 Spec No 1*, R69-73.

Mill, P., Mo, R., Fu, H., Grachtchouk, M., Kim, P.C., Dlugosz, A.A., and Hui, C.C. (2003). Sonic hedgehog-dependent activation of Gli2 is essential for embryonic hair follicle development. *Genes Dev 17*, 282-294.

Miller, J., McLachlan, A.D., and Klug, A. (1985). Repetitive zinc-binding domains in the protein transcription factor IIIA from Xenopus oocytes. *The EMBO journal 4*, 1609-1614.

Mills, A.A., Zheng, B., Wang, X.J., Vogel, H., Roop, D.R., and Bradley, A. (1999). p63 is a p53 homologue required for limb and epidermal morphogenesis. *Nature 398*, 708-713.

Mina, M., and Kollar, E.J. (1987). The induction of odontogenesis in non-dental mesenchyme combined with early murine mandibular arch epithelium. *Archives of oral biology 32*, 123-127.

Molyneaux, B.J., Arlotta, P., Hirata, T., Hibi, M., and Macklis, J.D. (2005). Fezl is required for the birth and specification of corticospinal motor neurons. *Neuron 47*, 817-831.

Moradian-Oldak, J. (2001). Amelogenins: assembly, processing and control of crystal morphology. *Matrix Biol 20*, 293-305.

Moran, J.L., Qiu, H., Turbe-Doan, A., Yun, Y., Boeglin, W.E., Brash, A.R., and Beier, D.R. (2007). A mouse mutation in the 12R-lipoxygenase, Alox12b, disrupts formation of the epidermal permeability barrier. *J Invest Dermatol 127*, 1893-1897.

Morris, R.J., and Potten, C.S. (1994). Slowly cycling (label-retaining) epidermal cells behave like clonogenic stem cells in vitro. *Cell proliferation 27*, 279-289.

Murawsky, C.M., Brehm, A., Badenhorst, P., Lowe, N., Becker, P.B., and Travers, A.A. (2001). Tramtrack69 interacts with the dMi-2 subunit of the Drosophila NuRD chromatin remodelling complex. *EMBO* Rep *2*, 1089-1094.

Nagel, S., Kaufmann, M., Drexler, H.G., and MacLeod, R.A. (2003). The cardiac homeobox gene NKX2-5 is deregulated by juxtaposition with BCL11B in pediatric T-ALL cell lines via a novel t(5;14)(q35.1;q32.2). *Cancer research 63*, 5329-5334.

Nakamura, T., de Vega, S., Fukumoto, S., Jimenez, L., Unda, F., and Yamada, Y. (2008). Transcription factor epiprofin is essential for tooth morphogenesis by regulating epithelial cell fate and tooth number. *The Journal of biological chemistry 283*, 4825-4833.

Nakamura, T., Yamazaki, Y., Saiki, Y., Moriyama, M., Largaespada, D.A., Jenkins, N.A., and Copeland, N.G. (2000). Evi9 encodes a novel zinc finger protein that physically interacts with BCL6, a known human B-cell proto-oncogene product. *Mol Cell Biol 20*, 3178-3186.

Okazuka, K., Wakabayashi, Y., Kashihara, M., Inoue, J., Sato, T., Yokoyama, M., Aizawa, S., Aizawa, Y., Mishima, Y., and Kominami, R. (2005). p53 prevents maturation of T cell

development to the immature CD4-CD8+ stage in Bcl11b-/- mice. *Biochem Biophys Res Commun 328*, 545-549.

Parraga, G., Horvath, S.J., Eisen, A., Taylor, W.E., Hood, L., Young, E.T., and Klevit, R.E. (1988). Zinc-dependent structure of a single-finger domain of yeast ADR1. *Science* (New York, NY *241*, 1489-1492.

Parrish, M., Ott, T., Lance-Jones, C., Schuetz, G., Schwaeger-Nickolenko, A., and Monaghan, A.P. (2004). Loss of the Sall3 gene leads to palate deficiency, abnormalities in cranial nerves, and perinatal lethality. *Molecular and cellular biology 24*, 7102-7112.

Pelengaris, S., Littlewood, T., Khan, M., Elia, G., and Evan, G. (1999). Reversible activation of c-Myc in skin: induction of a complex neoplastic phenotype by a single oncogenic lesion. *Mol Cell 3*, 565-577.

Polimeni, M., Giorgi, S., De Gregorio, L., Dragani, T.A., Molinaro, M., Cossu, G., and Bouche, M. (1996). Differentiation dependent expression in muscle cells of ZT3, a novel zinc finger factor differentially expressed in embryonic and adult tissues. *Mechanisms of development 54*, 107-117.

Przybylski, G.K., Dik, W.A., Wanzeck, J., Grabarczyk, P., Majunke, S., Martin-Subero, J.I., Siebert, R., Dolken, G., Ludwig, W.D., Verhaaf, B*., et al.* (2005). Disruption of the BCL11B gene through inv(14)(q11.2q32.31) results in the expression of BCL11B-TRDC fusion transcripts and is associated with the absence of wild-type BCL11B transcripts in T-ALL. *Leukemia 19*, 201-208.

Qiu, Y., Pereira, F.A., DeMayo, F.J., Lydon, J.P., Tsai, S.Y., and Tsai, M.J. (1997). Null mutation of mCOUP-TFI results in defects in morphogenesis of the glossopharyngeal ganglion, axonal projection, and arborization. *Genes Dev 11*, 1925-1937.

Relaix, F., Weng, X., Marazzi, G., Yang, E., Copeland, N., Jenkins, N., Spence, S.E., and Sassoon, D. (1996). Pw1, a novel zinc finger gene implicated in the myogenic and neuronal lineages. *Developmental biology 177*, 383-396.

Rodius, S., Indra, G., Thibault, C., Pfister, V., and Georges-Labouesse, E. (2007). Loss of alpha6 integrins in keratinocytes leads to an increase in TGFbeta and AP1 signaling and in expression of differentiation genes. *J Cell Physiol 212*, 439-449.

Rodriguez, C.I., Buchholz, F., Galloway, J., Sequerra, R., Kasper, J., Ayala, R., Stewart, A.F., and Dymecki, S.M. (2000). High-efficiency deleter mice show that FLPe is an alternative to Cre-loxP. *Nature genetics 25*, 139-140.

Ronnov-Jessen, L., Petersen, O.W., and Bissell, M.J. (1996). Cellular changes involved in conversion of normal to malignant breast: importance of the stromal reaction. *Physiological reviews 76*, 69-125.

Roop, D.R., Hawley-Nelson, P., Cheng, C.K., and Yuspa, S.H. (1983). Keratin gene expression in mouse epidermis and cultured epidermal cells. *Proceedings of the National Academy of Sciences of the United States of America 80*, 716-720.

Ruch, J.V., Lesot, H., and Begue-Kirn, C. (1995). Odontoblast differentiation. *The International journal of developmental biology 39*, 51-68.

Sakata, J., Inoue, J., Ohi, H., Kosugi-Okano, H., Mishima, Y., Hatakeyama, K., Niwa, O., and Kominami, R. (2004). Involvement of V(D)J recombinase in the generation of intragenic deletions in the Rit1/Bcl11b tumor suppressor gene in gamma-ray-induced thymic lymphomas and in normal thymus of the mouse. *Carcinogenesis 25*, 1069-1075.

Satterwhite, E., Sonoki, T., Willis, T.G., Harder, L., Nowak, R., Arriola, E.L., Liu, H., Price, H.P., Gesk, S., Steinemann, D.*, et al.* (2001). The BCL11 gene family: involvement of BCL11A in lymphoid malignancies. *Blood 98*, 3413-3420.

Schluter, C., Duchrow, M., Wohlenberg, C., Becker, M.H., Key, G., Flad, H.D., and Gerdes, J. (1993). The cell proliferation-associated antigen of antibody Ki-67: a very large, ubiquitous nuclear protein with numerous repeated elements, representing a new kind of cell cycle-maintaining proteins. *The Journal of cell biology 123*, 513-522.

Schultz, D.C., Friedman, J.R., and Rauscher, F.J., 3rd (2001). Targeting histone deacetylase complexes via KRAB-zinc finger proteins: the PHD and bromodomains of KAP-1 form a cooperative unit that recruits a novel isoform of the Mi-2alpha subunit of NuRD. *Genes Dev 15*, 428-443.

Segre, J. (2003). Complex redundancy to build a simple epidermal permeability barrier. *Curr Opin Cell Biol 15*, 776-782.

Segre, J.A. (2006). Epidermal barrier formation and recovery in skin disorders. *J Clin Invest 116*, 1150-1158.

Segre, J.A., Bauer, C., and Fuchs, E. (1999). Klf4 is a transcription factor required for establishing the barrier function of the skin. *Nature genetics 22*, 356-360.

Senawong, T., Peterson, V.J., Avram, D., Shepherd, D.M., Frye, R.A., Minucci, S., and Leid, M. (2003). Involvement of the histone deacetylase SIRT1 in chicken ovalbumin upstream promoter transcription factor (COUP-TF)-interacting protein 2-mediated transcriptional repression. *J Biol Chem 278*, 43041-43050.

Senawong, T., Peterson, V.J., and Leid, M. (2005). BCL11A-dependent recruitment of SIRT1 to a promoter template in mammalian cells results in histone deacetylation and transcriptional repression. *Arch Biochem Biophys 434*, 316-325.

Shastry, B.S. (1996). Transcription factor IIIA (TFIIIA) in the second decade. *Journal of cell science 109 (Pt 3)*, 535-539.

Shaulian, E., and Karin, M. (2002). AP-1 as a regulator of cell life and death. *Nature cell biology 4*, E131-136.

Siddiqui, H., Solomon, D.A., Gunawardena, R.W., Wang, Y., and Knudsen, E.S. (2003). Histone deacetylation of RB-responsive promoters: requisite for specific gene repression but dispensable for cell cycle inhibition. *Mol Cell Biol 23*, 7719-7731.

Simbulan-Rosenthal, C.M., Trabosh, V., Velarde, A., Chou, F.P., Daher, A., Tenzin, F., Tokino, T., and Rosenthal, D.S. (2005). Id2 protein is selectively upregulated by UVB in primary, but not in immortalized human keratinocytes and inhibits differentiation. *Oncogene 24*, 5443-5458.

Slack, J.M. (2000). Stem cells in epithelial tissues. *Science* (New York, NY) *287*, 1431-1433.

Smith, J.S., Brachmann, C.B., Celic, I., Kenna, M.A., Muhammad, S., Starai, V.J., Avalos, J.L., Escalante-Semerena, J.C., Grubmeyer, C., Wolberger, C*., et al.* (2000). A phylogenetically conserved NAD+-dependent protein deacetylase activity in the Sir2 protein family. *Proc Natl Acad Sci U S A 97*, 6658-6663.

Solari, F., Bateman, A., and Ahringer, J. (1999). The Caenorhabditis elegans genes egl-27 and egr-1 are similar to MTA1, a member of a chromatin regulatory complex, and are redundantly required for embryonic patterning. *Development 126*, 2483-2494.

Stenman, J., Toresson, H., and Campbell, K. (2003). Identification of two distinct progenitor populations in the lateral ganglionic eminence: implications for striatal and olfactory bulb neurogenesis. *J Neurosci 23*, 167-174.

Stone, S.J., Myers, H.M., Watkins, S.M., Brown, B.E., Feingold, K.R., Elias, P.M., and Farese, R.V., Jr. (2004). Lipopenia and skin barrier abnormalities in DGAT2-deficient mice. *The Journal of biological chemistry 279*, 11767-11776.

Su, X.Y., Busson, M., Della Valle, V., Ballerini, P., Dastugue, N., Talmant, P., Ferrando, A.A., Baudry-Bluteau, D., Romana, S., Berger, R*., et al.* (2004). Various types of rearrangements target TLX3 locus in T-cell acute lymphoblastic leukemia. *Genes Chromosomes Cancer 41*, 243-249.

Szabowski, A., Maas-Szabowski, N., Andrecht, S., Kolbus, A., Schorpp-Kistner, M., Fusenig, N.E., and Angel, P. (2000). c-Jun and JunB antagonistically control cytokine-regulated mesenchymal-epidermal interaction in skin. *Cell 103*, 745-755.

Thesleff, I. (2003). Epithelial-mesenchymal signalling regulating tooth morphogenesis. *Journal of cell science 116*, 1647-1648.

Thesleff, I., Keranen, S., and Jernvall, J. (2001). Enamel knots as signaling centers linking tooth morphogenesis and odontoblast differentiation. *Advances in dental research 15*, 14-18.

Thesleff, I., and Sharpe, P. (1997). Signalling networks regulating dental development. *Mechanisms of development 67*, 111-123.

Topark-Ngarm, A., Golonzhka, O., Peterson, V.J., Barrett, B., Jr., Martinez, B., Crofoot, K., Filtz, T.M., and Leid, M. (2006). CTIP2 associates with the NuRD complex on the promoter of p57KIP2, a newly identified CTIP2 target gene. *J Biol Chem 281*, 32272-32283.

Trappe, R., Buddenberg, P., Uedelhoven, J., Glaser, B., Buck, A., Engel, W., and Burfeind, P. (2002). The murine BTB/POZ zinc finger gene Znf131: predominant expression in the developing central nervous system, in adult brain, testis, and thymus. *Biochemical and biophysical research communications 296*, 319-327.

Trempus, C.S., Morris, R.J., Bortner, C.D., Cotsarelis, G., Faircloth, R.S., Reece, J.M., and Tennant, R.W. (2003). Enrichment for living murine keratinocytes from the hair follicle bulge with the cell surface marker CD34. *The Journal of investigative dermatology 120*, 501-511.

Tsai, R.Y., and Reed, R.R. (1997). Cloning and functional characterization of Roaz, a zinc finger protein that interacts with O/E-1 to regulate gene expression: implications for olfactory neuronal development. *J Neurosci 17*, 4159-4169.

Tsai, S.Y., and Tsai, M.J. (1997). Chick ovalbumin upstream promoter-transcription factors (COUP-TFs): coming of age. *Endocrine reviews 18*, 229-240.

Tucker, A., and Sharpe, P. (2004). The cutting-edge of mammalian development; how the embryo makes teeth. *Nature reviews 5*, 499-508.

Tummers, M., and Thesleff, I. (2003). Root or crown: a developmental choice orchestrated by the differential regulation of the epithelial stem cell niche in the tooth of two rodent species. *Development* (Cambridge, England) *130*, 1049-1057.

Tupler, R., Perini, G., and Green, M.R. (2001). Expressing the human genome. *Nature 409*, 832-833.

Tydell, C.C., David-Fung, E.S., Moore, J.E., Rowen, L., Taghon, T., and Rothenberg, E.V. (2007). Molecular dissection of prethymic progenitor entry into the T lymphocyte developmental pathway. *J Immunol 179*, 421-438.

Vaahtokari, A., Aberg, T., Jernvall, J., Keranen, S., and Thesleff, I. (1996). The enamel knot as a signaling center in the developing mouse tooth. *Mechanisms of development 54*, 39-43.

Vasireddy, V., Uchida, Y., Salem, N., Jr., Kim, S.Y., Mandal, M.N., Reddy, G.B., Bodepudi, R., Alderson, N.L., Brown, J.C., Hama, H*., et al.* (2007). Loss of functional ELOVL4 depletes very long-chain fatty acids (> or =C28) and the unique omega-O-acylceramides in skin leading to neonatal death. *Hum Mol Genet 16*, 471-482.

Vassar, R., Rosenberg, M., Ross, S., Tyner, A., and Fuchs, E. (1989). Tissue-specific and differentiation-specific expression of a human K14 keratin gene in transgenic mice. *Proceedings of the National Academy of Sciences of the United States of America 86*, 1563-1567.

von Zelewsky, T., Palladino, F., Brunschwig, K., Tobler, H., Hajnal, A., and Muller, F. (2000). The C. elegans Mi-2 chromatin-remodelling proteins function in vulval cell fate determination. *Development 127*, 5277-5284.

Waikel, R.L., Wang, X.J., and Roop, D.R. (1999). Targeted expression of c-Myc in the epidermis alters normal proliferation, differentiation and UV-B induced apoptosis. *Oncogene 18*, 4870-4878.

Wakabayashi, Y., Inoue, J., Takahashi, Y., Matsuki, A., Kosugi-Okano, H., Shinbo, T., Mishima, Y., Niwa, O., and Kominami, R. (2003a). Homozygous deletions and point mutations of the Rit1/Bcl11b gene in gamma-ray induced mouse thymic lymphomas. *Biochemical and biophysical research communications 301*, 598-603.

Wakabayashi, Y., Watanabe, H., Inoue, J., Takeda, N., Sakata, J., Mishima, Y., Hitomi, J., Yamamoto, T., Utsuyama, M., Niwa, O.*, et al.* (2003b). Bcl11b is required for differentiation and survival of alphabeta T lymphocytes. *Nature immunology 4*, 533-539.

Wang, Y., Wysocka, J., Perlin, J.R., Leonelli, L., Allis, C.D., and Coonrod, S.A. (2004). Linking covalent histone modifications to epigenetics: the rigidity and plasticity of the marks. *Cold Spring Harb Symp Quant Biol 69*, 161-169.

Werner, S., and Smola, H. (2001). Paracrine regulation of keratinocyte proliferation and differentiation. *Trends in cell biology 11*, 143-146.

Williams, C.J., Naito, T., Arco, P.G., Seavitt, J.R., Cashman, S.M., De Souza, B., Qi, X., Keables, P., Von Andrian, U.H., and Georgopoulos, K. (2004). The chromatin remodeler Mi-2beta is required for CD4 expression and T cell development. *Immunity 20*, 719-733.

Wolfe, S.A., Nekludova, L., and Pabo, C.O. (2000). DNA recognition by Cys2His2 zinc finger proteins. *Annual review of biophysics and biomolecular structure 29*, 183-212.

Xue, Y., Wong, J., Moreno, G.T., Young, M.K., Cote, J., and Wang, W. (1998). NURD, a novel complex with both ATP-dependent chromatin-remodeling and histone deacetylase activities. *Mol Cell 2*, 851-861.

Yamaguchi, H., Zhou, C., Lin, S.C., Durand, B., Tsai, S.Y., and Tsai, M.J. (2004). The nuclear orphan receptor COUP-TFI is important for differentiation of oligodendrocytes. *Dev Biol 266*, 238-251.

Yang, A., Schweitzer, R., Sun, D., Kaghad, M., Walker, N., Bronson, R.T., Tabin, C., Sharpe, A., Caput, D., Crum, C*., et al.* (1999). p63 is essential for regenerative proliferation in limb, craniofacial and epithelial development. *Nature 398*, 714-718.

Yao, Y.L., and Yang, W.M. (2003). The metastasis-associated proteins 1 and 2 form distinct protein complexes with histone deacetylase activity. *J Biol Chem 278*, 42560-42568.

Yokota, Y., Mansouri, A., Mori, S., Sugawara, S., Adachi, S., Nishikawa, S., and Gruss, P. (1999). Development of peripheral lymphoid organs and natural killer cells depends on the helix-loop-helix inhibitor Id2. *Nature 397*, 702-706.

Yu, Z., Lin, K.K., Bhandari, A., Spencer, J.A., Xu, X., Wang, N., Lu, Z., Gill, G.N., Roop, D.R., Wertz, P*., et al.* (2006). The Grainyhead-like epithelial transactivator Get-1/Grhl3 regulates epidermal terminal differentiation and interacts functionally with LMO4. *Dev Biol 299*, 122-136.

Zeichner-David, M., Diekwisch, T., Fincham, A., Lau, E., MacDougall, M., Moradian-Oldak, J., Simmer, J., Snead, M., and Slavkin, H.C. (1995). Control of ameloblast differentiation. *The International journal of developmental biology 39*, 69-92.

Zeichner-David, M., Vo, H., Tan, H., Diekwisch, T., Berman, B., Thiemann, F., Alcocer, M.D., Hsu, P., Wang, T., Eyna, J*., et al.* (1997). Timing of the expression of enamel gene products during mouse tooth development. *The International journal of developmental biology 41*, 27-38.

Zenz, R., and Wagner, E.F. (2006). Jun signalling in the epidermis: From developmental defects to psoriasis and skin tumors. *The international journal of biochemistry & cell biology 38*, 1043-1049.

Zhang, X., Azhar, G., Zhong, Y., and Wei, J.Y. (2006). Zipzap/p200 is a novel zinc finger protein contributing to cardiac gene regulation. *Biochemical and biophysical research communications 346*, 794-801.

Zhang, Y., Ng, H.H., Erdjument-Bromage, H., Tempst, P., Bird, A., and Reinberg, D. (1999). Analysis of the NuRD subunits reveals a histone deacetylase core complex and a connection with DNA methylation. *Genes Dev 13*, 1924-1935.

Zhou, Y.L., Lei, Y., and Snead, M.L. (2000). Functional antagonism between Msx2 and CCAAT/enhancer-binding protein alpha in regulating the mouse amelogenin gene expression is mediated by protein-protein interaction. *The Journal of biological chemistry 275*, 29066-29075.